geodiversitas

2023 • 45 • 15

New remains of Neotropical bunodont litopterns and the systematics of Megadolodinae (Mammalia: Litopterna)

Juan D. CARRILLO, Catalina SUAREZ, Aldo Marcelo BENITES-PALOMINO, Andrés VANEGAS, Andrés LINK, Aldo F. RINCÓN, Javier LUQUE, Siobhán B. COOKE, Melissa TALLMAN & Guillaume BILLET

in Juan D. CARRILLO (ed.),
Neotropical palaeontology:
the Miocene La Venta biome

art. 45 (15) — Published on 31 August 2023
www.geodiversitas.com

PUBLICATIONS SCIENTIFIQUES

MUSÉUM NAL HIST NATURELLE

Geodiversitas est indexé dans / Geodiversitas *is indexed in:*
– Science Citation Index Expanded (SciSearch®)
– ISI Alerting Services®
– Current Contents® / Physical, Chemical, and Earth Sciences®
– Scopus®

Geodiversitas est distribué en version électronique par / Geodiversitas *is distributed electronically by:*
– BioOne® (http://www.bioone.org)

Les articles ainsi que les nouveautés nomenclaturales publiés dans *Geodiversitas* sont référencés par / *Articles and nomenclatural novelties published in* Geodiversitas *are referenced by:*
– ZooBank® (http://zoobank.org)

Geodiversitas est une revue en flux continu publiée par les Publications scientifiques du Muséum, Paris
Geodiversitas *is a fast track journal published by the Museum Science Press, Paris*

Les Publications scientifiques du Muséum publient aussi / *The Museum Science Press also publish:* ***Adansonia***, ***Zoosystema***, ***Anthropozoologica***, ***European Journal of Taxonomy***, ***Naturae***, ***Cryptogamie*** **sous-sections** ***Algologie***, ***Bryologie***, ***Mycologie, Comptes Rendus Palevol***

Diffusion – Publications scientifiques Muséum national d'Histoire naturelle
CP 41 – 57 rue Cuvier F-75231 Paris cedex 05 (France)
Tél. : 33 (0)1 40 79 48 05 / Fax : 33 (0)1 40 79 38 40
diff.pub@mnhn.fr / http://sciencepress.mnhn.fr

ISSN (imprimé / *print*) : 1280-9659/ ISSN (électronique / *electronic*) : 1638-9395

New remains of Neotropical bunodont litopterns and the systematics of Megadolodinae (Mammalia: Litopterna)

Juan D. CARRILLO
Muséum national d'Histoire naturelle, Centre de Recherche en Paléontologie – Paris (CR2P, UMR 7207), CNRS/MNHN/Sorbonne Université, cp 38, 57 rue Cuvier, F-75231 Paris cedex 05 (France)
and Department of Biology, University of Fribourg, and Swiss Institute of Bioinformatics, Chemin du Musée 10, Fribourg (Switzerland)
and Smithsonian Tropical Research Institute, 0843-03092, Balboa (Panama)
juan.carrillo@unifr.ch (corresponding author)

Catalina SUAREZ
Grupo de Paleontología Neotropical Tradicional y Molecular (PaleoNeo), Facultad de Ciencias Naturales, Universidad del Rosario, Bogotá (Colombia)
and Smithsonian Tropical Research Institute, 0843-03092, Balboa (Panama)
Current address: Instituto Argentino de Nivología, Glaciología y Ciencias Ambientales, CCT-CONICET Mendoza, Av. Ruiz Leal s/n, Parque General San Martín, Mendoza, 5500 (Argentina)

Aldo Marcelo BENITES-PALOMINO
Smithsonian Tropical Research Institute, 0843-03092, Balboa (Panama)
and Paläontologisches Institut und Museum, Universität Zurich, Karl-Schmid-Strasse 4, 8006, Zurich (Switzerland)

Andrés VANEGAS
Museo de Historia Natural La Tatacoa, Centro Poblado La Victoria, Villavieja (Colombia)

Andrés LINK
Departamento de Ciencias Biológicas, Universidad de Los Andes, Bogotá (Colombia)

Aldo F. RINCÓN
Universidad del Norte, Km 5 vía Puerto Colombia, Barranquilla (Colombia)

Javier LUQUE
Museum of Zoology, Department of Zoology, University of Cambridge, Downing Street, Cambridge CB2 3EJ (United Kingdom)
and Smithsonian Tropical Research Institute, 0843-03092, Balboa (Panama)
and Museum of Comparative Zoology and Department of Organismic and Evolutionary Biology, Harvard University, 26 Oxford Street, Cambridge, MA, 02138 (United States)

Siobhán B. COOKE
Center for Functional Anatomy and Evolution, Johns Hopkins University School of Medicine, Baltimore MD, 21205 (United States)

Melissa TALLMAN
Department of Biomedical Sciences, Grand Valley State University, Allendale, MI, 49401 (United States)

Guillaume BILLET
Muséum national d'Histoire naturelle, Centre de Recherche en Paléontologie – Paris (CR2P, UMR 7207), CNRS/MNHN/Sorbonne Université, c.p. 38, 57 rue Cuvier, F-75231 Paris cedex 05 (France)

Submitted on 26 July 2022 | accepted on 24 February 2023 | published on 31 August 2023

urn:lsid:zoobank.org:pub:B826F25C-33D7-4AEF-9FF8-8B1CBAC28823

Carrillo J. D., Suarez C., Benites-Palomino A. M., Vanegas A., Link A., Rincón A. F., Luque J., Cooke S. B., Tallman M. & Billet G. 2023. — New remains of Neotropical bunodont litopterns and the systematics of Megadolodinae (Mammalia: Litopterna), *in* Carrillo J. D. (ed.), Neotropical palaeontology: the Miocene La Venta biome. *Geodiversitas* 45 (15): 409-447. https://doi.org/10.5252/geodiversitas2023v45a15. http://geodiversitas.com/45/15

ABSTRACT
Litopterna is one the most diverse and long–lived clades of South American native ungulates. *Megadolodus* and *Neodolodus* are bunodont litoptern genera recorded in the middle Miocene tropical faunistic assemblage of La Venta (Colombia). Both taxa were initially identified as didolodontid 'condylarths', but later reclassified into Proterotheriidae, within Litopterna. Previous studies proposed their inclusion within Proterotheriidae, but possible affinities with early litopterns and didolodontids have not been properly tested in phylogenetic analyses. We report new material of *Megadolodus* and *Neodolodus* from La Venta, which document new aspects of their upper and lower dentition, and we reassess their phylogenetic relationships with Litopterna and Didolodontidae. Using pre-existing matrices, we tested two alternative approaches of character construction for serial characters on the dentition in our phylogenetic analyses. Based on previously known and new fossil material, our analyses with both coding approaches support a close relationship between *Megadolodus* and *Neodolodus*, within Litopterna, and do not support a close relationship with Didolodontidae. At a less inclusive level, the relationships of Megadolodinae within Litopterna vary depending on the coding approach used. However, all of our analyses unambiguously support the monophyly of Megadolodinae as a clade of Neotropical bunodont litopterns. While the discovery of these new remains enlightens part of the litoptern phylogeny, the sensitivity of our analyses to coding approaches further highlights the importance of critical evaluation of character construction in morphological phylogenetics.

KEY WORDS
La Venta,
Litopterna,
Miocene,
South America.

RÉSUMÉ
Nouveaux restes de litopternes bunodontes néotropicaux et la systématique des Megadolodinae (Mammalia: Litopterna).
Les Litopterna constituent l'un des clades les plus diversifiés des ongulés natifs d'Amérique du Sud. *Megadolodus* et *Neodolodus* sont deux genres de litopternes bunodontes connus dans la faune tropicale du Miocène moyen de La Venta (Colombie). Les deux taxons ont été initialement identifiés comme des condylarthres didolodontidés, puis transférés parmi les Proterotheriidae, au sein des Litopterna. Cependant, leurs affinités possibles avec les plus anciens litopternes et didolodontidés n'ont jamais été testées dans les analyses phylogénétiques. Dans ce travail, nous rapportons du nouveau matériel attribué à *Megadolodus* et *Neodolodus* et réévaluons leurs relations phylogénétiques avec les Litopterna et les Didolodontidae. Dans nos analyses phylogénétiques, nous avons testé deux approches alternatives de construction de caractères pour les caractères sériels sur la dentition, en se fondant sur des matrices pré-existantes. Sur la base du matériel déjà connu et du nouveau matériel fossile, nos analyses avec l'une ou l'autre approche de codage soutiennent une relation étroite entre *Megadolodus* et *Neodolodus*, au sein des Litopterna, mais pas de relation étroite avec les Didolodontidae. À un niveau moins inclusif, les relations des Megadolodinae au sein des Litopterna varient selon l'approche de codage utilisée. Cependant, toutes nos analyses soutiennent sans ambiguïté la monophylie des Megadolodinae comme un clade de litopternes néotropicaux bunodontes. Si la découverte de ces nouveaux restes éclaire une partie de la phylogénie des litopternes, la sensibilité de nos analyses aux approches de codage souligne l'importance de l'évaluation critique de la construction des caractères morphologiques en amont des reconstructions phylogénétiques.

MOTS CLÉS
La Venta,
Litopterna,
Miocène,
Amérique du Sud.

RESUMEN
Nuevos restos de litopternos bunodontes neotropicales y la sistemática de Megadolodinae (Mammalia: Litopterna).
Litopterna es uno de los clados más diversos de ungulados nativos sudamericanos. *Megadolodus* y *Neodolodus* son géneros de litopternos bunodontes registrados en la fauna tropical de La Venta (Mioceno medio, Colombia). Ambos taxones fueron inicialmente identificados como didolodóntidos 'condilártos', pero posteriormente fueron reclasificados como Proterotheriidae, dentro de Litopterna. Estudios anteriores propusieron su inclusión dentro de Proterotheriidae, pero las posibles afinidades con litopternos basales y didolodóntidos no han sido debidamente evaluada a través de análisis filogenéticos. En este trabajo presentamos nuevo material de *Megadolodus* y *Neodolodus* y reevaluamos sus relaciones filogenéticas con Litopterna y Didolodontidae. En nuestros análisis filogenéticos, utilizamos dos enfoques alternativos de construcción de caracteres para el caso de caracteres seriados de la dentición. Basándonos en material anteriormente conocido y el nuevo material fósil, nuestros análisis con uno u otro enfoque de codificación apoyan una relación estrecha entre *Megadolodus* y *Neodolodus*, dentro de Litopterna, y no una relación

PALABRAS CLAVE
La Venta,
Litopterna,
Mioceno,
South America.

con Didolodontidae. A un nivel menos inclusivo, las relaciones de Megadolodinae dentro de Litopterna varían dependiendo del enfoque de codificación utilizado. Sin embargo, todos nuestros análisis apoyan inequívocamente la monofilia de Megadolodinae como un clado de litopternos Neotropicales bunodontes. Aunque el descubrimiento de estos nuevos restos aclara parte de la filogenia de los litopternos, la sensibilidad de nuestros análisis a los enfoques de codificación muestra la importancia de una evaluación crítica en la construcción de caracteres utilizados en filogenética morfológica.

INTRODUCTION

South American native ungulates (SANUs) represent an assemblage of hoofed placental mammals that radiated in South America (see Croft *et al.* 2020 and references therein) while this continent was isolated from other landmasses throughout most of the Cenozoic (Simpson 1980; Croft 2016; Defler 2019). Whether the SANUs, formerly classified into Meridiungulata (McKenna 1975; McKenna & Bell 1997), constitute a monophyletic group or not and what are their interrelationships remain unresolved fundamental questions in palaeomammalogy (Kramarz & MacPhee 2022).

Litopterna and Notoungulata were the most taxonomically diverse and long-lived SANU clades, with a fossil record extending until the late Pleistocene (Croft *et al.* 2020 and references therein). Data from alpha 1 and 2 collagen chains from Pleistocene representatives of Litopterna (*Macrauchenia* Owen, 1838) and Notoungulata (*Toxodon* Owen, 1837a) supports a close relationship between these two clades and extant Perissodactyla (Buckley 2015; Welker *et al.* 2015). Mitochondrial DNA data from *Macrauchenia* further supports that litopterns are closer to perissodactyls among extant mammals (Westbury *et al.* 2017). Although molecular data enabled major progress in understanding their position among placentals, the relationships of Litopterna with other extinct ungulate-like placentals are not fully resolved. Dental morphology supports a close relationship between Litopterna, two groups of early South American 'condylarths' (Kollpaniinae and Didolodontidae), and the North American Mioclaenidae (Muizon & Cifelli 2000; Gelfo 2004, 2007, 2010; but see Williamson & Carr 2007). The auditory and inner ear morphology does not unequivocally support nor contradict the affinities of Litopterna with North American 'condylarths' (e.g., Phenacodontidae, Billet *et al.* 2015; Kramarz *et al.* 2017). Phylogenetic analyses based on different morphological partitions (cranial, dental and postcranial) and using a molecular constraint have suggested a close relationship of litopterns and other SANUs with North American 'condylarths' (Muizon *et al.* 2015; Kramarz *et al.* 2017), of Notoungulata and Litopterna with 'condylarths' and Euungulata (i.e., Perissodactyl and Artiodactyla) (Carrillo & Asher 2017), or of Litopterna with some 'condylarths' and Euungulata to the exclusion of other SANU clades (O'Leary *et al.* 2013), which conflicts with the close relationship between Litopterna and Notoungulata supported by molecular evidence (Buckley 2015; Welker *et al.* 2015).

Litopterna includes nine families and 67 genera with records from the Paleocene (Peligran South American land mammal age [SALMA]; *c.* 63 Ma) to the late Pleistocene-Holocene (Lujanian SALMA; 0.13-0.01 Ma) (Bonaparte & Morales 1997; Ubilla *et al.* 2011; Croft *et al.* 2020). Within Litopterna, Proterotheriidae and Macrauchenidae are the two most diverse sub-clades (Soria 2001; Villafañe *et al.* 2006; Schmidt & Ferrero 2014; Forasiepi *et al.* 2016; McGrath *et al.* 2018, 2020a). Proterotheriidae includes small-to-medium-sized cursorial taxa, characterized by a brachydont dentition. The clade shows a trend towards functional monodactyly, with the enlargement of digit III, the reduction of digits II and IV, and loss of digits I and V (Soria 2001; McGrath *et al.* 2020a; Croft & López 2020). Proterotheriidae (McGrath *et al.* 2020b) ranges from the Eocene (Itaboraian SALMA; *c.* 53 Ma) to late Pleistocene (Lujanian SALMA) (Cifelli 1983; Soria 2001; Villafañe *et al.* 2006; Ubilla *et al.* 2011; McGrath *et al.* 2020a), and it includes *c.* 26 genera widely distributed across the continent (Croft *et al.* 2020). Proterotheriid diversity peaked in the Miocene and gradually decreased until the demise of the group in the Pleistocene (Villafañe *et al.* 2006; McGrath *et al.* 2020a, and references therein).

Phylogenetic analyses identified *Megadolodus molariformis* as the earliest-diverging proterotheriid (McGrath *et al.* 2020a, 2020b). *Megadolodus* is only known from the middle Miocene (Laventan SALMA; *c.* 11.8-13.5 Ma) assemblage of La Venta, Colombia (Kay *et al.* 1997). It was first described from a partial mandible with p4 and m1, and identified as a didolodontid 'condylarth' based on its bunodont dentition (McKenna 1956). However, additional craniodental and postcranial material supported the identification of *Megadolodus* as a proterotheriid, principally based on its tarsal and pedal morphology. Cifelli & Villarroel (1997) referred *Megadolodus* to its own subclade (Megadolodinae), within Proterotheriidae. Megadolodinae includes *Megadolodus molariformis* and *Bounodus enigmaticus* (Carlini *et al.* 2006). The latter was collected in the late Miocene sediments of the Urumaco Formation in northwestern Venezuela, and it is known from a poorly preserved maxillary fragment (Carlini *et al.* 2006; Bond & Gelfo 2010). The peculiar morphology and distribution of Megadolodinae suggests that it represents a tropical lineage within Protherotheriidae (Carlini *et al.* 2006; McGrath *et al.* 2020b).

Neodolodus colombianus is another litoptern recorded in La Venta that was initially described on the basis of a partial mandible and identified as a didolodontid 'condylarth'

(Hoffstetter & Soria 1986). However, additional dental and postcranial material supported the inclusion of *Neodolodus* within Proterotheriidae (Cifelli & Guerrero Díaz 1989). *Neodolodus* cf. *colombianus* is also recorded in the middle Miocene sediments of the Castilletes Formation (*c.* 14.2-16.7 Ma) in northern Colombia (Carrillo *et al.* 2018). *N. colombianus* was first transferred to *Prothoatherium* (Cifelli & Guerrero Díaz 1989), and then to *Lambdaconus* (Carrillo *et al.* 2018). Recent phylogenetic analyses supported the recognition of *Neodolodus* as a distinct genus, being closely related with *Protheosodon* within Proterotheriidae (McGrath *et al.* 2020a, 2020b). Despite some resemblance to *Megadolodus*, like its similar bunodonty, *Neodolodus* has never been included in Megadolodinae.

The Miocene assemblage of La Venta (Laventan SALMA) in Colombia is one of the best known extinct mammalian assemblages in tropical South America (Kay *et al.* 1997; Defler 2019). Paleoecological evidence indicates that La Venta assemblage inhabited a tropical forested environment, with an estimated annual rainfall of 1800-2500 mm and average temperatures > 25°C (Kay *et al.* 1997; Kay & Madden 1997; Croft 2001; Spradley *et al.* 2019). The mammalian assemblage includes a high diversity of litopterns, with one macraucheniid taxon and five proterotheriid taxa (Table 1). Among the litopterns from La Venta, *Megadolodus* and *Neodolodus* are perhaps the most enigmatic, and they are important to elucidate the evolution and biogeography of Proterotheriidae (Cifelli & Villarroel 1997; McGrath *et al.* 2020b). Here, we report new material of *Megadolodus* and *Neodolodus,* and we reassess their phylogenetic position in Proterotheriidae and Litopterna.

GEOLOGICAL SETTING

The specimens described in this work come from La Victoria and Villavieja Formations that crop out in the Upper Magdalena valley, Colombia (Fig. 1) in an area locally known as La Tatacoa Desert but commonly known in scientific literature as "La Venta" (Kay *et al.* 1997). The Villavieja Formation, which lies stratigraphically above the La Victoria Formation, has traditionally been known for containing the richest fossiliferous levels, especially in its lower part (Guerrero 1997). Consequently, historically the collecting efforts have been concentrated in this upper formation. Recent field work has, however, focused on the exploration of the older La Victoria Formation, thereby considerably increasing the number of fossils collected from this unit. This is the case of three of the four new specimens reported here (VPPLT 183, 974, 1588 and 1696), which were collected from mudstone levels close to the top (bed set below Cerbatana Conglomerate; Mora-Rojas *et al.* 2023) and bottom (bed set below Cerro Gordo; Mora-Rojas *et al.* 2023) of the La Victoria Formation. The fourth specimen comes from one of the most fossiliferous layers of the Villavieja Formation, the Monkey Beds (Mora-Rojas *et al.* 2023) (Fig. 1; Table 2).

The fossiliferous sediments of the Honda Group (the sedimentary unit that comprise the La Victoria and the Villavieja formations) span from *c.* 10.5 Ma to 16 Ma (Flynn *et al.* 1997; Montes *et al.* 2021; Mora-Rojas *et al.* 2023), with most of the sediment accumulation occurring between *c.* 11.8 and *c.* 13.8 Ma (Laventan SALMA; Madden *et al.* 1997; Mora-Rojas *et al.* 2023). The probabilistic age model of Mora-Rojas *et al.* (2023) estimate an age of *c.* 13.1 Ma for the upper levels of the bed set below Cerro Gordo, an age of *c.* 12.3 Ma for the bed set below Cerbatana Conglomerate, and an age of *c.* 12.0 Ma for the Monkey beds.

MATERIAL AND METHODS

The specimens described here were collected during different palaeontological expeditions in 2019 in partnership with a group of leaders of the local community (Vigías del Patrimonio Paleontológico La Tatacoa). They are housed in the Museo de Historia Natural La Tatacoa, in La Victoria (Villavieja, Huila, Colombia).

For metric comparisons, we took linear measurements of the dentition with a caliper to the nearest 0.1 mm. We follow Smith & Dodson (2003) for the orientation of the dentition, where the four cardinal directions are mesial, distal, lingual and labial. Dental terminology follows Soria (2001) and Muizon & Cifelli (2000). Three-dimensional surface models of the skull of the new described specimens of *Neodolodus colombianus* (VPPLT 1696) and *Megadolodus molariformis* (VPPLT 974) are available in MorphoMuseum (Carrillo *et al.* 2022). The surface scan of *N. colombianus* (VPPLT 1696) was made with a 3D structural light scanner HP Pro S3 with a resolution of 0.05 mm. The specimen of *M. molariformis* (VPPLT 974) was CT scanned using high resolution microtomography (CT) at the Montpellier Rio Imaging (MRI: Microtomograph RX EasyTom 150, X-ray source 40-150 kV) platform. Voxel size was 0.063 mm. Three-dimensional reconstruction of selected teeth of VPPLT 974 and visualization of 3D models were done using a stack of digital CT images with AVIZO v.9.7.0 software (Visualization Sciences Group, Burlington, MA, United States), and Biomedisa (Lösel *et al.* 2020). The scan is available in MorphoSource (https://www.morphosource.org/).

FIG. 1. — Geographical and stratigraphic occurrence of the new specimens of *Megadolodus molariformis* McKenna, 1956 and *Neodolodus colombianus* Hoffstetter & Soria, 1986: **A**, map of northern South America showing the location where other Neotropical bunodont litopterns have been found including La Venta (that records *Megadolodus* McKenna, 1956 and *Neodolodus* Hoffstetter & Soria, 1986), the Cocinetas basin (that records *Neodolodus*) and Urumaco (that records *Bounodus enigmaticus* (Carlini, Gelfo & Sánchez, 2006); **B**, geologic map of La Venta area (modified from Montes *et al.* 2021) showing the localities where the new specimens of *Megadolodus* and *Neodolodus* where found. The colors in the map correspond to the cartographic units shown in the stratigraphic scheme; **C**, stratigraphic scheme of the Honda Group (modified from Benites-Palomino *et al.* 2020) showing the cartographic units of Montes *et al.* (2021), the stratigraphic levels (**StL**) of (Mora-Rojas *et al.* 2023), and the stratigraphic position of the new *Megadolodus* and *Neodolodus* specimens. Bed abbreviations: **StL 1**, Bed set be-

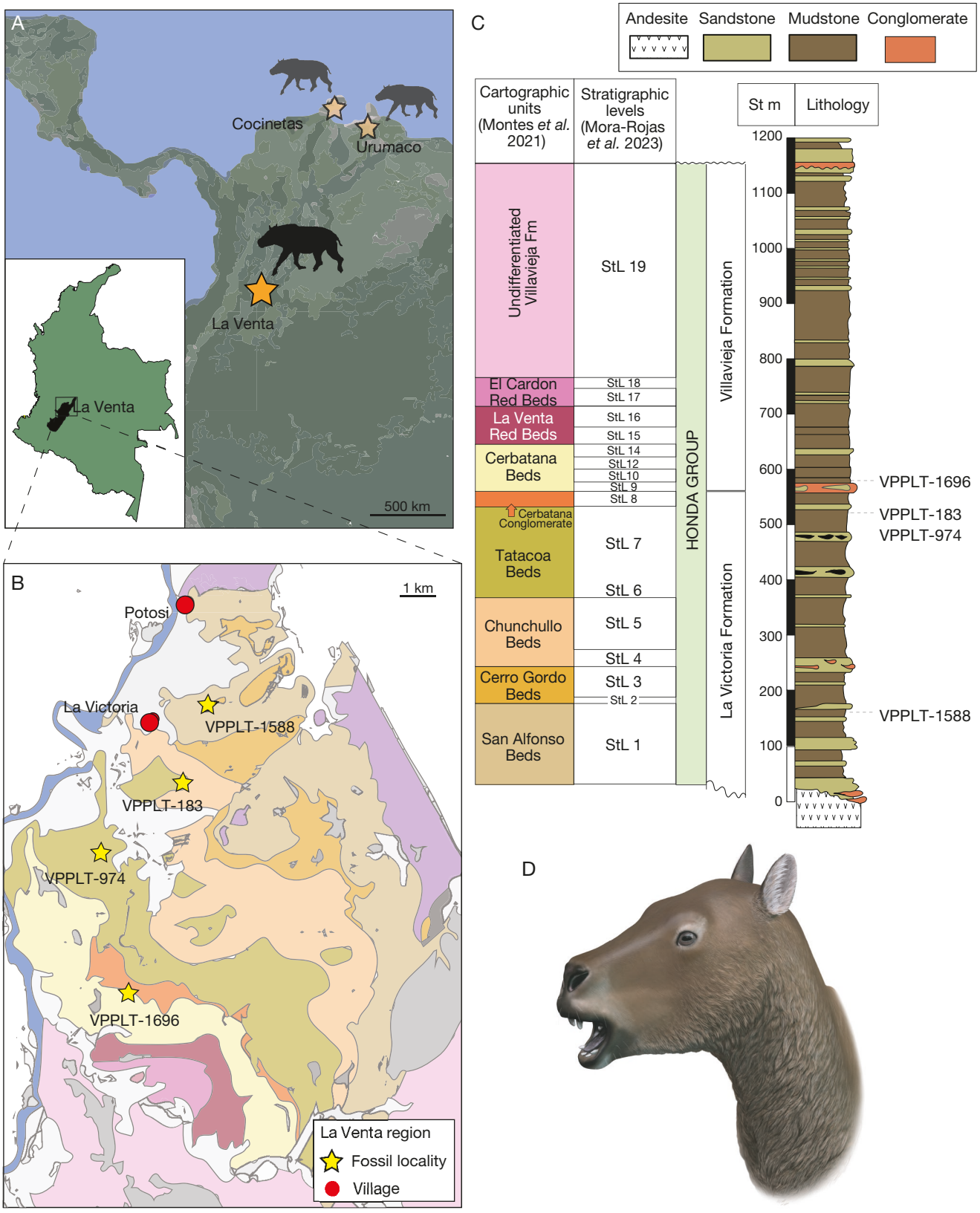

low Cerro Gordo; **StL 2**, Cerro Gordo sandstone; **StL 3**, between Cerro Gordo and Chunchullo; **StL 4**, Chunchullo sandstone; **StL 5**, bed set between Chunchullo and Tatacoa; **StL 6**, Tatacoa sandstone; **StL 7**, bed set below Cerbatana conglomerate; **StL 8**, Cerbatana conglomerate; **StL 9**, Monkey beds; **StL 10**, bed set above Monkey beds; **StL 12**, bed set above Fish bed; **StL 14**, bed set below La Venta red beds; **StL 15**, La Venta red beds; **StL 16**, bed set between La Venta red beds and El Cardón red beds; **StL 17**, El Cardón red beds; **StL 18**, San Francisco sandstone; **StL 19**, Polonia red beds; **D**, reconstruction of the head of *Neodolodus colombianus* based on the 3D model of the almost complete skull of the specimen VPPLT 1696. Abbreviations: **Fm**, Formation; **St m**, Stratigraphic meter. Reconstruction of *N. colombianus* made by Tatsuya Shimura.

TABLE 1. — Litopterna from La Venta faunal assemblage, Colombia.

Clade	Taxon	References
Proterotheriidae	*Megadolodus molariformis* McKenna, 1956	McKenna (1956); Cifelli & Villarroel (1997);
	Neodolodus colombianus Hoffstetter & Soria, 1986	Hoffstetter & Soria (1986); Cifelli & Guerrero Díaz (1989); Cifelli & Guerrero (1997); McGrath *et al.* (2020a)
	Mesolicaphrium sanalfonense	Cifelli & Guerrero (1997); McGrath *et al.* (2020a)
	Villarroelia totoyoi	Cifelli & Guerrero (1997)
	Proterotheriidae gen. et sp. indet	Cifelli & Guerrero (1997)
Macraucheniidae	*Theosodon* sp.	Cifelli & Guerrero (1997)

ABBREVIATIONS

Institutional abbreviations

FMNH	Field Museum of Natural History, Chicago;
MACN	Museo Argentino de Ciencias Naturales, Buenos Aires;
MLP	Museo de La Plata, La Plata;
MNHN	Muséum national d'Histoire naturelle, Paris;
UCMP	University of California Museum of Paleontology, Berkeley;
VPPLT	Vigías del Patrimonio Paleontológico, Museo de Historia Natural La Tatacoa, Villavieja;
YPM	Yale Peabody Museum, New Haven.

Teeth

C, c	upper canine, lower canine;
I, i	upper incisor, lower incisor;
P, p	upper premolar, lower premolar;
M, m	upper molar, lower molar;
dP, dp	deciduous upper premolar, deciduous lower premolar.

PHYLOGENETIC ANALYSES

TAXONOMIC SAMPLING

To test for the relationships of *Megadolodus molariformis* and *Neodolodus colombianus* within Litopterna and Didolotontidae, we performed phylogenetic analyses using data matrices published in previous studies (Cifelli 1993; Muizon & Cifelli 2000; Schmidt 2015; McGrath *et al.* 2020b). The taxonomic sampling (Appendix 1) reflects this aim. We did not include *Bounodus*, which is also referred to Megadolodinae (Carlini *et al.* 2006), due to the fragmentary nature and poor preservation of the known material.

As our goal was not to solve intra-generic relationships within derived proterotheriids, we included in our analyses only the best-documented species (anatomically complete) for some derived proterotheriid genera (e.g., *Tetramerorhinus*). Kollpaniinae were chosen as outgroups, represented by *Simoclaenus sylvaticus* and *Tiuclaenus* spp. (Muizon & Cifelli 2000; Muizon *et al.* 2019). We also included all the litoptern species from La Venta (Table 1), for which we used the new material described here and deposited in the collections of the VPPLT, as well as previous descriptions (McKenna 1956; Hoffstetter & Soria 1986; Cifelli & Guerrero Díaz 1989; Cifelli & Guerrero 1997; Cifelli & Villarroel 1997; McGrath *et al.* 2020a, 2020b). Finally, we included several early litopterns and didolodontids; their scoring was based on published descriptions (Simpson 1948; Simpson & Minoprio 1949; Paula Couto 1952; Bond & Vucetich 1983; Cifelli 1983; Cifelli & Soria 1983; Soria 2001; Dozo & Vera 2010; Zanesco *et al.* 2019), and observation of the specimens themselves, and casts of specimens in the collections of the MNHN. In total, 44 taxa were included in our phylogenetic analyses. Appendix 1 provides the list of taxa and the material available to us (original specimen, casts, photos, and references).

CHARACTER SAMPLING AND SCORING

Our character list is based on Cifelli (1993), Muizon & Cifelli (2000), Schmidt (2015), and McGrath *et al.* (2020b). Some characters were excluded, and others were modified; the justification for these modifications is provided in the character lists (Appendices 2; 3). For *Megadolodus, Neodolodus* and *Villarroelia*, the scoring of some characters was modified according to the new material described in this work and to new specimens deposited in the VPPLT collection. Character scoring of *Protolipterna ellipsodontoides* was modified when pertinent following a recent redescription of the species (Zanesco *et al.* 2019). For the remaining taxa, if a character score differs from the original character matrices, this is indicated and justified in the character lists (Appendices 2; 3). Scoring of the modified characters and new taxa was undertaken by JDC and GB.

The character list made from these previous studies contains a wealth of characters repeated at successive dental loci. A recent study has demonstrated that such characters on serial variations may not be independent from each other and may thereby mislead phylogenetic analyses (Billet & Bardin 2019). To test the effects of alternative approaches of character construction on this issue within litopterns, we produced two matrices, an "extended matrix" with five continuous and 109 discrete characters (Appendix 2) and a "reduced matrix" with five continuous and 91 discrete characters (Appendix 3). The extended matrix favours the reductive coding approach, which assumes that the observed morphological variations (the characters) are independent and thus scores characters separately (Wilkinson 1995; Billet & Bardin 2019). The reduced matrix uses the composite coding approach, which favours the construction of a single composite character when the observed variation is hypothesized to be biologically non-independent (Wilkinson 1995; Billet & Bardin 2019). Composite coding with constrained paths for transitions among character states might be a more appropriate approach to score variation in serially homologous structures (e.g., premolars and molars) (Billet & Bardin 2019). For example, in the extended matrix, the absence or presence of the metaconule is scored independently for the P3 and P4 (characters 28 and 29 in Appendix 2), whereas in the reduced matrix, it is scored in

TABLE 2. — Stratigraphic and locality information of the specimens described in this work.

Species	Specimen	Locality	Formation	Stratigraphic level	GPS
Megadolodus molariformis McKenna, 1956	VPPLT 974	Las Gaviotas 1	La Victoria	Below the Cerbatana conglomerate	3°18'41"N, 75°12'27"W
	VPPLT 1588	Cerro Pan de Azúcar	La Victoria	Below Cerro Gordo	3°21'26"N, 75°10'33"W
Neodolodus colombianus Hoffstetter & Soria, 1986	VPPLT 183	Kilómetro 121	La Victoria	Below the Cerbatana conglomerate	3°19'29"N, 75°10'55"W
	VPPLT 1696	Piedra Gorda, San Nicolás	Villavieja	Monkey beds	3°16'45"N, 75°11'46"W

a single composite character for the two premolars (character 18 in Appendix 3).

We acknowledge that in some cases, our approach to construct the reduced matrix might represent an oversimplified solution to the problem of character correlations. For example, when merging characters scored separately in the extended matrix, some trait combinations were not observed in our taxonomic sampling and therefore are not represented in the character states. However, future studies with a larger taxonomic sampling may find that these trait combinations exist and may need to revise the number and definition of the character states proposed here and set another geometry for authorized transitions. In the present case, the alternative coding strategies were explored in order to address the potential effects of these strategies on the phylogenies recovered for litopterns. A more satisfactory treatment of character correlations would undoubtedly deserve a more thorough revision of the data matrices, more complex character construction and extensive testing (Billet & Bardin 2019).

Phylogenetic analyses

The extended and reduced matrices were constructed in MorphoBank and analysed using TNT 1.5 (Goloboff & Catalano 2016) with maximum parsimony. The extended matrix (Appendix 2; Morphobank Project 3399) included 44 taxa and 114 characters (five continuous and 107 discrete), among which five multistate discrete characters were ordered. Simulations and empirical data suggest that parsimony analyses with ordered characters perform better when using characters that form morphoclines (Grand *et al.* 2013). The reduced matrix (Appendix 3; Morphobank Project 3401) included 44 taxa and 96 characters (five continuous and 91 discrete); four multistate discrete characters were ordered. We used equally weighted characters, treated gaps as missing, and treated taxa with multiple states as polymorphic. Searches used 500 replicates of random addition sequences holding 20 trees per replication, using tree bisection reconnection (TBR) for branch swapping. For the reduced matrix, we used step matrices (Appendix 4) to set the costs and constrain the paths for transitions among character states for five characters (characters 12, 13, 48, 53 and 60 in Appendix 3) that were scored using a composite coding approach. The step matrices were constructed in such a way that they allowed simultaneous changes on all teeth being included in the composite character, but also allowed changes along an anteroposterior gradient among these teeth (see Billet & Bardin 2019). Additional explanations on the construction of step matrices are given in Appendix 3. To obtain the list of unambiguous synapomorphies common to all the most parsimonious trees, we use the "apo -[" command in TNT (Goloboff *et al.* 2008). Annotated TNT files with the character matrices and the commands used in all analyses are available in Morphobank (Projects 3399 and 3401).

In addition, in order to evaluate the phylogenetic relationships of *Megadolodus* and *Neodolodus* and jointly estimate possible divergence dates for Megadolodinae, we conducted a Bayesian time-calibrated phylogenetic analysis on the discrete characters of the reduced matrix using BEAST 2 (version 2.6.7; Bouckaert *et al.* 2019). The stratigraphic ranges of the taxa were compiled from the literature. The age ranges and corresponding references are in Appendix 5. For time calibration, we used the oldest (maximum age within the age range) of each taxon. We used the Fossilized Birth-Death (FBD) model (Stadler 2010; Heath *et al.* 2014) that models diversification and fossil sampling. The FBD model estimates phylogenetic relationships and divergence times within a single framework.

We analysed the matrix with the Lewis Mk model (Lewis 2001), which is a widely-used model for morphological data in Bayesian analytical software, although it most certainly needs to be improved to better model morphological evolution (Goloboff *et al.* 2019). For the Bayesian analysis we used the composite character coding (reduced matrix) allowing for all possible character transitions (MUL model of Billet & Bardin 2019), because it has been shown that it performs better than independent scoring of characters (reductive coding) on successive teeth of a same class (IND model of Billet & Bardin 2019). We used 10 000 000 iterations, sampling every 5000 iterations. We used four chains (three heated one cold) with a delta temperature of 0.03 and the coupled Markov chain Monte Carlo (MCMC) algorithm (Müller & Bouckaert 2019). We used Tracer (version 1.7.1; Rambaut *et al.* 2018) for the visualization and diagnostics of the MCMC output. When summarizing the results, we discarded the first 10% of the samples as burn-in. For all the analyses tree annotation was done using the R packages Phytools (Revell 2012), Ggtree (Yu *et al.* 2017), and Deeptime (Gearty 2022).

SYSTEMATIC PALAEONTOLOGY

MAMMALIA Linnaeus, 1758
PLACENTALIA Owen, 1837b
LITOPTERNA Ameghino, 1889
Family PROTEROTHERIIDAE Ameghino, 1887

Subfamily MEGADOLODINAE Cifelli & Villarroel, 1997

EMENDED DIAGNOSIS. — Bunodont litopterns with two lower incisors, the distal (lateral) being significantly larger (tusk-like) than the mesial (central). Metaconid absent on p2. Metaconule of P4 isolated. Mesostyle absent on P3-4 but present on M1-3. Strong paracone and metacone folds on upper molars. M3 with well-developed hypocone. Megadolodinae is supported by the following synapomorphies: bunodont cheek teeth; small parastyle on P3-4; and m1-3 without paralophid.

Genus *Megadolodus* McKenna, 1956

EMENDED DIAGNOSIS. — The dental formula is I ?/2 C ?/1 P 4/4 M 3/3. Large, brachydont and bunodont megadolodine litoptern. Robust mandible. It differs from non-megadolodine proterotheriids in having the following combination of characters: The distal-most lower incisor is tusk-like, and the lower canine is small. Paraconid absent on p3-m3. The p3-4 are molariform and lack a hypoconulid. P3-4 without hypocone and with paraconule and metaconule. Upper molars with hypocone. M2 larger than the M1 and M3. Limbs more robust and with shorter distal elements in comparison with other proterotheriids for which the skeleton is known (Cifelli & Villarroel 1997). *Megadolodus* differs from *Neodolodus* in its larger size, the position of the posterior-most point of symphysis at the level of p3, and the hypoconid of the p4 located directly distal to the protoconid. It differs from *Bounodus* in having a proportionally larger P4 and M1, the latter and having an a quadrangular outline (not elongated mesiodistally) (Carlini *et al.* 2006).

Megadolodus molariformis McKenna, 1956
(Figs 1-4)

HOLOTYPE. — UCMP 39270, partial left mandible bearing the labial portion of the crown of p4, the m1, and the alveoli of p3 and m2 (Fig. 3B).

NEW REFERRED MATERIAL. — VPPLT 974, partial mandible with the symphysis and left body, bearing the alveoli of ?i2, right and left ?i3, alveolus of right c and p1, roots of left p1, and the left p2-m3 (Fig. 3A, C-E). VPPLT 1588, isolated left P1 and P2, right P3/P4, left P3/P4, and partial left maxilla with M1, M2 and lingual part of M3 (Fig. 2).

TYPE LOCALITY AND HORIZONS. — La Victoria Formation. VPPLT 974 comes from Las Gaviotas 1 (3°18'41"N, 75°12'27"W) in the bed set below the Cerbatana conglomerate (StL 7; Mora-Rojas *et al.* 2023) and VPPLT 1588 comes from Cerro Pan de Azúcar (3°21'26"N, 75°10'33"W) in the bed set below Cerro Gordo (StL1; Mora-Rojas *et al.* 2023) (Fig. 1).

DIAGNOSIS. — Same as for the genus due to monotypy.

REMARKS

The upper and lower incisors, canines and most rostral premolars were only partially preserved in known specimens of *Megadolodus molariformis*. Previously known craniodental material included partial mandibles that preserved dp3-4, p1-p3, fragmentary p4, m1-m3. Fragments of maxilla and isolated upper teeth included the dP3-4, P2-M2 and fragmentary M3 (Table 3; Cifelli & Villarroel 1997). The known postcranial elements include an almost complete vertebral column, ribs, fragments of the humerus, radius and ulna, most of the manus, pelvis and almost all the elements of the hind limbs (Cifelli & Villarroel 1997).

Fragments of the rostral upper and lower dentition have been previously identified, but given that these were isolated and fragmentary elements there has been uncertainty regarding the number and morphology of the upper and lower incisors, canines and most rostral premolars (p1-2 and P1-2) (Cifelli & Villarroel 1997). VPPLT 974 provides new evidence that clarifies for the first time the number of lower incisors and shows that the lower tusks are incisors (Fig. 3A, C), not lower canines as previously hypothesized (Cifelli & Villarroel 1997). The dental formula of Proterotheriidae is characterized by having one upper incisor, which is enlarged and developed into a tusk, and two lower incisors, the most mesial one is small and the most distal one is tusk-like (Scott 1910; Soria 2001). The homology of the upper and the two lower incisors is uncertain since it has not been established which loci were lost (Soria 2001). Scott (1910) hypothesized that the upper tusk corresponded to I2, whereas the mesial-most lower incisor was the i2 and the distal one was the i3, as in toxodontid notoungulates. Although we acknowledge the uncertainty in the homology on the upper and lower incisors, we follow Scott (1910) and tentatively identify the upper incisor as ?I2, and the two lower incisors as ?i2 and ?i3.

DESCRIPTION

VPPLT 1588 and VPPLT 974 have large bunodont dentitions (Table 4) with thick enamel characteristic of *Megadolodus* (McKenna 1956; Cifelli & Villarroel 1997). In addition, VPPLT 1588 is referred to *Megadolodus* based on the partly molariform P3/P4 (with a triangular arrangement of the metacone with the protocone, paracone, the presence of paraconule and metaconule, but without a hypocone; Fig. 2C, E), and the presence of a hypocone in the upper molars (Fig. 2D, F) (Cifelli & Villarroel 1997). The referral of VPPLT 974 to *Megadolodus* is further supported by the robust mandible, the p4 fully molariform, and the absence of paraconid in p3-m3 (Fig. 3A, D) (McKenna 1956; Cifelli & Villarroel 1997).

VPPLT 1588 preserves two isolated teeth, here interpreted as left P1 (Fig. 2A) and P2 (Fig. 2B), because the crowns are not molariform, as is the case in P3 and P4 (Cifelli & Villarroel 1997). The crown of the putative P1 is simple and it has a single cusp with crests extending mesially and distally. It is triangular in labial view, with some wear on the lingual side (Fig. 2A). P2 is similar to P1, but with a more extended lingual edge. The crown of the putative P2 is also triangular in labial view, as it has one main cusp on the labial side of the crown with crests extending mesially and distally from it and an extended lingual edge. The latter is composed of a basin lingual to the main cusp and exhibits a low cusp on its lingual aspect, which resembles an incipiently developed

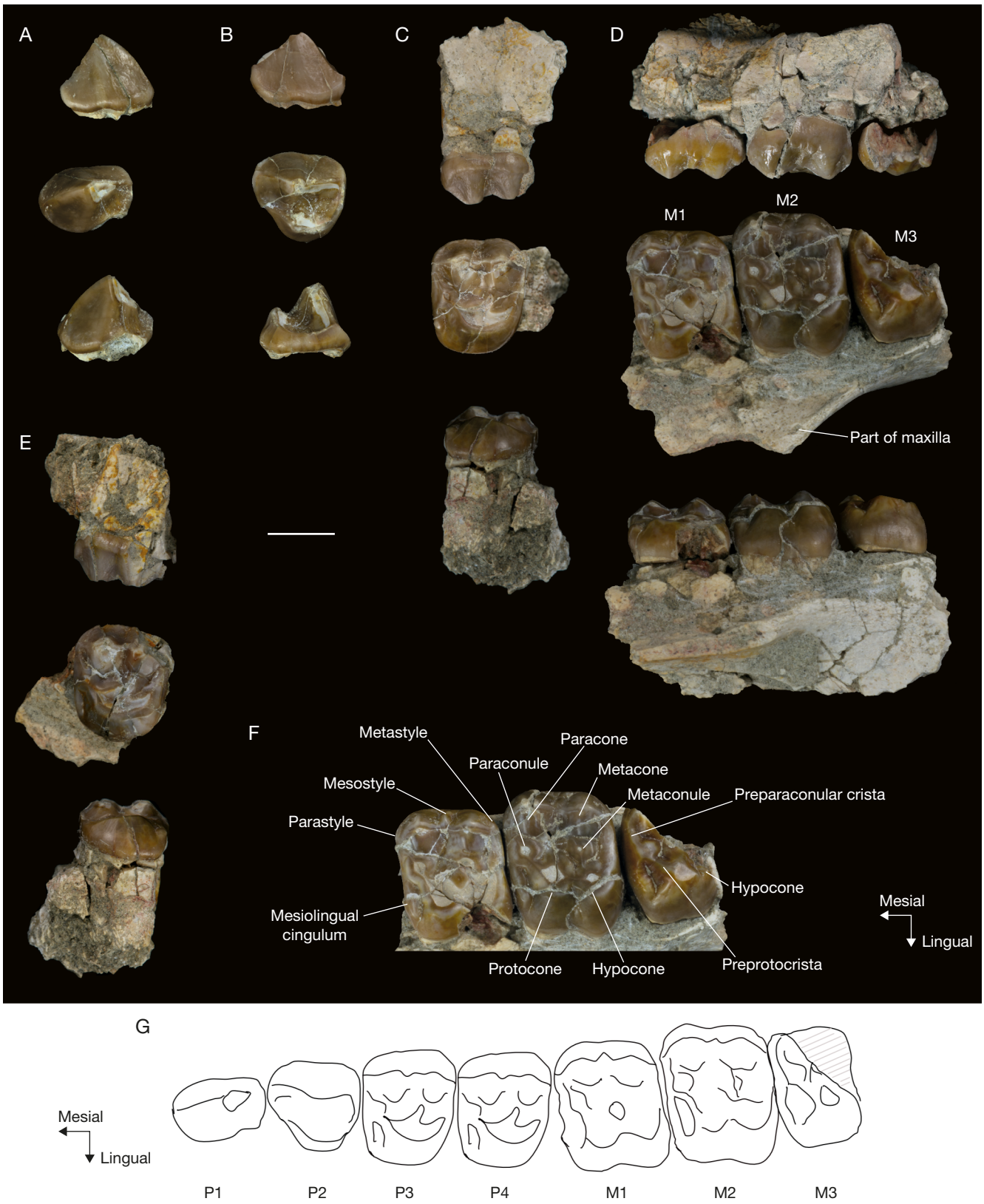

Fig. 2. — Upper dentition of *Megadolodus molariformis* McKenna, 1956 (VPPLT 1588): **A**, left P1 in labial (top), occlusal (middle) and distal (bottom) views; **B**, left P2 in labial (**top**), occlusal (**middle**) and distal (**bottom**) views; **C**, left P3 or P4 in labial (**top**), occlusal (**middle**) and lingual (**bottom**) views; **D**, fragment of left maxilla with M1-3 in labial (**top**), occlusal (**middle**) and lingual (**bottom**) views; **E**, right P3 or P4 in labial (**top**), occlusal (**middle**) and lingual (**bottom**) views; the photos were digitally reversed to show the same orientation as the left dentition; **F**, detail of M1-3 in occlusal view; **G**, reconstruction of the left upper cheekteeth of *M. molariformis* based on VPPLT 1588. Scale bar: 1 cm.

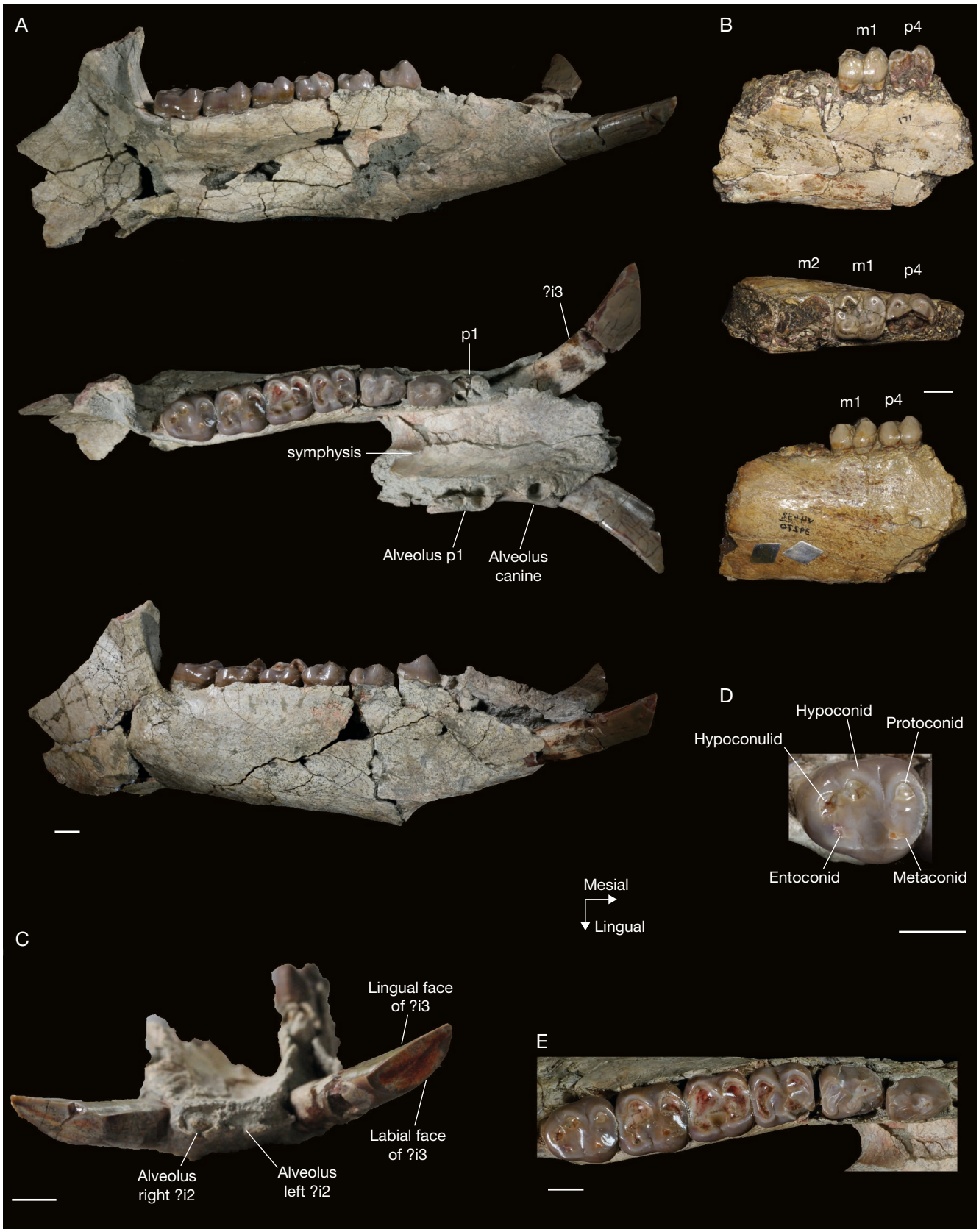

FIG. 3. — Mandible and lower dentition of *Megadolodus molariformis* McKenna, 1956: **A**, VPPLT 974 in medial (**top**), occlusal (**middle**) and lateral (**bottom**) views; the lateral view was digitally reversed to show the same orientation as the lingual view; **B**, holotype of *M. molariformis* (UCMP 39270) in lingual (**top**), occlusal (**middle**) and labial (**bottom**) views; the labial view was digitally reversed to show the same orientation as the lingual view; **C**, VPPLT 974 in rostral view showing the alveoli of ?i2; **D**, detail of m3 (VPPLT 974) in occlusal view; **E**, detail of the p2-m3. Scale bars: 1 cm.

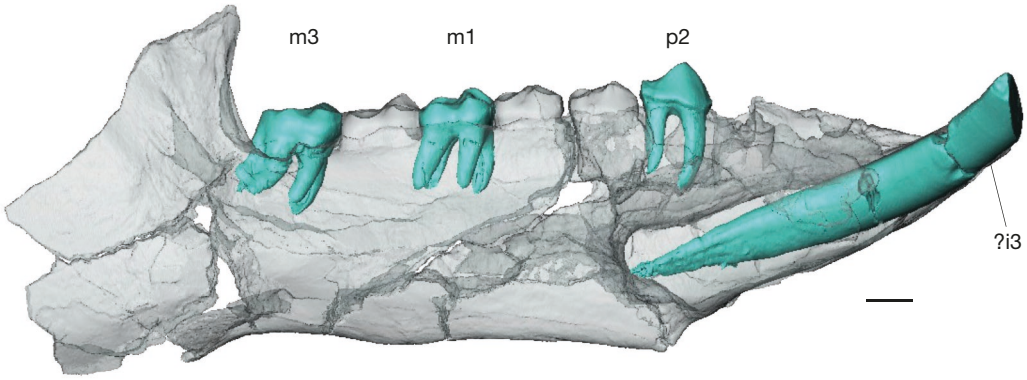

FIG. 4. — Lateral view of the virtually reconstructed mandible of *Megadolodus molariformis* McKenna, 1956. Bone transparency shows the dentary, and the crowns and roots of m3, m1, p2 and ?i3 are shown in light blue. Scale bar: 1 cm.

TABLE 3. — Dental loci known for the bunodont litopterns from La Venta. Abbreviations: **al**, alveolus; **T**, tooth; **pT**, partial tooth. New data from the specimens described in this work are marked **in red**.

	I1/i1	I2/i2	I3/i3	C/c	P1/p1	P2/p2	P3/p3	P4/p4	M1/m1	M2/m2	M3/m3
Megadolodus molariformis	–	–	–	–	–	–	–	–	–	–	–
upper teeth	–	–	–	–	T	T	T	T	T	T	pT
lower teeth	–	al	T	al	T	T	T	T	T	T	T
Neodolodus colombianus	–	–	–	–	–	–	–	–	–	–	–
upper teeth	–	T	–	–	T	T	T	T	T	T	T
lower teeth	–	T	T	T	T	T	T	T	T	T	T

protocone. A faint cingular crest extends from the low lingual cusp along the mesial and distal edges of the tooth (Fig. 2B).

In *Megadolodus*, the P3 and P4 have a very similar morphology and size, being partly molariform, but without an hypocone (Cifelli & Villarroel 1997). Therefore, we cannot establish if the isolated left and right upper premolars correspond to P3 or P4 (Fig. 2C, E; Table 4). Both have a well-developed protocone, paracone, metacone, and worn metaconule, the paraconule is only visible in the left tooth (Fig. 2C, E), as in other specimens of *Megadolodus* (Cifelli & Villarroel 1997). The P3/P4 have mesiolingual and labial cingula. The mesiolingual cingulum isolates a small basin and forms a small cuspule on its lingual end. The lingual face of the P3/P4 is rounded, in contrast to lingual face of the molars which is straight (Fig. 2C-E). There is no mesostyle in the P3/P4, the parastyle is present and the metastyle region of the crown is not well-preserved in both teeth.

The upper molars show a more quadrangular outline in occlusal view than P3/P4 due to the presence of the cingulum-derived hypocone (Cifelli & Villarroel 1997). The crown of M1 is broken in the distolingual portion where the hypocone would be found, and the crown of M3 is broken, missing most of its labial and distal portions (Fig. 2D). We identified the M1 because of its more quadrangular outline in occlusal view and larger size in comparison with the P3 and P4 (Fig. 2D, F). It also shows more advanced occlusal wear than P3 and/or P4, M2 and M3, as expected for the M1 given that is the first permanent tooth to erupt. All upper molars have a strong mesiolingual cingulum that isolates a small basin (narrower on M1-2), similar to what is seen on P3 and/or P4. M1 and M2 have a small mesostyle in addition to the faint parastyle and metastyle (Fig. 2F). There are two faint labial ridges, one on the paracone and one in the metacone on M1-2 (Fig. 2F). The paraconule and metaconule are well developed. On the M1 and M2 the paraconule is equidistant between the protocone and paracone, as in other specimens of *Megadolodus* (Cifelli & Villarroel 1997). The molars of VPPLT 1588 have a preprotocrista (connecting the protocone with the paraconule) and a preparaconular crista (connecting the paraconule with the parastyle). There is no postprotocrista that would connect the protocone and metaconule (Fig. 2F). The metaconule is isolated and closer to the metacone than the protocone, as seen in other specimens of *Megadolodus* (Cifelli & Villarroel 1997). The hypocone is well-developed and isolated. The labial cingula, which can be seen on M1 and M2, are very thin and extending across the whole labial side (Fig. 2F). Although M1 and M3 are only partially preserved, it appears that M2 is the largest molar, especially in the labiolingual dimension (i.e., width; Table 4).

The mandible of *Megadolodus* (VPPLT 974) is robust with a deep horizontal ramus that appears to reach its maximum depth at the level of p2-3 (Figs 3-4). No foramina are observed. The rostroventral portion of the left ascending ramus is preserved; it is wide and suggests that the masseteric fossa was large (Fig. 3A). The symphysis extends caudally up to the level of p3 (Fig. 3A). Only the alveoli of the of right and left ?i2 were preserved (Fig. 3C). The ?i3 is tusk-like and extroverted (projecting anterolaterally). It is not ever-growing, and its root closes at the level of the distal edge of p2 (Fig. 4). The lingual face of ?i3 is flat, the labial face is convex, giving a nearly

TABLE 4. — Craniodental measurements (in mm) of specimens of *Megadolodus molariformis* from La Venta assemblage. Symbols: *, type specimen, taken from McKenna (1956) and Cifelli & Villarroel (1997); **, taken from Cifelli & Villarroel (1997); #, estimated due to specimen breakage. +, identified as P3 or P4.

		UCMP 39270*	IGM 183282**	IGM 183544, 183916**	IGM 184019**	TATAC 1**	TATAC 2**	IGM 250400**	VPPLT 974 left	VPPLT 974 right	VPPLT 1588
?i2	Antero-posterior length	–	–	–	–	–	–	–	–	6.8	–
	Transverse length	–	–	–	–	–	–	–	–	9.3	–
?i3	Antero-posterior length	–	–	–	–	–	–	–	15.3	15.7	–
	Transverse length	–	–	–	–	–	–	–	11.3	12.2	–
Diastema ?i3-c	Length	–	–	–	–	–	–	–	–	–	–
c	Length	–	–	–	–	–	–	–	7.3#	–	–
	Width	–	–	–	–	–	–	–	7.1#	–	–
Diastema c-p1	Length	–	–	–	–	–	–	–	–	–	–
p1	Length	–	13.0	13.4	–	–	–	–	–	–	–
	Width	–	7.5	6.8	–	–	–	–	–	–	–
p2	Length	–	–	–	–	–	14.4	–	15.8	–	–
	Width	–	–	–	–	–	9.4	–	10.4	–	–
p3	Length	–	–	–	13.6	–	12.8	–	15.4	–	–
	Width	9#	–	–	12.2	–	12.9#	–	12.4	–	–
p4	Length	15.3#	–	–	–	–	14.6	–	14.8	–	–
	Width	14#	–	–	–	–	15.7**	–	14.2	–	–
m1	Length	16.4	15.1	15.6	–	–	14.8**	–	15.1	–	–
	Width	15.5	16.4#	16.0	–	–	–	–	15.7	–	–
m2	Length	19#	16.8	17.8	–	–	15.6	–	16.6	–	–
	Width	17#	17.7#	16.6	–	–	15.9	–	16.7	–	–
m3	Length	–	–	–	–	–	–	19.1	17.4	–	–
	Width	18#	–	–	–	–	–	15.7	16.4	–	–
Mandible	Depth at m1	47	–	–	–	–	–	–	46.7	–	–
	Maximum thickness at m3	23	–	–	–	–	–	–	28.8	–	–
P1	Length	–	–	6.0	–	–	–	–	–	–	14.2
	Width	–	–	4.9	–	–	–	–	–	–	10.1
P2	Length	–	–	–	–	–	–	–	–	–	14.1
	Width	–	–	–	–	–	–	–	–	–	13.6
P3	Length	–	14.2	–	–	–	–	–	–	–	14.1+
	Width	–	17.5	–	–	–	–	–	–	–	17.1+
P4	Length	–	14.5	–	–	13.8	–	–	–	–	–
	Width	–	17.5	–	–	18.6	–	–	–	–	–
M1	Length	–	–	–	–	14.4	–	–	–	–	14.9
	Width	–	–	–	–	19.9	–	–	–	–	18.6
M2	Length	–	17.2	–	–	15.1	–	–	–	–	15.2
	Width	–	–	–	–	–	–	–	–	–	19.0
M3	Length	–	–	–	–	13.7	–	–	–	–	NA
	Width	–	–	–	–	18.6	–	–	–	–	NA

oval shape in cross-section. The anterior tip bears an oblique wear-facet marking the occlusion with the upper dentition (Fig. 3C). Only the alveoli of the right canine and of the p1 are preserved (Fig. 3A). There is a short diastema (8.6 mm) between the right ?i3 and the alveolus of the canine, and a slightly longer diastema (13.5 mm) between the alveoli of the right canine and the p1 (Fig. 3A). The alveolus of the canine indicates it was single rooted, and the p1 has two roots, as shown by the preserved part of the left p1 and alveolus of the right p1. The p2 has one main cuspid which is located approximately at the mid-length of the tooth. It is connected distally to a crest directed downwards and towards a small distal basin. This basin (incipient talonid) is bordered distally by a small cuspulid. A crest also connects the mesial edge of the crown with the main cuspid, and there is no mesial bulge, as described in other specimens of *Megadolodus* (Cifelli & Villarroel 1997). The p2 has two roots, one mesial and one distal, the latter divides in two smaller roots at the apical end, one labial and one lingual (Fig. 4).

The p3-4 are molariform and lack a hypoconulid (Fig. 3A, E), as in other specimens of *Megadolodus* (Cifelli & Villarroel 1997). There is an increase in size from the p3 to m1 (Table 4). The p3 has three roots, a large distal one, and two mesial. It lacks a paraconid and the paracristid forms a small

bulge at the anterolingual border of tooth. The protoconid, metaconid, hypoconid and entoconid are similar in size. The p4 has four roots, two mesial and two distal.

The p4 and the lower molars of VPPLT 974 show an advanced state of wear, and no crest are visible. The trigonid and talonid of the molars are comparable in length and width (Cifelli & Villarroel 1997). The paraconid is absent in all the lower molars. The protoconid, metaconid, and hypoconid have similar size, while the entoconid and hypoconulid are smaller. Due to wear, the hypoconulid is only distinct in the m3, where it is located distal to the other talonid cusps (Fig. 3D). The hypoconulid is slightly closer to the hypoconid, whereas in other *Megadolodus* specimens it is closer to the entoconid (Cifelli & Villarroel 1997). Unlike upper molars (VPPLT 1588) where M2 is bigger than M1 and M3, the lower molars (VPPLT 974) have a similar size (Table 4). The lower molars have four roots, two mesial and two distal (Fig. 4).

Genus *Neodolodus* Hoffstetter & Soria, 1986

EMENDED DIAGNOSIS. — The dental formula is I 1/2 C 0/1 P 4/4 M 3/3. Small, brachydont and bunodont megadolodine litoptern. *Neodolodus* differs from *Megadolodus* in its smaller size and having labial and lingual cingulids on m1-3. *Neodolodus* differs from *Bounodus* in its smaller size, the P4 being of similar size (not smaller) than M1, and the P4-M1 with a quadrangular outline (not elongated mesiodistally).

REMARKS

In comparison with other Laventan litopterns, *Neodolodus* differs from *Mesolicaphrium sanalfonense* (Cifelli & Guerrero 1997; McGrath *et al.* 2020a) in the absence of a connection between the protocone and metaconule, having well-developed styles on the upper molars, and the absence of a mesostyle on P3. It differs from *Villarroelia totoyoi* in that P3-4 are not fully molariform lacking an hypocone, the absence of a mesostyle on P3 and P4, and the presence of a hypocone on M3 (Cifelli & Guerrero 1997).

Neodolodus colombianus Hoffstetter & Soria, 1986 (Figs 1; 5-8)

HOLOTYPE. — Specimen MNHN.F.VIV9, partial right mandible bearing p3-m3 (Fig. 7C).

REFERRED MATERIAL. — VPPLT 183, isolated right M1 (Fig. 6B). VPPLT 1696, almost complete skull with left and right ?I2 and P1-M3 (Figs 5-6A). Partial mandible with complete right and left dentition except for left ?i2 (Fig. 7A-B, D). Partial right scapula (Fig. 8A), partial right tibia (Fig. 8B), left metacarpal III (Fig. 8C), right metatarsal III (Fig. 8D), and fragments of undetermined (possibly for metapodials III) phalanx.

TYPE LOCALITY AND HORIZONS. — VPPLT 183 comes from Kilómetro 121 (3°19'29"N, 75°10'55"W), La Victoria Formation in the bed set below the Cerbatana conglomerate (StL 7; Mora-Rojas *et al.* 2023). VPPLT 1696 comes from Piedra Gorda, San Nicolás (3°16'45"N, 75°11'46"W), Villavieja Formation, Monkey beds (StL 9; Mora-Rojas *et al.* 2023) (Fig. 1).

DIAGNOSIS. — Same as for the genus due to monotypy.

REMARKS

Previously known craniodental and postcranial material referred to *Neodolodus colombianus* included partial mandibles that preserved p2, p3, p4, m1, m2 and m3. Partial premaxilla with ?I2, and maxillae that preserved P2, P3, P4, M1, M2 and M3 (Table 3). The known postcranial elements include partial humerus, radii, metacarpal III and II or IV, manual phalanx, partial pelvis, femur, tibia, astragalus, calcaneus, metatarsal III and pedal phalange (Cifelli & Guerrero Díaz 1989).

Previously known specimens referred to *Neodolodus* did not preserve the rostral portion of the cranium and mandible, and the new material clarifies the number and morphology of the upper and lower incisors, canines and anterior premolars (Table 3).

DESCRIPTION

VPPLT 1696 preserves most of the cranium although many parts are damaged with cracks and crushed fragments of bone. Parts of the maxilla, palatines, the left zygomatic arch, the nasal, frontal, squamosal, parietal, alisphenoid and occipital bones, and most of the mandible are preserved but, except for teeth, the bad state of preservation does not permit to describe subtle anatomical details (Figs 5; 6A; 7A, B, D). VPPLT 1696 is referred to *Neodolodus* based on its small size (Table 5), brachydont and bunodont dentition, the absence of a mesostyle on P3-4 (Figs 5B; 6A), a small paraconid present on p3 but absent on p4-m3, and the isolated entoconid on m1-3 (Fig. 7B, D) (Hoffstetter & Soria 1986; Cifelli & Guerrero Díaz 1989; McGrath *et al.* 2020a).

The cranium measures *c.* 10.5 cm from the most caudal point of the sagittal crest to the most rostral point of the snout between the incisors. It is damaged, lacking portions of the prexamilla and maxilla. Due to the preservation, no sutures or synchondrosis are clearly visible. In ventral view, the palate looks narrow, but it is unclear whether this is due to a slight post-mortem mediolateral compression of the cranium or represents the unaltered morphology. The choanae open directly posteromedially to the distal edges of the M3, with a rounded rostral edge. From there, the basipharyngeal canal is bordered laterally by the sagittally-oriented ectopterygoid crests, up to the auditory region caudally. In lateral view, the rostrum is low and elongated (Fig. 5A). The orbit is large, with a large frontal postorbital process of the frontal posteriorly. The zygomatic arch does not extend much laterally but this might be due in part to postmortem deformation. In dorsal view, the temporal lines are concave caudally, extending from the caudal margin of the orbit and meeting on the roof of the cranium at the level of the rostral edge of the posterior root of the zygomatic arch (Fig. 5A). The union of these temporal lines forms a well-defined sagittal crest caudally.

The mesial-most pair of the upper teeth (?I2) are developed into tusks, which are triangular in cross-section and curved ventrally (Fig. 5A). The most apical portion of the tusks is not preserved, and is not possible to assess if the upper tusks touched with the lower ones, as it appears to be the case in

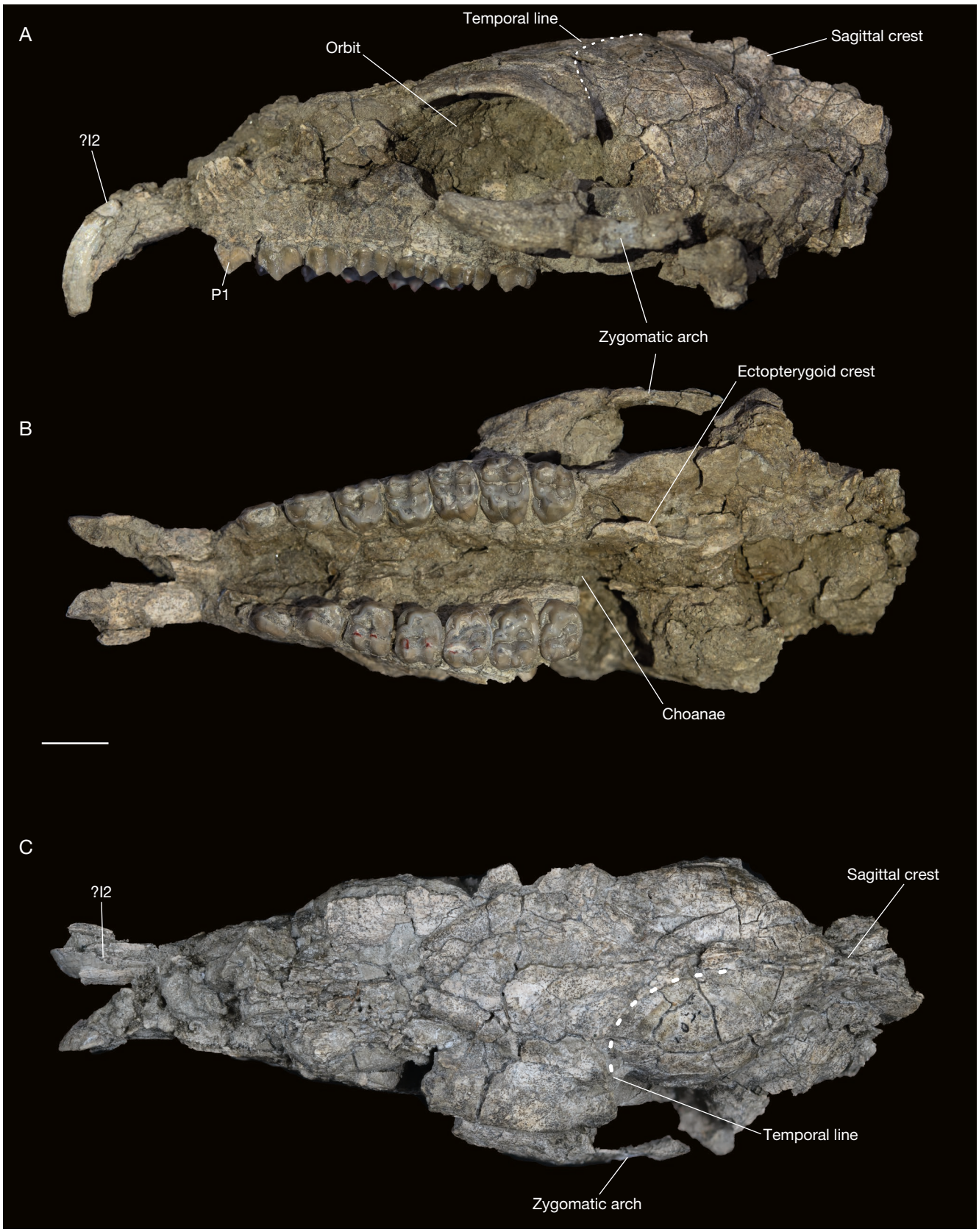

Fig. 5. — Skull and upper dentition of *Neodolodus colombianus* Hoffstetter & Soria, 1986: **A**, cranium (VPPLT 1696) in left lateral view; **B**, cranium in ventral view; **C**, cranium in dorsal view. Scale bar: 1 cm.

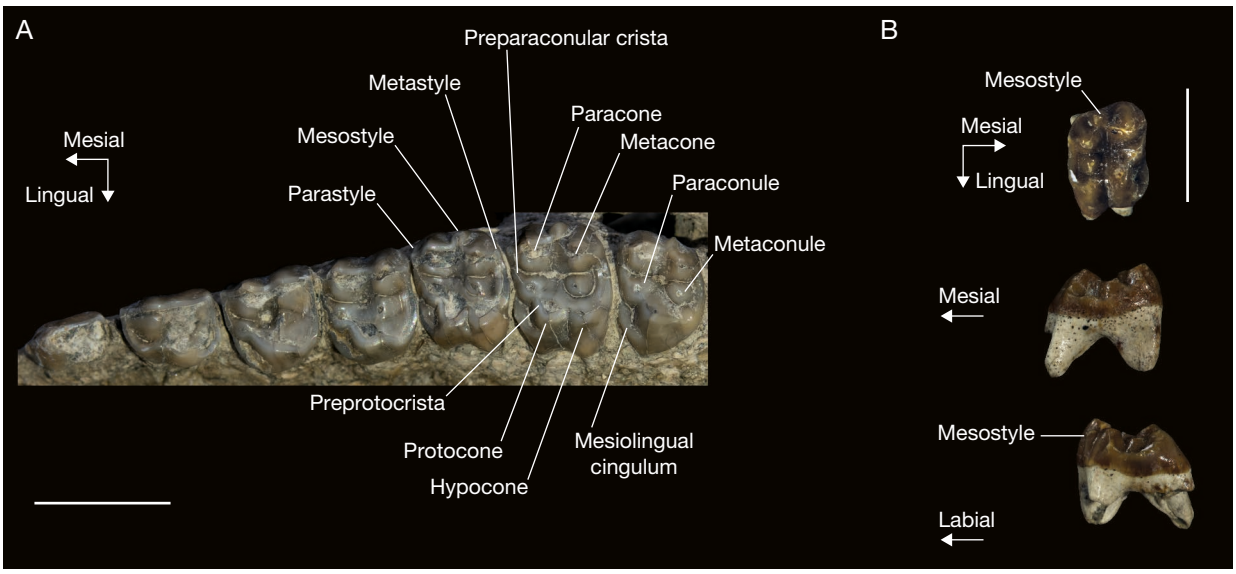

FIG. 6. — Detail of upper dentition of *Neodolodus colombianus* Hoffstetter & Soria, 1986: **A**, left upper cheekteeth in occlusal view (VPPLT 1696); **B**, right M1 (VPPLT 183) in occlusal (**top**), lingual (**middle**) and distal (**bottom**) views. Scale bars: 1 cm.

Megadolodus (Fig. 3C). In *Neodolodus*, the crown of P1 is simple with a single centrally-located cusp with a crest extending mesially, as in *Megadolodus*. The distal portion of the crown has an oblique wear facet oriented distolingually (Figs 5B; 6A). The P2 also has one cusp, located on the labial side and positioned mesial of the midline of the tooth. The tooth exhibits a lingual basin which is stretched distomesially and bordered by a distolingual cingulum (Figs 5B; 6A). A small cusp was also likely present on the distolingual edge of this basin, but the wear stage of the tooth precludes a definite statement on this morphology. On the distolabial border of the crown there is a metastyle.

The upper premolars and molars of VPPLT 1696 increase in size from P3 to M2 (Table 5), and the M3 is similar in size to P4, as in *Megadolodus* (Cifelli & Villarroel 1997), *Anisoplophus, Diadiaphorus, Megadolodus* and *Villarroelia,* and unlike *Tetramerorhinus* where the M3 is larger or of similar size to M1-2. The P3-4 are partly molariform, they have a well-developed protocone, paracone and metacone, but they lack a fully individualized hypocone (an incipient cingulum-derived hypocone is visible on P4) (Figs 5B; 6A). As in *Megadolodus* (Fig. 2C, E), there is a parastyle and metastyle on the ectoloph of the P3 and P4 of *Neodolodus*, but no mesostyle (Fig. 6A). Two faint labial ridges are visible on the labial wall of the paracone and metacone (Figs 5B; 6A). As seen in other specimens of *Neodolodus* (Cifelli & Guerrero Díaz 1989), the posterior premolars of VPPLT 1696 have a thick mesiolingual cingulum that defines a small basin directed labiolingually. The paraconule and metaconule are distinct, the former being connected to the protocone by the preprotocrista, whereas the latter is isolated (Fig. 6A).

The upper molars exhibit a labially protruding mesostyle, especially on M1-2. The parastyle and metastyle are less developed than the mesostyle (Fig. 6A). A cingulum of varying thickness is present at both labial corners at the base of the crown, as described in other specimens of *Neodolodus* (Cifelli & Guerrero Díaz 1989). All the upper molars have a postcingulum-derived hypocone (Figs 5B; 6A). The paracone and metacone are well-defined and not connected to the paraconule or metaconule. As in *Megadolodus,* there are two ridges on the labial flank of the paracone and metacone, although in *Neodolodus* these ridges are more developed (Figs 2F; 6A). The upper molars of *Neodolodus* also exhibit a thick mesiolingual cingulum that forms a basin just like on P3-4 (Figs 5B; 6A) (Cifelli & Guerrero Díaz 1989). The paraconule is connected by the preprotocrista to the protocone, as in *Megadolodus*, (Cifelli & Villarroel 1997). The metaconule is isolated from other cusps in all the molars. The hypocone is small and connected to the protocone on M3 by a small lingual crista (Fig. 6A), as in other specimens of *Neodolodus* (McGrath *et al.* 2020a).

The mandible of VPPLT 1696 preserves most of the right and left horizontal rami and part of the left ascending ramus (Fig. 7A). The mandibular symphysis extends caudally until the level of the p2 (Fig. 7B). Of the two mesial-most incisors, only the crown of the right ?i2 is preserved. It is spatulate with flat lingual and labial faces. The base of the crown of the right and left ?i3 are preserved (Fig. 7A, B). The ?i3 have flat lingual and convex labial faces, separated by medial and labial ridges. The ?i3 are considerably larger than the ?i2. As in *Megadolodus*, there are two short diastemata (Fig. 7B), one between the ?i3 and the canine (5.0 and 4.0 mm in right and left side respectively), and one between the canine and the p1 (4.0 and 3.0 mm in right and left side respectively). The canine is small and somewhat spatulate, with a flat lingual face and a convex labial one (Fig. 7A, B).

The p1-2 are simple with a single cuspid located slightly mesial to the centre of the tooth, which results in a nearly triangular shape in labial view. On both teeth, crests extend downward mesially and distally from the main cuspid

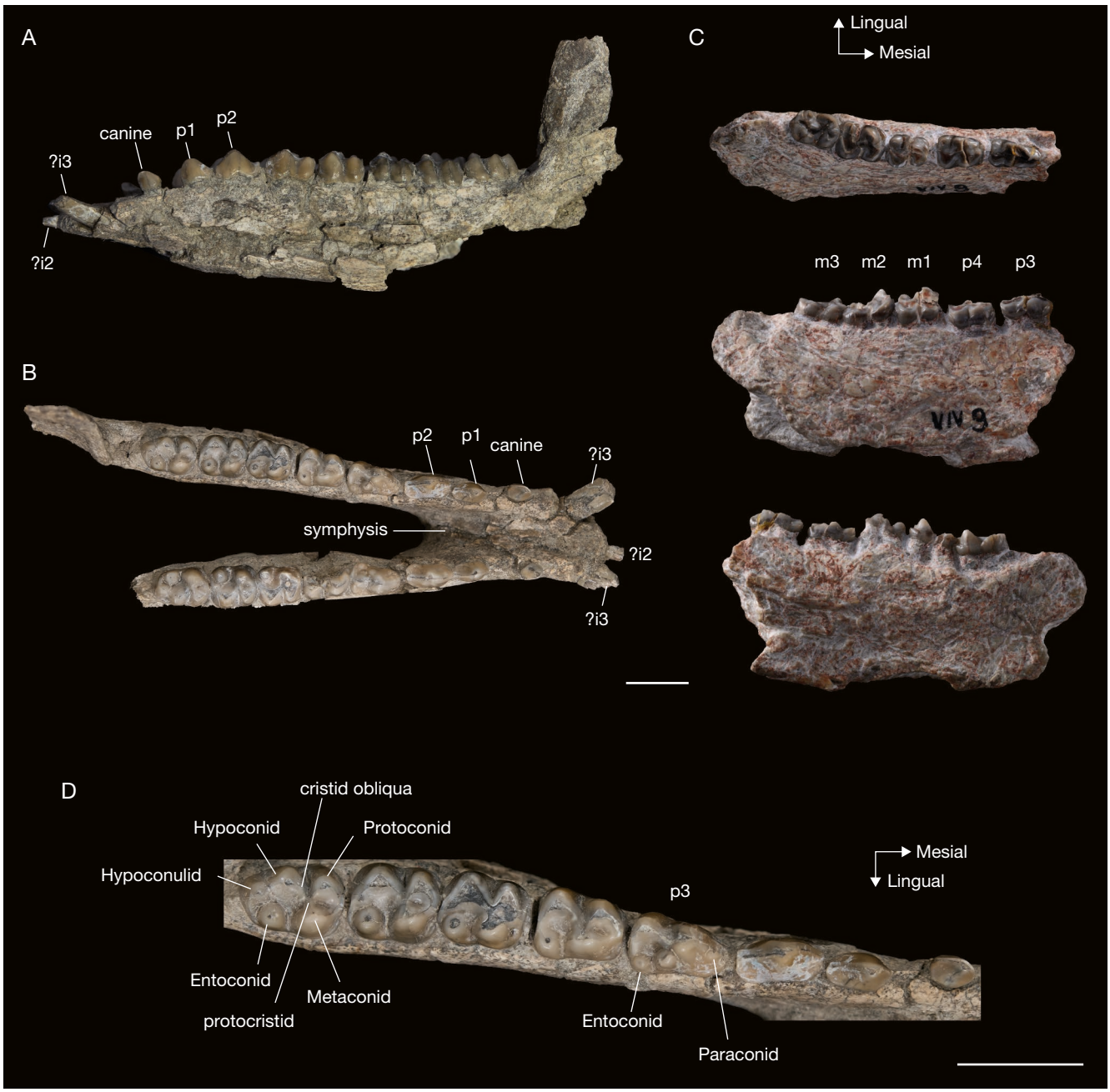

Fig. 7. — Mandible and lower dentition of *Neodolodus colombianus* Hoffstetter & Soria, 1986: **A**, partial mandible (VPPLT 1696) in left lateral view; **B**, partial mandible (VPPLT 1696) in dorsal view; **C**, holotype (MNHN.F.VIV9) in occlusal (**top**), labial (**middle**) and lingual (**bottom**) views; **D**, detail of the left lower dentition (c-m3) of VPPLT 1696 in occlusal view. Scale bars: 1 cm.

(Fig. 7B). On p2, the distal crest gently curves lingually and upwards at its distal end which resembles an incipient talonid (Cifelli & Guerrero Díaz 1989). The size of the premolars increases from p1 to p4. The p3 is bicrescentic, with the trigonid being narrower than the talonid (Fig. 7D). A low cuspid is present at the mesial edge of p3, which may well represent an incipient paraconid; this cuspid is absent on p4 and lower molars, as already described for this species (Hoffstetter & Soria 1986; Cifelli & Guerrero Díaz 1989). The p4 is molariform, without paraconid (Fig. 7D). The lingual portion of the crown of the right p4 of VPPLT 1696 is broken, but the left p4 is complete. In *Neodolodus*, the hypoconulid is absent on p3-4 (Fig. 7D). There is a low metaconid on p3, and the same cuspid is more developed on p4. The metaconid is separated from the protoconid by a sulcus on its mesial edge. The entoconid is isolated from other cuspids on both teeth (Fig. 7D).

The lower molars of *Neodolodus* are bicrescentic and increase in length from m1 to m3 (Cifelli & Guerrero Díaz 1989). VPPLT 1696 has high wear on m1 and moderate wear on m2, whereas the m3 is only slightly worn (Fig. 7B, D). The less worn state of m3 allows the preservation of

TABLE 5. — Craniodental measurements (in mm) of specimens of *Neodolodus colombianus* Hoffstetter & Soria, 1986 from La Venta assemblage. *, type specimen, taken from Hoffstetter & Soria (1986); **, taken from Cifelli & Guerrero Díaz (1989); #, estimated due to specimen breakage.

		MNHN. F.VIV9*	Duke-ING 86-093**	Duke-ING 86-274**	Duke-ING 86-288**	UCMP 37691**	Duke-ING 88-332**	IGN 182578**	UCMP 38910**	IGN 182568**	VPPLT 1696 left	VPPLT 1696 right	VPPLT 183
?i2	Antero-posterior length	–	–	–	–	–	–	–	–	–	–	–	–
	Transverse length	–	–	–	–	–	–	–	–	–	–	–	–
?i3	Antero-posterior length	–	–	–	–	–	–	–	–	–	4.1	4.2	–
	Transverse length	–	–	–	–	–	–	–	–	–	2.6	2.6	–
Diastema ?i3-c	Length	–	–	–	–	–	–	–	–	–	6.2	6.9	–
c	Length	–	–	–	–	–	–	–	–	–	3.2	3.0	–
	Width	–	–	–	–	–	–	–	–	–	2.0	2.2	–
Diastema c-p1	Length	–	–	–	–	–	–	–	–	–	3.6	4.9	–
p1	Length	–	–	–	–	–	–	–	–	–	4.8	4.9	–
	Width	–	–	–	–	–	–	–	–	–	2.9	2.6	–
p2	Length	–	–	–	–	–	–	7.3	–	–	6.8	6.4	–
	Width	–	–	–	–	–	–	3.6	–	–	3.6	3.3	–
p3	Length	8.2	–	–	–	–	–	–	–	–	7.1	6.7	–
	Width	4.5	–	–	–	–	4.6	–	–	–	4.5	4.6	–
p4	Length	7.5	–	7.3	–	7.5	7.4	–	–	–	6.6	6.8	–
	Width	5.6	–	5.8	–	6.0	5.8	–	–	–	5.4	–	–
m1	Length	6.5	6.7	6.7	–	6.9	6.6	–	–	–	6.3	6.1	–
	Width	5.8	5.4	6.1	–	6.0	6.8#	–	–	–	5.5	5.7	–
m2	Length	7.5	7.6	–	6.8	7.3	7.9	–	–	–	6.7	6.1	–
	Width	6.5	5.9	6.0	5.6	6.7	6.2	–	–	–	5.8	6.1	–
m3	Length	8.0	9.2	–	8.7	9.3	8.0	–	–	–	7.4	7.9	–
	Width	6.0	5.6	–	5.5	6.1	5.0	–	–	–	5.8	5.6	–
Mandible	Depth at m1	–	–	–	–	–	–	–	–	–	6.2#	–	–
	Maximum thickness at m3	–	–	–	–	–	–	–	–	–	7.5	7.5	–
C	Maximum diameter	–	–	–	–	–	–	–	–	–	6.4	5.3	–
P1	Length	–	–	–	–	–	–	–	–	–	6.7	5.8	–
	Width	–	–	–	–	–	–	–	–	–	3.5	3.5	–
P2	Length	–	–	–	–	–	–	–	–	–	6.3	5.7	–
	Width	–	–	–	–	–	–	–	–	–	5.4	5.6	–
P3	Length	–	–	–	–	–	–	–	6.8	7.0	6.1	5.8	–
	Width	–	–	–	–	–	–	–	8.2	8.3	7.5	7.2	–
P4	Length	–	–	–	–	–	–	–	7.3	7.3	6.0	6.0	–
	Width	–	–	–	–	–	–	–	8.9	8.9	7.9	7.2	–
M1	Length	–	–	–	–	–	–	–	–	7.2	6.0	6.0	7.0
	Width	–	–	–	–	–	–	–	–	9.0	7.9	7.2	9.4
M2	Length	–	–	–	–	–	–	–	7.0	7.9	6.8	6.2	–
	Width	–	–	–	–	–	–	–	9.4	10.3	9.1	8.7	–
M3	Length	–	–	–	–	–	–	–	7.0	–	5.9	5.4	–
	Width	–	–	–	–	–	–	–	8.2	–	7.4	8.0	–

the protocristid, which connects the protoconid and the metaconid along their distal edges (Fig. 7D). There is a mesial crest extending from the protoconid. The absence of paraconid results in an ovate outline of the trigonid. The hypoconid is the largest cusp on the molar talonid. It is connected to the base of the metaconid and trigonid through a low cristid obliqua and to the hypoconulid through a low distal cristid (hypocristid). The entoconid is isolated from other cusps on all the lower molars (Hoffstetter & Soria 1986) and located in a more lingual position than the hypoconulid (Cifelli & Guerrero 1997; McGrath *et al.* 2020a). The hypoconulid is smaller than the entoconid on m1-2 (Fig. 7D). The hypoconulid on m3 is located distally from the hypoconid and entoconid and is connected to a cristid extending lingually from it, without reaching the entoconid (Fig. 7D).

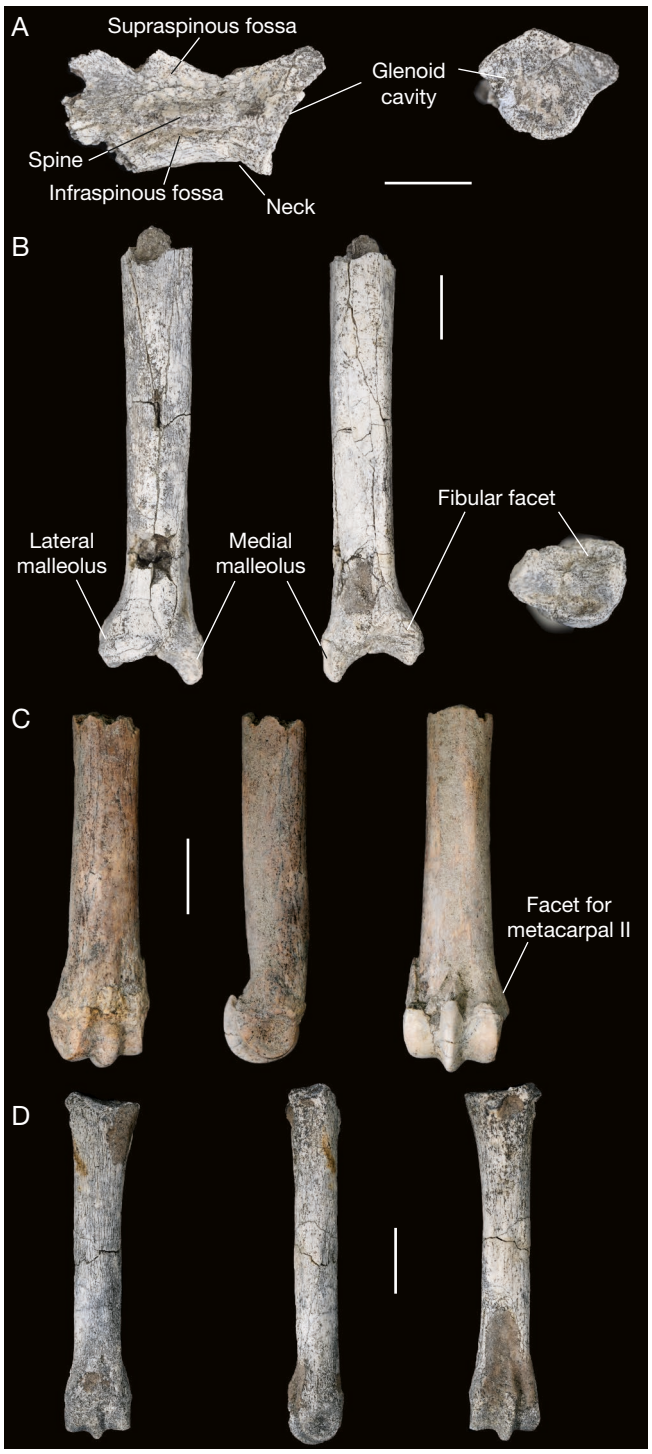

Fig. 8. — Scapula and limb bones of *Neodolodus colombianus* (VPPLT 1606): **A**, partial right scapula in dorsolateral view (**left**) and proximal view (**right**); **B**, partial right tibia in anterior (**left**), posterior (**middle**) and distal (**right**) views; **C**, left metacarpal III in anterior (**left**), medial (**middle**) and posterior (**right**) views; **D**, right metatarsal III in anterior (**left**), medial (**middle**) and posterior (**right**) views. Scale bars: 1 cm.

Associated postcranial elements of VPPLT 1696 include a partial scapula and limb bones. The right scapula preserves the glenoid fossa, part of the spine and the blade (Fig. 8A). The glenoid fossa is semi-circular, being rounded on the lateral edge and straighter in the dorsal edge. The neck is short and wide. The spine is broken, it is narrow and located in the middle of the blade. Most of the blade is not preserved and the relative size and shape of the supraspinous and infraspinous fossae cannot be assessed. The right tibia preserves the shaft and the distal epiphysis (Fig. 8B). The medial malleolus extends further distally than the lateral malleolus, as in *Diadiaphorus majusculus* (Schmidt *et al.* 2019b). On the latero-posterior part of the distal end of the tibia, there is a facet for the articulation with the fibula (Fig. 8B). The metapodials III (Fig. 8C-D) have a straight and long diaphyses, and the distal a well-defined keels, as seen in other proterotheriids (Carrillo *et al.* 2018; Schmidt *et al.* 2019b). By comparison with the known metapodials III of *Megadolodus* (Cifelli & Villarroel 1997), we tentatively identify one element as left metacarpal III (Fig. 8C) because it is shorter and more robust than the other element, which we identify as the right metatarsal III (Fig. 8D). The metacarpal III has a small facet for the articulation with the metacarpal II on the medial side, and the proximal epiphysis is not fused (Fig. 8C).

PHYLOGENETIC ANALYSES

Extended matrix

The parsimony analysis of the extended matrix yielded 281 trees, 405 steps long, with a consistency index of 0.344 and a retention index of 0.688. A strict consensus of these trees (Fig. 9) shows a polytomy at the base of the ingroup including members of Didolodontidae, represented in our taxonomic sample by *Didolodus*, *Ricardocifellia,* and *Lamegoia* (Croft *et al.* 2020), and Protolipternidae (Cifelli 1983), represented by *Miguelsoria*, *Protolipterna*, and *Asmithwoodwardia* (Fig. 9). The polytomy includes *Miguelsoria,* a clade formed by *Protolipterna* + Didolodontidae (Bremer support = 1), and a clade including all the remaining ingroup taxa (Bremer support = 1), with *Asmithwoodwardia* as the earliest diverging taxon within this clade.

The *Prolipterna* + Didolodontidae clade is supported by one unambiguous synapomorphy (see characters [and states] in Appendix 2): metastyle absent on P4 (36[0]). Didolodontidae is recovered as monophyletic (Bremer support = 2), and it is supported by 14 unambiguous synapomorphies: presence of hypocone on M3 (66[1]), low astragalar body, without sharp crests (101[0]) , tibial trochlea of the astragalus restricted to the dorsal surface (102[0]), ovoid astragalar head (103[0]) , navicular facet of the astragalus restricted to the distoinferior part of the head (104[0]), presence of the cuboid facet on the astragalus (105[0]), presence of a medial collateral ligament facet on the astragalus(106[0]), a shallow astragalar ectal facet facing inferiorly (107[0]), medial malleolar facet of the astragalus restricted to medial side of the body (108[1]), medial side of the astragalus with a strong anterior flare (109[1]), the presence of a medial expansion of the astragalar head (110[1]), short calcaneal neck with the cuboid facet nearly perpendicular to the axis of the calcaneus (111[0]), subplanar sustentacular facet of calcaneus, facing dorsodistally (112[0]), and presence of a dorsal beak on the distal end of the calcaneus (113[1]).

FIG. 9. — Hypothesis of phylogenetic relationships within Didolodontidae and Litopterna based on the analysis of the extended matrix. Strict consensus of the 281 most parsimonious trees resulting from the analysis. The numbers at the nodes indicate the Bremer support. The nodes indicated with letters are discussed in the text.

A large clade (node A1 in Fig. 9; Bremer support = 3) includes all the remaining ingroup taxa and is supported by 11 synapomorphies: parastyle forming a strong projection in P3 (31[1]), and P4 (32[1]), cheek teeth bunoselenodont (37[1]), presence of metaconid on p2 (40[1]), presence of a labial cingulid on p3 (41[1]), and p4 (51[1]), lophate talonid on p4 (49[2]), paralophid on m1-2 terminating near the midline (80[1]), lingual attachment of the lower molar cristid obliqua to the trigonid (90[1]), and presence of lingual cingulids on m1-2 (94[1]), and m3 (95[1]).

Adiantoides and *Indalecia* (classified as Indaleciidae, Cifelli & Soria 1983) form a politomy at the base of node A1, together with a clade formed by all the remaining litopterns (node B, Bremer support = 2) (Fig. 9). The node B is supported by seven unambiguous synapomorphies: posteriormost point of the mandibular symphysis at the level of p2 (11[1]), presence of metaconule on P4 (29[1]), paracone and metacone subequal and well separated from each other (33[1]), presence of mesostyle in upper molars (59[1]), and mesiolingual cingulum connected to protocone on M1 (73[1]), M2 (74[1]), and M3 (75[1]).

The adianthid *Proectocion* (Cifelli & Soria 1983) is recovered as closely related to *Polymorphis* (Bremer support = 1), nested within Macraucheniidae (Bremer support = 1), which is represented by three taxa in our sample (*Polymorphis, Theosodon* and *Cramauchenia*) (Fig. 9). The Macraucheniidae + *Proectocion* clade diverges at the base of node B and is supported by three unambiguous synapomorphies: upper molar hypocone developed as crescent (64[1]), presence of hypocone on M3 (66[1]), and lower molar metaconid developed as a distinct column (82[1]). The close relationship between the more recent macraucheniids in our sample (*Theosodon* and *Cramauchenia*; Bremer support = 2) is supported by three unambiguous synapomorphies: postcingulum in upper molars enlarged enclosing a basin (70[1]), anterior attachment of the lower molar entoconid to the hypolophid (86[1]), and the lower molar entoconid developed as an entolophid (87[1]).

A less inclusive clade defined by node C (Bremer support = 1) includes proterotheriids and closer allies (Fig. 9). Anisolambdidae (represented in our sample by *Paranisolambda, Anisolambda,* and *Protheosodon*; Croft *et al.* 2020) is not recovered as a monophyletic group (Fig. 9). *Protheosodon* is the earliest taxon to diverge at the base of node C, whereas *Paranisolambda* and *Anisolambda* are nested within a less inclusive clade defined by node D (Bremer support = 1). Within this clade, *Paranisolambda* is recovered as the sister taxon of *Victorlemoinea*, and *Anisolambda* as the sister taxon of *Lambdaconus suinus* (Fig. 9).

Megadolodus and *Neodolodus* are recovered as sister taxa (Bremer support = 5; Fig. 9), supporting the inclusion of *Neodolodus* in Megadolodinae (Cifelli & Villarroel 1997). Megadolodinae is nested within the clade defined by node D, and it is supported by 10 unambiguous synapomorphies: P4 metaconule isolated (30[2]), small parastyle on P3 (31[0]) and P4 (32[0]), bunodont cheek teeth (37[0]), absence of metaconid on p2 (40[0]), parastyle of upper molars not forming a labial projection (58[0]), presence of hypocone on M3 (66[1]), absence of paralophid on m1-2 (80[0]) and m3 (81[0]), and a median attachment of the cristid obliqua to the trigonid (90[0]).

In the analysis of the extended matrix, the other litopterns reported from La Venta (Table 1) also branch within the clade that includes protherotheriids and close allies (node C in Fig. 9). *Mesolicaphrium sanalfonense* is recovered forming a politomy at base of the clade together with *Diaplasotherium robustum*, *Picturotherium migueli,* the clade defined by node D, and a a large proterotheriid clade (node E, Bremer support =1) (Fig. 9). At the base of the clade defined by node E is a polytomy that includes *Anisolophus floweri, Anisolophus australis, Prolicaphrium specillatum* and a less inclusive clade of proterotheriids (node F1, Bremer support =1). *Villarroelia totoyoi* is the earliest taxon to diverge within this clade, which also includes the more derived proterotheriids (Fig. 9).

Overall, the Bremer support for the nodes of the phylogenetic hypothesis obtained with the extended matrix is low (Fig. 9), with most nodes having a Bremer support of one or two. Only two nodes show relatively high Bremer support values: the node defining the Megadolodinae clade with a support of five, and the node that includes the advanced litopterns (node A1) with a support of three (Fig. 9).

Reduced matrix

The parsimony analysis of the reduced matrix yielded 580 trees, 367 steps long, with a consistency index of 0.365 and a retention index of 0.675. The strict consensus of these trees (Fig. 10) is poorly resolved and shows a basal polytomy including the representatives of Didolodontidae and Protolipternidae, and a larger clade (node A2 in Fig. 10; Bremer support = 2) formed by all the remaining ingroup taxa (Fig. 10). Didolodontidae is not recovered as monophyletic, but *Lamegoia* and *Ricardocifellia* are recovered as sister taxa (Bremer support = 1). All the representatives of Protolipternidae (*Miguelsoria, Protolipterna,* and *Asmithwoodwardia*) are recovered as part of the polytomy (Fig. 10).

The clade A2 issued from the analysis of the reduced matrix (Fig. 10) is similar in its taxonomical content, but not in its topology, to the clade A1 obtained with the extended matrix (Fig. 9). In the analysis of the reduced matrix, there is indeed a large polytomy at base of node A2, which includes representatives of Indaleciidae and Anisolambdidae, *Victorlemoinea, Paramacrauchenia, Anisolophus, Diplasiotherium, Lambdaconus, Picturotherium, Mesolicaphrium, Prolicaphrium,* Megadolodinae, a clade including macraucheniids, *Proectocion* and *Protheosodon* (node G), and a clade including later diverging proterotheriids (node F2) (Fig. 10). The clade defined by node A2 is supported by three unambiguous synapomorphies: bunoselenodont cheek teeth (30[1]; also a synapomorphy for node A1 in the extended matrix analysis), M3 larger or of similar size than M1-2 (61[1]), and lingual attachment of the lower molar cristid obliqua to the trigonid (74[1]; also a synapomorphy for node A1 in the extended matrix analysis).

The Anisolambdidae (*Paranisolambda, Anisolambda,* and *Protheosodon*) is not recovered as monophyletic, with *Protheosodon* appearing within the clade defined by node G (Bremer support = 1), as the sister taxon to macraucheniids and *Proectocion* (Fig. 10). As in the analysis of the extended matrix (Fig. 9), the adianthid *Proectocion* is recovered as closely related to *Polymorphis,* nested within Macraucheniidae (*Polymorphis, Theosodon* and *Cramauchenia*) (Fig. 10). The Macraucheniidae + *Proectocion* clade (Bremer support = 1) is supported by five unambiguous synapomorphies: reduced talonid on p3 (35[1]), p3 trigonid mesiodistally longer than talonid (36[0]), p3 hypoconid positioned lingual of protoconid (37[1]), presence of hypocone in all the upper molars (55[2]), and lower molar metaconid developed as a distinct column (67[1]; a synapomorphy also indicated in the extended matrix analysis). The close relationship between the more derived macraucheniids (*Theosodon* and *Cramauchenia*) is supported by two unambiguous synapomorphies: anterior attachment of the lower molar entoconid to the hypolophid (71[1]; a synapomorphy also indicated in the extended matrix analysis), and the lower molar entoconid developed as an entolophid 72([1]; a synapomorphy also indicated in the extended matrix analysis).

The analysis of the reduced matrix also recovered *Megadolodus* and *Neodolodus* as sister taxa, forming the clade Megadolodinae (Bremer support = 2; Fig. 10). This clade is supported by six unambiguous synapomorphies: absence of mesostyle and paracone and metacone broadly space on P3 (19[1]), small parastyle on P3-P4 (25[0]; a synapomorphy also indicated in the extended matrix analysis), absence of mesostyle on P4 (28[0]), bunodont cheek teeth (30[0]; a synapomorphy also indicated in the extended matrix analysis), and absence of paralophid on m1-2 (65[0]), and m3 (66[0]; synapomorphies also indicated in the extended matrix analysis).

One litoptern taxa from La Venta, *Villarroelia totoyoi*, is found within in a large clade that includes the more derived protherotheriids (node F2 in Fig. 10; Bremer support =1), whereas the other Laventan litoptern, *Mesolicaphrium sanalfonense,* is recovered at the polytomy at the base of node A2

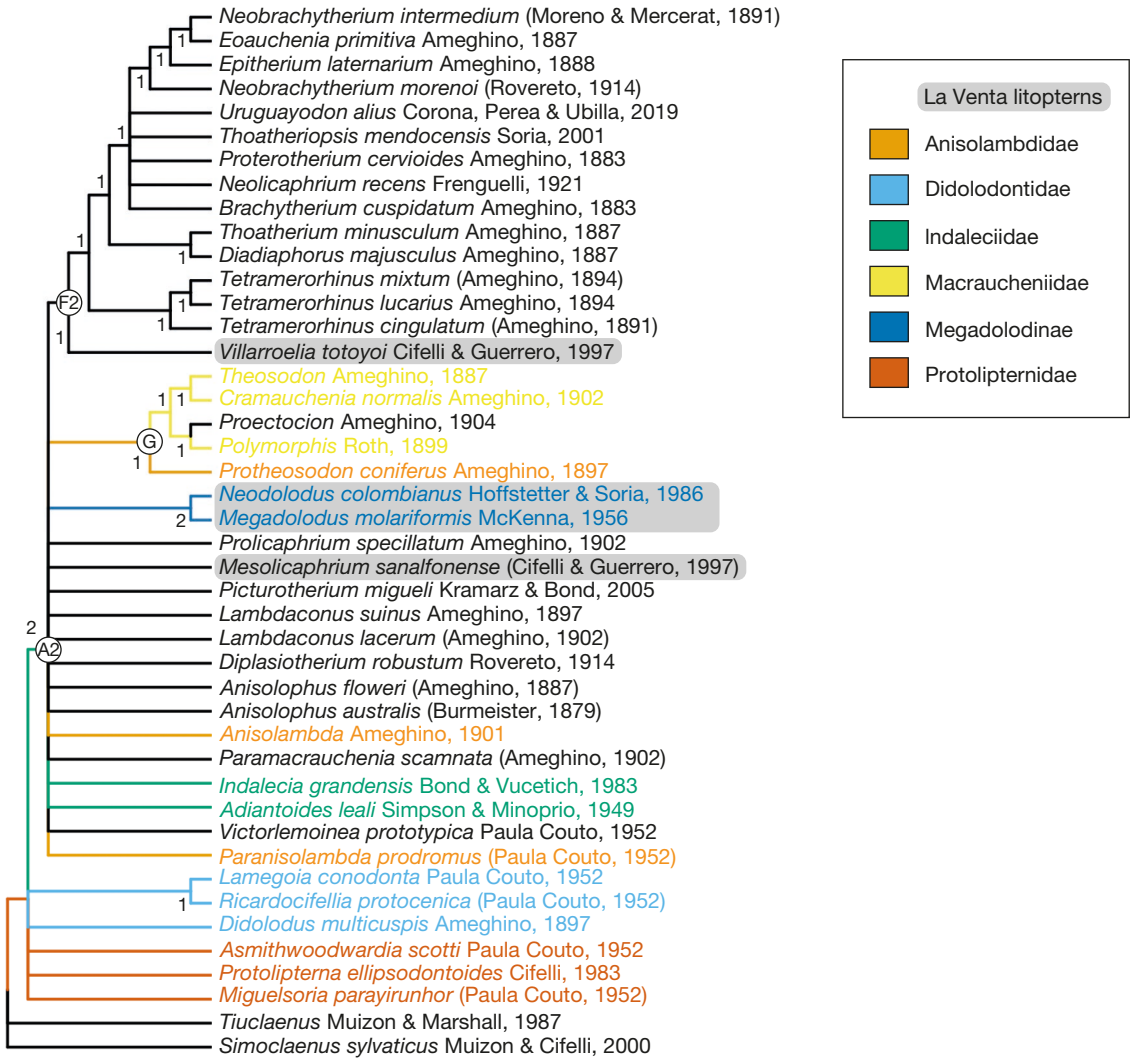

Fig. 10. — Hypothesis of phylogenetic relationships within Didolodontidae and Litopterna based on the analysis of the reduced matrix and using maximum parsimony. Strict consensus of the 580 most parsimonious trees resulting from the analysis. The numbers at the nodes indicate the Bremer support. The numbers at the nodes indicate the Bremer support. The nodes indicated with letters are discussed in the text.

(Fig. 10). The Bremer support of the nodes within the clade defined by the node F2 are low, with all the nodes having a value of 1.

The Bayesian phylogenetic analysis of the reduced matrix (Fig. 11) recovers two basal clades. One clade (node H in Fig. 11; posterior support = 0.8) includes the Didolodontidae (posterior support = 1) and Protolipternidae (posterior support = 0.8), each one recovered as monophyletic and being sister clades (Fig. 11). The second clade (node A3 in Fig. 11; posterior support = 0.9) includes all the remaining ingroup taxa, and is similar in its content to the clades recovered in the analyses using parsimony (nodes A1 [Fig. 9] and A2 [Fig. 10]). In the Bayesian analysis, the clade defined by node A3 contains two main clades. In one clade (node I in Fig. 11), *Paranisolambda* is the earliest taxon to diverge, followed by *Adiantoides, Proectocion* and Macraucheniidae (composed by *Polymorphis, Cramauchenia* and *Theosodon*), which is recovered as monophyletic, although with a low posterior support (< 0.5). The second main clade in A3 (node J in Fig. 11) includes *Indalecia, Victorlemoinea,* the anisolambdis *Anisolambda* and *Protheosodon* and most of the taxa recognized as proterotheriids in previous studies (e.g., McGrath *et al.* 2020b).

The Bayesian analysis also strongly supports a monophyletic Megadolodinae (represented by *Megadolodus* and *Neodolodus*; posterior support = 1), with an estimated time of origin of 14 Ma (95% credible interval = 12.9-15.8 Ma; Fig. 11). Megadolodinae is recovered within the clade defined by node J, and, within it, in a less inclusive clade that also includes the two other Laventan protherotheriids (*Villarroelia* and *Mesolicaphrium*). The latter clade (node K in Fig. 11; posterior support < 0.5) was not recovered by any of the two analyses using maximum parsimony (Figs 9-10). Within it, *Picturotherium* is the earliest taxon to diverge, and it is sister to a clade defined by node L, which has two subclades. One includes Megadolodinae as the sister group of *Anisolophus australis*. In the second subclade, *Anisolophus floweri* is the earliest taxon to diverge, followed by *Villarroelia*. *Mesolicaphrium* appears as the sister taxon of *Diaplasiotherium* (Fig. 11).

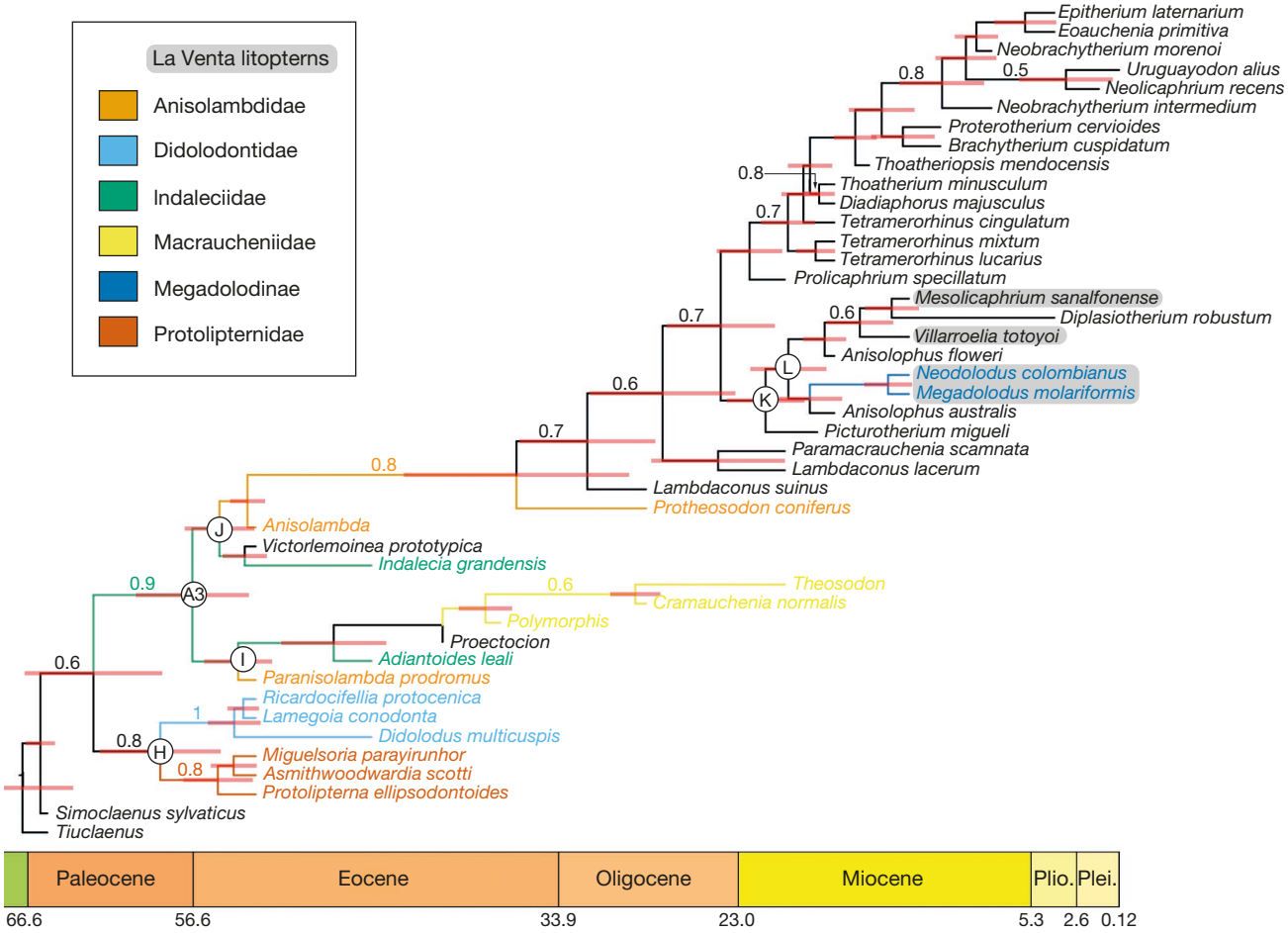

FIG. 11. — Hypothesis of phylogenetic relationships within Didolodontidae and Litopterna based on the reduced matrix and using Bayesian inference. Maximum clade credibility tree. The numbers show the clade posterior values larger than 0.5. The red horizontal bars are the 95% highest probability density intervals for the divergence times. Abbreviations: **Plio.**, Pliocene; **Plei.**, Pleistocene; **Ma**, millions of years. The nodes indicated with letters are discussed in the text.

DISCUSSION

SYSTEMATICS OF MEGADOLODINAE AND PROTEROTHERIIDAE

Megadolodus and *Neodolodus* are enigmatic bunodont native ungulates found in Miocene faunal assemblages of tropical South America (Cifelli & Guerrero Díaz 1989; Cifelli & Villarroel 1997; Carrillo *et al.* 2018). Both taxa were initially identified as didolodontid 'condylarths' (McKenna 1956; Hoffstetter & Soria 1986). If affinities with didolodontids were accepted, it would imply the survival into the middle Miocene of a clade that is otherwise only known from the Palaeocene and Eocene (McKenna 1956; Gelfo *et al.* 2020). *Megadolodus* and *Neodolodus* were later classified into Proterotheriidae, within Litopterna (Cifelli & Guerrero Díaz 1989; Cifelli & Villarroel 1997; McGrath *et al.* 2020b). However, the possible affinities of these bunodont taxa with early litopterns and didolodontids had not been properly tested in phylogenetic analyses. This work presents such an analysis.

The new material described here substantially increased the information on the craniodental anatomy of *Megadolodus* and *Neodolodus* (Figs 2-8; Table 3), enabling us to better test the phylogenetic relationships of these taxa. We found no support of affinities of *Megadolodus* and *Neodolodus* with Didolondontidae. Instead, our results strongly support a close relationship between *Megadolodus* and *Neodolodus*. Based on the results of our phylogenetic analyses, we propose to include *Neodolodus* within Megadolodinae (Figs 9-11).

Megadolodinae is a clade of bunodont litopterns recorded in Neogene sediments of tropical South America (Cifelli & Villarroel 1997; Carlini *et al.* 2006; Carrillo *et al.* 2018). Studies on the palaeobiology of megadolodines indicate they inhabited tropical forests. Dental and postcranial evidence suggest that *Megadolodus* had a body size of 40-65 kg (Cifelli & Villarroel 1997; Croft 2016). The bunodont morphology suggests an omnivorous diet, including hard fruits (Cifelli & Villarroel 1997), which was also probably true for *Bonoudus* (Carlini *et al.* 2006). *Megadolodus* shows some similarities to living suids such as having large cheek teeth, protruding lower incisors, robust femora and short distal limb elements (Cifelli & Villarroel 1997). The small size, dental and postcranial anatomy of *Neodolodus* indicate cursorial adaptations and a browsing or frugivorous diet, similar to small cursorial and forest-dwelling living ungulates (e.g., tragulids) and rodents (e.g., agutis and pacas) (Cifelli & Guerrero Díaz 1989).

Given the uncertainties of the phylogenetic relationships of Megadolodinae within Litopterna (Figs 9-11), it is not possible to establish if the bunodont condition of megadolodines is the result of a reversal from a lophodont condition, or the retention of the plesiomorphic condition. *Megadolodus* and *Bounodus* (recorded in the late Miocene assemblage of Urumaco, Venezuela; Carlini *et al.* 2006; Bond & Gelfo 2010) had been previously included within Megadolodinae. Unfortunately, the fragmentary nature and poor preservation of the known material of *Bounodus* (Carlini *et al.* 2006) made it difficult to include it in phylogenetic analyses. Previous analyses supported a close relationship of *Neodolodus* with *Protheosodon* (McGrath *et al.* 2020a; McGrath *et al.* 2020b).

McGrath *et al.* (2020b) proposed a stem-based definition of Proterotheriidae: "Proterotheriidae is defined as the clade composed of *Tetramerorhinus lucarius* Ameghino, 1894, (*sensu* Soria 2001) and all litopterns more closely related to it than to *Macrauchenia patachonica* Owen, 1838, *Tricoelodus bicuspidatus* Ameghino, 1897, or *Protolipterna ellipsodontoides* Cifelli, 1983." The phylogenetic analysis of McGrath *et al.* (2020b) did not include macraucheniids (the clade to which *M. patachonica* belongs), whereas our taxon sampling includes three macraucheniids (*Polymorphis, Cramauchenia* and *Theosodon*).

Following the Protherotheriidae definition of McGrath *et al.* (2020b), it is unclear which node could represent Protherotheriidae in our phylogenetic analyses. The nodes A1, A2 and A3 (in Figs 9-11) include the advanced litopterns (all litopterns included in our analyses except protolipternids). The clades defined by these nodes include the macraucheniids *Polymorphis, Cramauchenia* and *Theosodon* and therefore do not correspond to Protheroriidae *sensu* McGrath *et al.* (2020b). The analysis of the extended matrix recovered a clade that includes Megadolodinae and the more derived proterotheriids to the exclusion of Macraucheniidae (node C, Fig. 9). However, this clade was not recovered in the analysis of the reduced matrix (Fig. 10). In fact, clades potentially corresponding to the definition of Proterotheriidae of McGrath *et al.* (2020b) strongly differ among our three analyses (node C in analysis with reduced matrix; node F2 in the parsimony analysis of extended matrix and node J in the Bayesian analysis of reduced matrix). Future studies that include a larger sample of macraucheniids may help to clarify the definition of Protherotheriidae, and whether Megadolodinae belongs to this clade.

Besides, we notice other major differences between the analyses using the extended (Fig. 9) and reduced (Fig. 10) matrices. Many of the subclades recovered within the clade including litopterns and close allies in the analysis of the extended matrix (node A1, Fig. 9), were not recovered in the analysis using the reduced matrix (node A2, Fig. 10). Only one subclade including the more derived proterotheriids was recovered in both parsimony analyses, but not in the Bayesian analysis, (nodes F1 [Fig. 9] and F2 [Fig. 10]), although their topologies differed. This indicates that most interrelationships within Litopterna are highly sensitive to coding strategies and character correlations. The three phylogenetic analyses are consistent in: 1) the recognition of a large clade that includes advanced litopterns to the exclusion of protolipternids (nodes A1 [Fig. 9] , A2 [Fig. 10] and A3 [Fig. 11]); 2) a clade formed by Macraucheniidae and *Proectocion*; and 3) a Megadolodinae clade.

McGrath *et al.* (2020b) recovered *Megadolodus* as the earliest diverging protherotheriid and *Adiantoides* as the second diverging taxon, a topology that requires a long ghost lineage for *Megadolodus* (Barrancan-Laventan SALMAs; *c.* 26 Ma; Appendix 4). *Neodolodus* was found more nested within Protherotheriidae, as sister taxa to *Protheosodon coniferus* (McGrath *et al.* 2020b: fig. 6). In contrast, most of our results support a later diverging position of Megadolodinae nested within a clade including most proterotheriids (Figs 9; 11), with an estimated time of origin of *c.* 14 Ma for the divergence time between *Megadolodus* and *Neodolodus*, as indicated by the Bayesian analysis (Fig. 11).

Systematics of Didolodontidae and Litopterna

Our phylogenetic analyses present several insights on the interrelationships of litopterns and some closely related SANU clades. The analyses using maximum parsimony (with the extended and reduced matrices) and the Bayesian analysis suggest varying affinities between Didolodontidae and Protolipternidae (Figs 9-11). Only the Bayesian analysis recovered Didolodontidae and Protolipternidae as sister clades (posterior support = 0.8).

Traditionally, Litopterna does not include Didolodontidae, but includes Protolipternidae and several other groups (Croft *et al.* 2020, and references therein). Our analyses failed to recover a monophyletic Litopterna, as we found that at least some members of Protolipternidae are closely related to Didolodontidae to the exclusion of other litopterns (Figs 9-11). As previously underlined by other authors (Billet *et al.* 2015), the monophyly of Litopterna remains to be properly tested with cladistic analyses using characters from different anatomical partitions and a large taxonomic sample. Although our character matrices include some postcranial characters (Cifelli 1993), most of the characters are from the dentition. Dental characters may show high levels of homoplasy (Sansom *et al.* 2016; Brocklehurst & Benevento 2020), and homoplasy in our analyses here is high (retention index is 0.688 in the extended matrix and 0.675 in the reduced matrix), which highlights the need for future analyses to include characters from different anatomical partitions (Billet *et al.* 2015).

Our analyses recovered *Proectocion*, traditionally classified within Adianthidae (Cifelli & Soria 1983; Croft *et al.* 2020), as a close relative to Macraucheniidae. Our taxonomic sampling reflects our goal to evaluate the relationships of Megadolodinae with didolodontids and other early diverging litopterns, as well as with proterotheriids. The taxonomic sampling and character scoring in our analyses were not suited to evaluate the relationships of Adianthidae within Litopterna, and the inclusion of additional adianthid taxa (e.g., *Adianthus, Proadianthus*) may confirm or refute their monophyly and potential affinities with macraucheniids.

Previous studies have evaluated the interrelationships within Macraucheniidae (Forasiepi *et al.* 2016; McGrath *et al.* 2018), but to our knowledge, only the work of Cifelli (1993) attempted

to evaluate the origins and relationships of Macraucheniidae within Litopterna. In this regard, our work is a preliminary contribution towards elucidating the interrelationships of litopterns and closely related SANUs (Kollpaniinae, Didolodontidae). Future studies might include more macraucheniids, but also modify and expand the character scoring to evaluate further the monophyly of Macraucheniidae and its relationships within Litopterna.

Anisolambidae and Indaleciidae were not recovered as monophyletic in any of the three analyses (Figs 9-11). As in previous studies (McGrath *et al.* 2020a; McGrath *et al.* 2020b), the three 'anisolambdid' taxa (*Paranisolambda, Anisolambda* and *Protheosodon*) were resolved in different branches (Figs 9-11). Therefore, our work shows that many aspects of the phylogenetic relationships and systematics within Litopterna deserve further analysis and call for more efforts in increasing anatomical and taxonomical sampling to make more progress regarding these long-standing issues.

Alternative approaches to character construction in Litopterna systematics

In our phylogenetic analyses, we tested two alternative approaches of character construction for serial characters on the dentition, since among-characters correlations in this anatomical partition may hinder phylogenetic constructions (Billet & Bardin 2019). The reductive coding approach scores characters separately assuming the observed morphological variations are independent, whereas the composite coding approach favours the construction of a single character when the observed variation is hypothesized to be biologically non-independent (Wilkinson 1995; Billet & Bardin 2019). Our analyses using the reductive and the composite coding approaches are congruent in the composition of nodes A1 and A2 (Figs 9-10) and a very limited number of other nodes (see above). However, the interrelationships within these clades varied substantially depending on the coding strategy, urging caution with regard to the phylogeny of this group. The sensitivity of our analyses to coding approaches highlights the importance of critical evaluation of character construction in morphological phylogenetics in general, and for litopterns in particular for which data matrices contain a wealth of serially repeated dental characters. Further research is also needed in that regard.

CONCLUSION

We report new material of *Megadolodus* and *Neodolodus* from La Venta, which clarifies the number of lower incisors in these taxa, and shows that the lower tusks are not lower canines as previously hypothesized. The relative low degree of dental wear undergone by the new specimens provided new information on their upper and lower dentition to reassess their phylogenetic relationships. The new fossil material described here supports a close relationship between *Megadolodus* and *Neodolodus* within Litopterna and no affinities with Didolodontidae. Our analyses unambiguously support the monophyly of Megadolodinae as a clade of bunodont Neotropical litopterns. While the discovery of the new remains enlightens part of the litoptern phylogeny, there are still significant uncertainties regarding many aspects of the phylogenetic interrelationships within Litopterna.

Acknowledgements

We thank the Servicio Geológico Colombiano for the permits to do the computed tomography on VPPLT 794. JDC was supported by the Swiss National Science Foundation Grant P400PB_186733 and P4P4PB_199187. This work was also supported by funds of the Smithsonian Tropical Research Institute and the Anders Foundation. Fieldwork conducted by AL, SBC, and MT was supported by a Leakey Foundation Research Grant and a National Geographic Society/Waitt Foundation Grant (Grant ID # 38715). We acknowledge the use of TNT sponsored by the Willi Henning Society. We thank M. Carvalho, C. Jaramillo, L. Mora, R. Vanegas and the group of Vigías del Patrimonio Paleonotológico La Tatacoa for valuable advice and assistance during fieldwork. We acknowledge the photos taken by D. Carvalho (VPPLT 1588; 794; 729), R. Vanegas (VPPLT 1696), P. Loubry (MNHN.F.VIV9) and D. Croft (UCMP 39270). We thank E. Cerdeño for sharing photos and information on the holotype of *A. leali*. We are grateful to A. Kramarz (MACN) and W. Simpson (FMNH) for sharing photos of *Cramauchenia* specimens, and J. Cantalapiedra for valuable comments. We thank A. Kramarz, an anonymous reviewer and the handling editor, E. Côtez, for constructive comments.

REFERENCES

Ameghino F. 1887. — Enumeración sistemática de las especies de mamíferos fósiles coleccionados por Carlos Ameghino en los terrenos eocenos de la Patagonia austral y depositados en el Museo La Plata. *Boletín del Museo de La Plata* 1: 1-26.

Ameghino F. 1889. — Contribución al conocimiento de los mamíferos fósiles de la República Argentina. *Actas Academia Nacional Ciencias Córdoba* 6: 1-1027. https://www.biodiversitylibrary.org/page/51769581

Ameghino F. 1894. — Énumération synoptique des espèces de mammifères fossiles des formations éocènes de Patagonie. *Boletín de la Academia Nacional de Ciencias de Córdoba* 13: 1-196. http://repositorio.anh.org.ar/jspui/handle/anh/397

Ameghino F. 1897. — Les mammifères crétacés de l'Argentine: deuxième contribution à la connaissance de la faune mammalogique des couches à *Pyrotherium*. *Boletin Instituto Geografico Argentino* 18: 406-521. http://repositorio.anh.org.ar/jspui/handle/anh/515

Benites-Palomino A., Aguirre-Fernández G., Moreno-Bernal J. W., Vanegas A. & Jaramillo C. 2020. — Miocene freshwater dolphins from La Venta, Huila, Colombia suggest independent Invasions of riverine environments in tropical South America. *Journal of Vertebrate Paleontology*: e1812078. https://doi.org/10.1080/02724634.2020.1812078

Billet G. & Bardin J. 2019. — Serial homology and correlated characters in morphological phylogenetics: modeling the evolution of dental crests in placentals. *Systematic Biology* 68 (2): 267-280. https://doi.org/10.1093/sysbio/syy071

Billet G. & Bardin J. 2021. — Segmental series and size: clade-wide investigation of molar proportions reveals a major evolutionary

allometry in the dentition of placental mammals. *Systematic Biology* 70 (6): 1101-1109. https://doi.org/10.1093/sysbio/syab007

Billet G., Muizon C. de, Schellhorn R., Ruf I., Ladevèze S. & Bergqvist L. 2015. — Petrosal and inner ear anatomy and allometry amongst specimens referred to Litopterna (Placentalia). *Zoological Journal of the Linnean Society* 173 (4): 956-987. https://doi.org/10.1111/zoj.12219

Bonaparte J. F. & Morales J. 1997. — An early Notonychopidae (Litopterna) from the Lower Paleocene of Punta Peligro, Chubut, Argentina. *Estudios Geologicos* 53 (5): 263-274. https://doi.org/10.3989/egeol.97535-6232

Bond M. & Gelfo J. N. 2010. — The South American Native Ungulates of the Urumaco Formation, *in* Sánchez-Villagra M. R., Aguilera O. A. & Carlini A. A. (eds), *Urumaco & Venezuelan Paleontology. The Fossil Record of the Northern Neotropics*. Bloomington & Indianapolis, Indiana University Press: 256-268.

Bond M. & Vucetich M. G. 1983. — *Indalecia grandensis* gen. et. sp. nov del Eoceno temprano del Noroeste argentino, tipo de una nueva subfamilia de los Adianthidae (Mammalia, Litopterna). *Asociación Geológica Argentina, Revista* 38 (1): 107-117

Bond M., Perea D., Ubilla M. & Tauber A. 2001. — *Neolicaphrium recens* frenguelli, 1921, the only surviving Proterotheriidae (Litopterna, Mammalia) into the South American Pleistocene. *Palaeovertebrata* 30 (1-2): 37-50.

Bouckaert R., Vaughan T. G., Barido-Sottani J., Duchêne S., Fourment M., Gavryushkina A., Heled J., Jones G., Kühnert D., Maio N. D., Matschiner M., Mendes F. K., Müller N. F., Ogilvie H. A., Plessis L. du, Popinga A., Rambaut A., Rasmussen D., Siveroni I., Suchard M. A., Wu C.-H., Xie D., Zhang C., Stadler T. & Drummond A. J. 2019. — BEAST 2.5: An advanced software platform for Bayesian evolutionary analysis. *PLOS Computational Biology* 15 (4): e1006650. https://doi.org/10.1371/journal.pcbi.1006650

Brocklehurst N. & Benevento G. L. 2020. — Dental characters used in phylogenetic analyses of mammals show higher rates of evolution, but not reduced independence. *PeerJ* 8: e8744. https://doi.org/10.7717/peerj.8744

Buckley M. 2015. — Ancient collagen reveals evolutionary history of the endemic South American 'ungulates'. *Proceedings of Royal Society of Biology* 282 (1806): 20142671. https://doi.org/10.1098/rspb.2014.2671

Cardini A. 2019. — Craniofacial allometry is a rule in evolutionary radiations of placentals. *Evolutionary Biology* 46 (3): 239-248. https://doi.org/10.1007/s11692-019-09477-7

Cardini A. & Polly P. D. 2013. — Larger mammals have longer faces because of size-related constraints on skull form. *Nature Communications* 4: 2458. https://doi.org/10.1038/ncomms3458

Carlini A. A., Gelfo J. N. & Sánchez R. 2006. — A new Megadolodinae (Mammalia, Litopterna, Protherotheriidae) from the Urumaco Formation (Late Miocene) of Venezuela. *Journal of Systematic Palaeontology* 4 (3): 279-284. https://doi.org/10.1017/S1477201906001830

Carrillo J. D. & Asher R. J. 2017. — An exceptionally well-preserved skeleton of *Thomashuxleya externa* (Mammalia, Notoungulata), from the Eocene of Patagonia, Argentina. *Paleontologia Electronica* 20.2.34.A: 1-33. https://doi.org/10.26879/759

Carrillo J. D., Amson E., Jaramillo C., Sánchez R., Quiroz L., Cuartas C., Rincón A. F. & Sánchez-Villagra M. R. 2018. — The Neogene Record of Northern South American Native Ungulates. *Smithsonian Contributions to Paleobiology* 101: 1-67. https://doi.org/10.5479/SI.1943-6688.101

Carrillo J. D., Suarez C., Benites-Palomino A., Vanegas A., Link A., Rincon A. F., Luque J., Cooke S. B., Tallman M. & Billet G. 2022. — 3D models related to the publication: New remains of Neotropical bunodont litopterns and the systematics of Megadolodinae (Mammalia: Litopterna). *MorphoMuseuM* 8: 174. https://doi.org/10.18563/journal.m3.174

Cifelli R. L. 1983. — The origin and affinities of the South American Condylarthra and early Tertiary Litopterna (Mammalia). *American Museum Novitates* 2772: 1-49. http://hdl.handle.net/2246/5256

Cifelli R. L. 1993. — The phylogeny of the native South American ungulates, *in* Szalay F. S., Novacek M. J. & McKenna M. C. (eds), *Mammal Phylogeny: Placentals*. New York, Springer-Verlag: 195-214.

Cifelli R. L. & Guerrero Díaz J. 1989. — New remains of *Prothoatherium colombianus* (Litopterna, Mammalia) from the Miocene of Colombia. *Journal of Vertebrate Paleontology* 9 (2): 222-231. https://www.jstor.org/stable/4523257

Cifelli R. L. & Guerrero J. 1997. — Litopterns, *in* Kay R. F., Madden R. H., Cifelli R. L. & Flynn J. J. (eds), *Vertebrate Paleontology in the Neotropics. The Miocene Fauna of La Venta, Colombia*. Smithsonian Institution Press, Washington and London: 289-302.

Cifelli R. L. & Ortiz-Jaureguizar E. 2014. — *Depaulacoutoia*, a replacement name for *Paulacoutoia* Cifelli, 1983, a preoccupied name. *Journal of Vertebrate Paleontology* 34 (3): 730-730. https://doi.org/10.1080/02724634.2013.820194

Cifelli R. L. & Soria M.F. 1983. — Systematics of the Adianthidae (Litopterna, Mammalia). *American Museum Novitates* 2771: 1-25. http://hdl.handle.net/2246/5255

Cifelli R. L. & Villarroel C. 1997. — Paleobiology and affinites of *Megadolodus*, *in* Kay R. F., Madden R. H., Cifelli R. L. & Flynn J. J. (eds), *Vertebrate Paleontology in the Neotropics. The Miocene Fauna of La Venta, Colombia*. Smithsonian Institution Press, Washington and London: 265-288.

Cione A. L. & Tonni E. P. 1995. — Chronostratigraphy and 'Land-Mammal Ages' in the Cenozoic of southern South America: principles , practices , and the 'Uquian' problem. *Journal of Paleontology* 69 (1): 135-159. https://doi.org/10.2307/1306287

Corona A., Perea D. & Ubilla M. 2019. — A new genus of Proterotheriinae (Mammalia, Litopterna) from the Pleistocene of Uruguay. *Journal of Vertebrate Paleontology* 39 (1). https://doi.org/10.1080/02724634.2019.1567523

Croft D. A. 2001. — Cenozoic environmental change in South America as indicated by mammalian body size distributions (cenograms). *Diversity and Distributions* 7: 271-287. https://doi.org/10.1046/j.1366-9516.2001.00117.x

Croft D. A. 2016. — *Horned Armadillos and Rafting Monkeys: The Fascinating Fossil Mammals of South America*. Bloomington and Indianapolis, Indiana University Press, 304 p. https://www.jstor.org/stable/j.ctt1ch76w4

Croft D. A. & López G. 2020. — Gondwanan perspectives: evolution, biogeography, and paleoecology of the native ungulates of South America. *Ameghiniana* 57 (2): 71-79. https://doi.org/10.5710/amgh.15.04.2020.3351

Croft D. A., Gelfo J. N. & López G. M. 2020. — Splendid innovation: the extinct South American native ungulates. *Annual Review of Earth and Planetary Sciences* 48 (1): 259-290. https://doi.org/10.1146/annurev-earth-072619-060126

Cuitiño J. I., Fernicola J. C., Kohn M. J., Trayler R., Naipauer M., Bargo M. S., Kay R. F. & Vizcaíno S. F. 2016. — U-Pb geochronology of the Santa Cruz Formation (early Miocene) at the Río Bote and Río Santa Cruz (southernmost Patagonia, Argentina): Implications for the correlation of fossil vertebrate localities. *Journal of South American Earth Sciences* 70: 198-210. https://doi.org/10.1016/j.jsames.2016.05.007

Defler T. 2019. — *History of Terrestrial Mammals in South America: How South American Mammalian Fauna Changed from Mesozoic to Recent Times*. Vol. 42. Cham, Springer International Publishing. 372 p. (Topics in Geobiology). https://doi.org/10.1007/978-3-319-98449-0

Dozo M. T. & Vera B. 2010. — First skull and associated postcranial bones of Macraucheniidae (Mammalia, Litopterna) from the Deseadan SALMA (late Oligocene) of Cabeza Blanca (Chubut, Argentina). *Journal of Vertebrate Paleontology* 30 (6): 1818-1826. https://www.jstor.org/stable/25790806

DUNN R. E., MADDEN R. H., KOHN M. J., SCHMITZ M. D., STRÖMBERG C. A. E., CARLINI A. A., RÉ G. H. & CROWLEY J. 2013. — A new chronology for middle Eocene-early Miocene South American Land Mammal Ages. *Bulletin of the Geological Society of America* 125 (3-4): 539-555. https://doi.org/10.1130/B30660.1

FLYNN J. J., GUERRERO J. & SWISHER C. C. 1997. — Geochronology of the Honda group, *in* KAY R. F., MADDEN R. H., CIFELLI R. L. & FLYNN J. J. (eds), *Vertebrate Paleontology in the Neotropics. The Miocene Fauna of La Venta, Colombia*. Smithsonian Institution Press, Washington and London: 44-59.

FORASIEPI A. M., MACPHEE R. D. E., HERNÁNDEZ DEL PINO S., SCHMIDT G. I., AMSON E. & GROHÉ C. 2016. — Exceptional skull of *Huayqueriana* (Mammalia, Litopterna, Macraucheniidae) from the late Miocene of Argentina: anatomy, systematics, and paleobiological implications. *Bulletin of American Musem of Natural History* 404: 1-76. https://doi.org/10.5531/sd.sp.23

GAUDRY A. 1904. — Fossiles de Patagonie. Dentition de quelques mammifères. *Mémoires de la Société géologique de France. Paléontologie* 31: 1-27. https://doi.org/10.5962/bhl.title.86388

GEARTY W. 2022. — Willgearty/deeptime: v0.2.2. https://doi.org/10.5281/zenodo.6560750

GELFO J. N. 2004. — A new South American mioclaenid (Mammalia : Ungulatomorpha) from the Tertiary of Patagonia , Argentina. *Ameghiniana* 41 (3): 475-484.

GELFO J. N. 2007. — The 'Condylarth' Raulvaccia peligrensis (Mammalia: Didolodontidae) from the Paleocene of Patagonia, Argentina. *Journal of Vertebrate Paleontology* 27 (3): 651-660. https://doi.org/10.1671/0272-4634(2007)27[651:TCRPMD]2.0.CO;2

GELFO J. N. 2010. — The 'condylarth' Didolodontidae from Gran Barranca: history of the bunodont South American mammals up to the Eocene-Oligocene transition, *in* MADDEN R. H., CARLINI A. A., VUCETICH M. G. & KAY R. F. (eds), *The Paleontology of Gran Barranca. Evolution and Environmental Change through the middle Cenozoic of Patagonia*. Cambridge, Cambridge University Press: 130-142.

GELFO J., ALONSO R., MADDEN R. & CARLINI A. 2020. — An Eocene bunodont South American native ungulate (Didolodontidae) from the Lumbrera Formation, Salta Province, Argentina. *Ameghiniana* 57 (2): 132-145. https://doi.org/10.5710/amgh.29.11.2019.3293

GOLOBOFF P. A. & CATALANO S. A. 2016. — TNT version 1.5, including a full implementation of phylogenetic morphometrics. *Cladistics* 32 (3): 221-238. https://doi.org/10.1111/cla.12160

GOLOBOFF P. A., FARRIS J. S. & NIXON K. C. 2008. — TNT, a free program for phylogenetic analysis. *Cladistics* 24 (5): 774-786. https://doi.org/10.1111/j.1096-0031.2008.00217.x

GOLOBOFF P. A., PITTMAN M., POL D. & XU X. 2019. — Morphological Data Sets Fit a Common Mechanism Much More Poorly than DNA Sequences and Call Into Question the Mkv Model. *Systematic Biology* 68 (3): 494-504. https://doi.org/10.1093/sysbio/syy077

GRAND A., CORVEZ A., DUQUE VELEZ L. M. & LAURIN M. 2013. — Phylogenetic inference using discrete characters: performance of ordered and unordered parsimony and of three-item statements. *Biological Journal of the Linnean Society* 110 (4): 914-930. https://doi.org/10.1111/bij.12159

GUERRERO J. 1997. — Stratigraphy, sedimentary environments, and the Miocene uplift of the Colombian Andes, *in* KAY R. F., MADDEN R. H., CIFELLI R. L. & FLYNN J. J. (eds), *Vertebrate Paleontology in the Neotropics. The Miocene Fauna of La Venta*. Smithsonian Institution Press, Washington and London: 15-43.

HEATH T. A., HUELSENBECK J. P. & STADLER T. 2014. — The fossilized birth-death process for coherent calibration of divergence-time estimates. *Proceedings of the National Academy of Sciences of the United States of America* 111 (29): e2957-66. https://doi.org/10.1073/pnas.1319091111

HOFFSTETTER R. & SORIA M. F. 1986. — *Neodolodus colombianus* gen. et sp. nov., un nouveau Condylarthre (Mammalia) dans le Miocène de Colombie. *Comptes Rendus de l'Académie des Sciences, série 2,* 303, *Mécanique-physique, Chimie, Sciences de l'Univers, Sciences de la Terre* 17: 1619-1622. https://gallica.bnf.fr/ark:/12148/bpt6k5664058j/f1625.item

JERNVALL J. 1995. — Mammalian molar cusp patterns: developmental mechanisms of diversity. *Acta Zoologica Fennica* 198: 1-61

JERNVALL J. 2000. — Linking development with generation of novelty in mammalian teeth. *Proceedings of the National Academy of Sciences* 97 (6): 2641-2645. https://doi.org/10.1073/pnas.050586297

KAY R. F. & MADDEN R. H. 1997. — Mammals and rainfall: paleoecology of the middle Miocene at La Venta (Colombia, South America). *Journal of Human Evolution* 32 (2-3): 161-199. https://doi.org/10.1006/jhev.1996.0104

KAY R. F., MADDEN R. H., CIFELLI R. L. & FLYNN J. J. (eds) 1997. — *Vertebrate Paleontology in the Neotropics. The Miocene Fauna of La Venta, Colombia*. Smithsonian Instituion Press, Washington and London, 592 p.

KRAMARZ A. G. & BOND M. 2005. — Los Litopterna (Mammalia) de la Formación Pinturas, Mioceno Temprano-Medio de Patagonia. *Ameghiniana* 42 (3): 30-39. http://ref.scielo.org/tr9f9h

KRAMARZ A. G. & MACPHEE R. D. E. 2022. — Did some extinct South American native ungulates arise from an afrothere ancestor? A critical appraisal of Avilla and Mothé's (2021) Sudamericungulata – Panameridiungulata hypothesis. *Journal of Mammalian Evolution* 30: 67-77. https://doi.org/10.1007/s10914-022-09633-5

KRAMARZ A. G., BOND M. & ROUGIER G. W. 2017. — Redescription of the auditory region of the putative basal astrapothere (Mammalia) *Eoastrapostylops riolorense* Soria and Powell, 1981. Systematic and phylogenetic considerations. *Annals of Carnegie Museum* 84 (2): 95-164. https://doi.org/10.2992/007.084.0204

LEWIS P. O. 2001. — A likelihood approach to estimating phylogeny from discrete morphological character data. *Systematic Biology* 50 (6): 913-25. https://doi.org/10.1080/106351501753462876

LINNAEUS C. 1758. — *Systema Naturae per Regna Tria Naturae, Secundum Classes, Ordines, Genera, Species cum Caracteribus, Differentiis, Synonymis, Locis*. Vol. I. Stockholm, Laurentii Salvii, 824 p. https://doi.org/10.5962/bhl.title.559

LÖSEL P. D., VAN DE KAMP T., JAYME A., ERSHOV A., FARAGÓ T., PICHLER O., TAN JEROME N., AADEPU N., BREMER S., CHILINGARYAN S. A., HEETHOFF M., KOPMANN A., ODAR J., SCHMELZLE S., ZUBER M., WITTBRODT J., BAUMBACH T. & HEUVELINE V. 2020. — Introducing Biomedisa as an open-source online platform for biomedical image segmentation. *Nature Communications* 11 (1): 5577. https://doi.org/10.1038/s41467-020-19303-w

MADDEN R. H., GUERRERO J., KAY R. F., FLYNN J. J., SWISHER III C. C. & WALTON A. H. 1997. — The Laventan Stage and Age, *in* KAY R. F., MADDEN R. H., CIFELLI R. L. & FLYNN J. J. (eds), *Vertebrate Paleontology in the Neotropics. The Miocene Fauna of La Venta, Colombia*. Smithsonian Institution Press, Washington and London: 355-381.

MCGRATH A. J., ANAYA F. & CROFT D. A. 2018. — Two new macraucheniids (Mammalia: Litopterna) from the late middle Miocene (Laventan South American Land Mammal Age) of Quebrada Honda, Bolivia. *Journal of Vertebrate Paleontology*: e1461632. https://doi.org/10.1080/02724634.2018.1461632

MCGRATH A., ANAYA F. & CROFT D. 2020a. — New Proterotheriids from the middle Miocene of Quebrada Honda, Bolivia, and body size and diversity trends in Proterotheriid and Macraucheniid Litopterns (Mammalia). *Ameghiniana* 57 (2): 159-188. https://doi.org/10.5710/amgh.03.03.2020.3268

MCGRATH A. J., FLYNN J. J. & WYSS A. R. 2020b. — Proterotheriids and macraucheniids (Litopterna: Mammalia) from the Pampa Castillo Fauna, Chile (early Miocene, Santacrucian SALMA) and a new phylogeny of Proterotheriidae. *Journal of Systematic Palaeontology* 18 (9): 717-738. https://doi.org/10.1080/14772019.2019.1662500

MCKENNA M. C. 1956. — Survival of primitive notoungulates and condylarths into the Miocene of Colombia. *American Journal of Science* 254: 736-743. https://doi.org/10.2475/ajs.254.12.736

McKenna M. C. 1975. — Toward a Phylogenetic Classification of the Mammalia, *in* Luckett W. P. & Szalay F. S. (eds), *Phylogeny of the Primates*. Springer, Boston: 21-46. https://doi.org/10.1007/978-1-4684-2166-8_2

McKenna M. C. & Bell S. K. 1997. — *Classification of Mammals above the Species Level*. Columbia University Press, New York, 631 p.

Mones A. 2015. — *Ricardocifellia*, a replacement name for *Paulacoutoia* Cifelli, 1983, and *Depaulacoutoia* Cifelli and Ortiz-Jaureguizar, 2014 (Mammalia, 'Condylarthra,' Didolodontidae), and the status of *Depaulacoutoia* Kretzoi and Kretzoi, 2000 (Mammalia, Australidelphia, Polydolopimorphia). *Journal of Vertebrate Paleontology* 35 (5): e973571. https://doi.org/10.1080/02724634.2015.973571

Montes C., Silva C. A., Bayona G. A., Villamil R., Stiles E., Rodriguez-Corcho A. F., Beltran-Triviño A., Lamus F., Muñoz-Granados M. D., Perez-Angel L. C., Hoyos N., Gomez S., Galeano J. J., Romero E., Baquero M., Cardenas-Rozo A. L., Von Quadt A., Ballato P., Maria Pinto Gama C., Matano F., J G. J. & Quadt von A. 2021. — A Middle to Late Miocene Trans-Andean Portal: Geologic Record in the Tatacoa Desert. *Frontiers in Earth Science* 8: 643. https://doi.org/10.3389/feart.2020.587022

Mora-Rojas L., Cárdenas A., Jaramillo C., Silvestro D., Bayona G., Zapata S., Moreno F., Silva C., Moreno-Bernal J. W., Jaramillo J. S., Valencia V. & Ibañez M. 2023. — Stratigraphy of a middle Miocene neotropical Lagerstätte (La Venta Site, Colombia). *Geodiversitas* 45 (6): 197-221. https://doi.org/10.5252/geodiversitas2023v45a6. http://geodiversitas.com/45/6

Muizon C. de & Cifelli R. L. 2000. — The 'condylarths' (archaic Ungulata, Mammalia) from the early Palaeocene of Tiupampa (Bolivia): implications on the origin of the South American ungulates. *Geodiversitas* 22 (1): 47-150.

Muizon C. de, Billet G., Argot C., Ladeveze S. & Goussard F. 2015. — *Alcidedorbignya inopinata*, a basal pantodont (Placentalia, Mammalia) from the early Palaeocene of Bolivia: anatomy, phylogeny and palaeobiology. *Geodiversitas* 37 (4): 397-634. https://doi.org/10.5252/g2015n4a1

Muizon C. de, Billet G. & Ladevèze S. 2019. — New remains of kollpaniine "condylarths" (Panameriungulata) from the early Palaeocene of Bolivia shed light on hypocone origins and molar proportions among ungulate-like placentals. *Geodiversitas* 41 (25): 841-874. https://doi.org/10.5252/geodiversitas2019v41a25. http://geodiversitas.com/41/25

Müller N. F. & Bouckaert R. 2019. — Coupled MCMC in BEAST 2. https://doi.org/10.1101/603514

O'Leary M. A., Bloch J. I., Flynn J. J., Gaudin T. J., Giallombardo A., Giannini N. P., Goldberg S. L., Kraatz B. P., Luo Z., Meng J., Ni X., Novacek M. J., Perini F. A., Randall Z. S., Rougier G. W., Sargis E. J., Silcox M. T., Simmons N. B., Spaulding M., Velazco P. M., Weksler M., Wible J. R. & Cirranello A. L. 2013. — The placental mammal ancestor and the post-K-Pg radiaton of placentals. *Science* 339 (6120): 662-667. https://doi.org/10.1126/science.1229237

Owen R. 1838. — Fossil Mammalia, *in The Zoology of the Voyage of the* HMS Beagle *under the Command of Captain Fitzroy, during the Years 1832 to 1836.* Vol. 1. Smith, Elder and Co., London: 13-40. https://doi.org/10.5962/bhl.title.109909

Owen R. 1837a. — A description of the cranium of the *Toxodon platensis*, a gigantic extinct mammiferous species, referrible by its dentition to the Rodentia, but with affinities to the Pachydermata and the herbivorous Cetacea. *Proceeding of the Geological Society* 2: 541-542. https://www.biodiversitylibrary.org/page/33880245

Owen R. 1837b. — Mammalia, *in The Cyclopaedia of Anatomy and Physiology*. Vol. III. Gilbert & Piper London, Sherwood: 234-244. https://www.biodiversitylibrary.org/page/848631

Paula Couto C. de 1952. — Fossil mammals from the beginning of the Cenozoic in Brazil: Condylarthra, Litopterna, Xenungulata and Astrapotheria. *Bulletin of the American Museum of Natural History* 99 (6): 355-394. http://hdl.handle.net/2246/417

Prevosti F. J., Romano C. O., Forasiepi A. M., Hemming S., Bonini R., Candela A. M., Cerdeño E., Madozzo Jaén M. C., Ortiz P. E., Pujos F., Rasia L., Schmidt G. I., Tagliorretti M., MacPhee R. D. E. & Pardiñas U. F. J. 2021. — New radiometric 40Ar-39Ar dates and faunistic analyses refine evolutionary dynamics of Neogene vertebrate assemblages in southern South America. *Scientific Reports* 11 (1): 9830. https://doi.org/10.1038/s41598-021-89135-1

Rambaut A., Drummond A. J., Xie D., Baele G. & Suchard M. A. 2018. — Posterior summarization in Bayesian phylogenetics using Tracer 1.7. *Systematic Biology* 67 (5): 901-904. https://doi.org/10.1093/sysbio/syy032

Revell L. J. 2012. — Phytools: an R package for phylogenetic comparative biology (and other things). *Methods in Ecology and Evolution* 3 (2): 217-223. https://doi.org/10.1111/j.2041-210X.2011.00169.x

Rovereto C. 1914. — Los Estratos Araucanos y sus fósiles. *Anales del Museo Nacional de Historia Natural de Buenos Aires.* 25: 1-249

Sansom R. S., Wills M. A. & Williams T. 2016. — Dental data perform relatively poorly in reconstructing mammal phylogenies: Morphological partitions evaluated with molecular benchmarks. *Systematic Biology*: syw116. https://doi.org/10.1093/sysbio/syw116

Schmidt G. I. 2015. — Actualización sistemática y filogenia de los Proterotheriidae (Mammalia, Litopterna) del 'Mesopotamiense' (Mioceno tardío) de Entre Ríos, Argentina. *Revista Brasileira de Paleontologia* 18 (3): 521-546. https://doi.org/10.4072/rbp.2015.3.14

Schmidt G. I. & Ferrero B. S. 2014. — Taxonomic reinterpretation of *Theosodon hystatus* Cabrera and Kraglievich, 1931 (Litopterna, Macraucheniidae) and phylogenetic relationships of the family. *Journal of Vertebrate Paleontology* 34 (5): 1231-1238. https://doi.org/10.1080/02724634.2014.837393

Schmidt G. I., Cerdeño E. & Pino S. H. D. 2019a. — Macraucheniidae and Proterotheriidae (Mammalia, Litopterna) from Quebrada Fiera (Late Oligocene), Mendoza Province, Argentina. *Andean Geology* 46 (2): 368-382. https://doi.org/10.5027/andgeoV46n2-3109

Schmidt G. I., Hernández del Pino S., Muñoz N. A. & Fernández M. 2019b. — Litopterna (Mammalia) from the Santa Cruz Formation (Early-Middle Miocene) at the Río Santa Cruz, Southern Argentina. *Publicación Electrónica de la Asociación Paleontológica Argentina* 19 (2): 170-192. https://doi.org/10.5710/PEAPA.13.08.2019.290

Scott W. B. 1910. — *Mammalia of the Santa Cruz Beds.* Part I. *Litopterna.*, *Reports of the Princeton University Expeditions to Patagonia (1896-1899)*. Vol. 7. Schweizerbartsche Verlaghandlung (E. Nagele), Princeton and Stuttgart, 156 p.

Simpson G. G. 1948. — The beginning of the age of mammals in South America. Part 1, Introduction. Systematics: Marsupialia, Edentata, Condylarthra, Litopterna, and Notioprogonia. *Bulletin of the American Museum of Natural History* 91 (1): 215-216. https://doi.org/10.1007/s10914-010-9153-7

Simpson G. G. 1980. — *Splendid Isolation. The Curious History of South American Mammals*. Yale University Press, New Haven and London, 266 p.

Simpson G. G. & Minoprio J. L. 1949. — A new Adianthinae Liptoptern and associated mammals from a Deseadan faunule in Mendoza, Argentina. *American Museum Novitates* 1434: 1-27. http://hdl.handle.net/2246/2349

Skinner M. M. & Gunz P. 2010. — The presence of accessory cusps in chimpanzee lower molars is consistent with a patterning cascade model of development. *Journal of Anatomy* 217 (3): 245-253. https://doi.org/10.1111/j.1469-7580.2010.01265.x

Smith J. B. & Dodson P. 2003. — A proposal for a standard terminology of anatomical notation and orientation in fossil vertebrate dentitions. *Journal of Vertebrate Paleontology* 23 (1): 1-12. https://doi.org/10.1671/0272-4634(2003)23[1:APFAST]2.0.CO;2

Soria M. F. 1981. — Los Litopterna del Colhuehuapense (Oligoceno tardío) de la Argentina. *Revista del Museo Argentino de Ciencias Naturales "Bernardino Rivadavia"* 3: 1-54

Soria M. F. 2001. — Los Proterotheriidae (Litopterna, Mammalia), sistemática, origen y filogenia. *Monografías del Museo Argentino de Ciencias Naturales* 1: 1-167

Spradley J. P., Glazer B. J. & Kay R. F. 2019. — Mammalian faunas, ecological indices, and machine-learning regression for the purpose of paleoenvironment reconstruction in the Miocene of South America. *Palaeogeography, Palaeoclimatology, Palaeoecology* 518: 155-171. https://doi.org/10.1016/j.palaeo.2019.01.014

Stadler T. 2010. — Sampling-through-time in birth-death trees. *Journal of Theoretical Biology* 267 (3): 396-404. https://doi.org/10.1016/j.jtbi.2010.09.010

Ubilla M., Perea D., Bond M. & Rinderknecht A. 2011. — The first cranial remains of the Pleistocene Proterotheriid *Neolicaphrium* Frenguelli, 1921 (Mammalia, Litopterna): a comparative approach. *Journal of Vertebrate Paleontology* 31 (1): 193-201. https://doi.org/10.1080/02724634.2011.539647

Villafañe A. L., Ortiz-Jaureguizar E. & Bond M. 2006. — Cambios en la riqueza taxonómica y en las tasas de primera y última aparición de los Proterotheriidae (Mammalia, Litopterna) durante el Cenozoico. *Estudios Geológicos* 62 (1): 155-166. https://doi.org/10.3989/egeol.0662115

Villafañe A. L., Schmidt G. I. & Cerdeño E. 2012. — Consideraciones sistemáticas y bioestratigráficas acerca de *Thoatheriopsis mendocensis* Soria, 2001 (Litopterna, Proterotheriidae). *Ameghiniana* 49 (3): 365-374. http://hdl.handle.net/11336/71246

Welker F., Collins M. J., Thomas J. A., Wadsley M., Brace S., Cappellini E., Turvey S. T., Reguero M., Gelfo J. N., Kramarz A., Burger J., Thomas-Oates J., Ashford D. A., Ashton P. D., Rowsell K., Porter D. M., Kessler B., Fischer R., Baessmann C., Kaspar S., Olsen J. V, Kiley P., Elliott J. A., Kelstrup C. D., Mullin V., Hofreiter M., Willerslev E., Hublin J.-J., Orlando L., Barnes I. & MacPhee R. D. E. 2015. — Ancient proteins resolve the evolutionary history of Darwin's South American ungulates. *Nature* 522: 81-84. https://doi.org/10.1038/nature14249

Westbury M., Baleka S., Barlow A., Hartmann S., Paijmans J. L. A., Kramarz A., Forasiepi A. M., Bond M., Gelfo J. N., Reguero M. A., López-Mendoza P., Taglioretti M., Scaglia F., Rinderknecht A., Jones W., Mena F., Billet G., De Muizon C., Aguilar J. L., MacPhee R. D. E. & Hofreiter M. 2017. — A mitogenomic timetree for Darwin's enigmatic South American mammal *Macrauchenia patachonica*. *Nature Communications* 8: 15951. https://doi.org/10.1038/ncomms15951

Wilkinson M. 1995. — A comparison of two methods of character construction. *Cladistics* 11 (3): 297-308. https://doi.org/10.1111/j.1096-0031.1995.tb00091.x

Williamson T. E. & Carr T. D. 2007. — *Bomburia* and *Ellipsodon* (Mammalia: Mioclaenidae) from the early Paleocene of New Mexico. *Journal of Paleontology* 81 (5): 966-985. https://doi.org/10.1666/pleo05-116.1

Woodburne M. O., Goin F. J., Bond M., Carlini A. A., Gelfo J. N., López G. M., Iglesias A. & Zimicz A. N. 2014. — Paleogene land mammal faunas of South America; a response to global climatic changes and indigenous floral diversity. *Journal of Mammalian Evolution* 21 (1): 1-73. https://doi.org/10.1007/s10914-012-9222-1

Yu G., Smith D. K., Zhu H., Guan Y. & Lam T. T.-Y. 2017. — ggtree: an r package for visualization and annotation of phylogenetic trees with their covariates and other associated data. *Methods in Ecology and Evolution* 8 (1): 28-36. https://doi.org/10.1111/2041-210X.12628

Zanesco T., Bergqvist L. P. & Pereira Á. A. 2019. — Intraspecific variation of one of the oldest Litopterna (Mammalia), *Protolipterna ellipsodontoides*, and redescription of the species. *Ameghiniana* 56 (5): 380-401. https://doi.org/10.5710/AMGH.11.08.2019.3250

Submitted on 26 July 2022;
accepted on 24 February 2023;
published on 31 August 2023.

APPENDICES

APPENDIX 1. — Taxon list, specimens, and references.

Photos of casts of specimens previously described from La Venta (Cifelli & Guerrero 1997) were kindly provided by A. McGrath. Unless otherwise state it in Appendices 2 and 3, we maintained the character scores for protherotheriid taxa of McGrath *et al.* (2020b).

Adiantoides leali
Pictures of MCNAM-PV 3004, kindly provided by Esperanza Cerdeño and Guillermo Campos, director of the Museo de Ciencias Naturales y Antropológicas J.C. Moyano (Simpson & Minoprio 1949; Cifelli & Soria 1983).

Anisolophus australis
Descriptions and figures of Scott (1910) and Soria (2001), and the revision of the following specimens: YPM PU 15368, YPM PU 15996, and MNHN.F.SCZ208.

Anisolophus floweri
Descriptions and figures of Scott (1910) and Soria (2001).

Asmithwoodwardia scotti
Photos and casts of DGM 358M (holotype) (Paula Couto 1952).

Brachytherium cuspidatum
Photos of MLP 70-I-10-3, and descriptions and figures of Soria (2001).

Cramauchenia normalis
Description, illustrations and photographs of MPEF-PV 2524, MACN A-52-219 (lectotype), MACN A-52-220 (paralectotype), MACN A-52-221, MACN A-52-233, MACN A-52-235, FMNH P13292 , FMNH P13293, FMNH P13301, FMNH P13586 (Soria 1981; Cifelli 1983; Dozo & Vera 2010).

Diadiaphorus majusculus
Descriptions and figures of Scott (1910) and Soria (2001), and the revision of the following specimens: MNHN.F.SCZ207, MNHN-1900-18 (uncatalogued MNHN.F.SCZ fossil), MLP 12-296, MLP 12-299, MLP 12-304.

Didolodus multicuspis
Cast of MACN A 10689 and MACN A 10690.

Indalecia grandensis
Description of PVL 4186, and PVL S-12 (Bond & Vucetich 1983).

Lambdaconus lacerum
MNHN.F.COL109, and description and illustrations of MACN A-52-246 (holotype), MACN A-52-247 (paratype), and MACN 18785 (cast of FMNH P 13432) (Gaudry 1904; Soria 2001).

Lambdaconus suinus
MNHN.F.DES159 and description and illustrations of MACN A-52-159, MACN A-12198, MACN A-12655, AMNH 29554 (Soria 2001; Schmidt *et al.* 2019a).

Lamegoia conodonta
Casts of MNRJ 1463-V (holotype), 1464V, and 1465V (paratypes). (Paula Couto 1952; Cifelli 1983).

Miguelsoria parayirunhor
Photos and casts of DGM 330M, DGM 397 M, DGM 402 M, DGM 966M, (Paula Couto 1952; Cifelli 1983). All the specimens have a cream and yellowish color indicating they come from the 'white fossil fissures' of Itaborai, and its referral to *Miguelsoria* is further supported by size and taxon abundance (Billet *et al.* 2015).

Megadolodus molariformis
VPPLT 974, VPPLT 1588. Photos of UCMP 39270 (holotype) kindly provided by D. Croft. Photos of casts of IGM 183282, IGM 183544, IGM 184019, TATAC 1, and TATAC 2 (McKenna 1956; Cifelli & Villarroel 1997).

Mesolicaphrium sanalfonense
VPPLT 1697, MNHN.F.VIV5. Photos of casts of IGM 182852, IGM 183246, IGM 183620, IGM 184499, IGM 250873, and UCMP 39254 (Cifelli & Guerrero 1997; McGrath *et al.* 2020a).

Neobrachytherium morenoi
MACN 8428 (holotype), MACN 8431 as described and figured by Soria (2001) and Rovereto (1914).

Neodolodus colombianus
MNHN.F.VIV9 (holotype), VPPLT 183, VPPLT 184, VPPLT 1696. Photos of casts of Duke-ING 86093, Duke ING 86288, ING 182568, and UCMP 38910 (Hoffstetter & Soria 1986; Cifelli & Guerrero Díaz 1989; McGrath *et al.* 2020a).

Neolicaphrium recens
MLP 34-V-22-12 (holotype) and additional specimens as figured and described by Bond *et al.* (2001).

Paranisolambda prodromus
Photos of DGM 262M (holotype), DGM 304M (paratype), DGM 307M, DGM 310M, and DGM 1421M (Paula Couto 1952; Cifelli 1983).

Protolipterna ellipsodontoides
Casts of DNPM LE444E, 1392M. Photos of MCT 1392a-M (Cifelli 1983; Zanesco *et al.* 2019).

Appendix 1. — Continuation.

Ricardocifellia protocenica
Casts of MNRJ 1432V, 1434V, 1438V, 1439V, 1451V, 1452V, 1453V. Photos of 698M and 2150M (Cifelli 1983; Cifelli & Ortiz-Jaureguizar 2014; Mones 2015).

Tetramerorhinus cingulatum
Descriptions and figures of Scott (1910) and Soria (2001).

Tetramerorhinus lucarius
Descriptions and figures of Scott (1910) and Soria (2001), and the revision of the following specimens: YPM PU 15722, MLP 12-323.

Tetramerorhinus mixtum
Descriptions and figures of Scott (1910) and Soria (2001), and the revision of the following specimens: YPM PU 15107, MLP 26 IV-15-17, MLP 12-297.

Theosodon spp.
Descriptions and figures of Scott (1910) and the revision of the following specimens: *Theosodon lydekkeri* (MNHN.F.1902-6; YPM PU 15717); *Theosodon garrrettorum* (YPM PU 15164); *Theoson lallemanti* (YPM PU 15359; YPM PU 16003); *Theosodon* sp (YPM PU 16041).

Thoatherium minusculum
Descriptions and figures of Scott (1910) and Soria (2001), and AMNH 9167 as illustrated by Cifelli & Guerrero (1989).

Villarroelia totoyoi
VPPLT 729. Photos of casts of 8638, 86028, 85471, 86539, IGM 183407, IGM 184501, IGM 250965, and UCMP 39970.

APPENDIX 2. — Character list extended matrix.

The character list below is largely based on the data matrices from Cifelli (1993) and McGrath *et al.* (2020b). We also selected relevant characters from Muizon & Cifelli (2000). The original numbers of characters in those works are indicated with a "C", "M-C" and "MG", respectively: for example, character 1 of Cifelli (1993) is noted "1C", and character 1 of McGrath *et al.* (2020b) is noted "1MG". If a character was modified from its original definition, it is indicated. For example, the modified character of McGrath *et al.* (2020b) "36MG", is listed as "36MG modified". When two characters were equal, we merged them as one. For example, character "31C" and "30MG" are listed as one character and noted "31C + 30MG". If a character is treated as an ordered character in the analysis, this is indicated in parenthesis.

In addition, some characters were excluded for the following reasons:

1MG and 2MG: are likely allometric, as has been shown in several mammal clades (Cardini & Polly 2013; Cardini 2019).

8MG: reflects size variation, which may not be phylogenetically informative to resolve the interrelationships of early litopterns.

12C, 26C, 33C, 34C, 42MG, 60MG: not informative in our data matrix.

27C: redundant with 66MG.

39C: redundant with character 15MG.

30C: redundant with characters 27MG and 28MG.

4M-C: redundant with character 15C.

5M-C: redundant with all the other P4 characters.

6M-C, 7M-C, 28C, 41C: redundant with 43MG, 53MG, 54MG, and 61MG.

24C, 38MG: the observed variation is difficult to score with confidence.

44MG: redundant with 13C and 14C.

25C, 45MG, 46MG: the criteria to separate the states is not clear to us and we could not reproduce the scoring of Cifelli (1993) and McGrath *et al.* (2020b).

47MG: redundant with 32C.

21M-C: redundant with 22C, 23C, and 48C.

18C: redundant with 77MG.

80MG: redundant with 17C.

57MG, 76MG: likely allometric (Billet & Bardin 2021) and they are redundant with character 49C. We decided to keep character 49C because it does not follow the allometric model and the largest M2 might be a synapomorphy of some SANUs (Muizon *et al.* 2019: fig. 15).

Note from Cifelli (1993): "Characters scored 0 indicate the presumed ancestral condition"

Note from McGrath *et al.* (2020b): "Characters involving cranial or mandibular dimensions were only recorded on adult specimens (i.e., M3/m3 fully erupted). Continuous characters rescaled to exhibit a range of 0-1 (see McGrath *et al.* 2020b; Table S2). All linear measurements taken to nearest 0.1 mm. *-continuous character. †-character adapted from Schmidt (2015)."

In the character list below, the comments and justifications on modifications of the character definitions and character scorings are in italics.

CONTINUOUS CHARACTERS

Skull

(3MG) Dorsoventral height of orbit/M1 mesiodistal length.*

(4MG) Width of palate between right and left M1/M1 mesiodistal length.*

Mandible

(5MG) Mandibular height (measured perpendicular to ventral edge of mandible) at posterior edge of m1/m1 length.*

(6MG) Mandibular height (measured perpendicular to ventral edge of mandible) at distal edge of m3/height at distal edge of p2.*

Upper incisors

(7MG) Length of upper incisor-P1 diastema/M1 mesiodistal length.*

DISCRETE CHARACTERS

Skull

(9MG) Orbit: open (0); closed (1).

(10MG modified – Ordered) Anterior edge of orbit directly over: P4 (0); M1 (1); M2 or M2-M3 (2).

We modified the definition of character state 2, to reflect the fact that in Cramauchenia normalis *the anterior edge of the orbit is at the boundary of M2-M3 (Dozo & Vera 2010).*

(11MG) Posterior edge of infraorbital foramen directly dorsal of: P4 (0); P3 (1).

(12MG) Lateral edges of premaxillae: convergent (0); parallel (1).

Mandible

(23M-C) Mandibular symphysis: unfused (0); ankylosed (1).

(13MG – Ordered) Posterior most point of symphysis at level of: p3 (0); p2 (1); p1 (2).

Upper incisors

(14MG) Number of upper incisors: three (0); one (1).

(15MG) Upper incisor(s): small and incisiform (0); hypertrophied and tusk-like (1).

We scored this character as "?" for Megadolodus considering that only fragments of the anterior dentition are known, and the morphology of the upper incisors is uncertain (Cifelli & Villarroel 1997). Our scoring differs from McGrath et al. *(2020b), which scored the character state as "small and incisiform".*

Lower incisors

(16MG) Number of lower incisors: three (0); two (1).

(17MG) External (distal-most) lower incisor relative to other incisors: subequal (0); significantly larger than internal (mesial) incisor(s) (1).

Appendix 2. — Continuation.

Upper canines

(18MG) Upper canine: present (0); absent (1).

We modified the score for Megadolodus *from "present (0)" to "?", since the recognition of an isolated tooth as being a canine was very uncertain (Cifelli & Villarroel 1997), and might in fact represent the upper tusk (I2).*

(19MG) Diastema between P1 and next-most mesial tooth: absent (0); present (1).

We modified the score for Villarroelia *from "present (1)" to "?", as we found no mention of the diastema in the description (Cifelli & Guerrero 1997), and observation of the cast of the specimen IGM 250965 shows no evidence of a diastema.*

Lower canines

(20MG modified) Lower canine: incisiform (0); tusk-like (1). We excluded character state 2 (absent), because no taxa in our sample was scored with that state.

(21MG) Diastema between c and p1: absent (0); present (1).

Upper premolars

(23MG) P2 protocone: absent (0); present (1).†
(3M-C) Postprotocrista of P3: P3 with an incipient or small protocone and a posterior edge not expanded posteriorly (0); small or medium-sized protocone present and postprotocrista expanded posteriorly (1).
(31C + 30MG) P3 mesostyle: absent (0); present (1).
(24MG) P3 paracone and metacone: incipient on each other (0); broadly spaced (1).
(26MG) P3 hypocone: absent (0); present (1).†
(32MG) P4 hypocone: absent (0); present (1).†
(25MG) P3 mesiolingual cingulum: not connected to protocone and not forming basin (0); connected to protocone forming basin (1); extends past protocone (2); absent (3).
(27MG) P3 paraconule: absent (0); present (1).
(28MG) P3 metaconule: absent (0); present (1).†
(29C) P4 metaconule: absent (0); present (1).

We followed Cifelli (1993) and scored the P4 metaconule as "absent" for Protolipterna *and* Didolodus. *This scoring differs from the McGrath* et al. *(2020b).*

(36MG modified) P4 metaconule connection: joined to protocone by crest (0); joined to hypocone by crest (1); isolated (2).

We modified the character definition to reflect the connection of metaconule, which is scored independently of its presence/absence.

(29MG modified) P3 parastyle: small (0); forming strong projection (1).

We modified the definition of character states to be consistent with character 27 (see below).

(40C + 33MG modified) P4 parastyle: small (0); forming strong projection (1).
(15C) P4 metacone: absent or closely appressed to paracone (0); subequal to paracone and well separated from it (1).
(31MG) P4 mesiolingual cingulum: not connected to protocone and not forming basin (0); connected to protocone forming basin (1); extends past protocone (2); absent (3).
(16C + 34MG) P4 mesostyle: absent (0); present (1).
(35MG) P4 metastyle: absent (0); present (1).
(22MG) Cheek teeth: bunodont (0); bunoselenodont (1).

Lower premolars

(62MG – Ordered) Ratio of p2/p1 mesiodistal length: p2/p1 < or = 1.25 (0); 1.25 < p2/p1 < 1.45 (1); p2/p1 > or = 1.45 (2).
(63MG) p1-2 implantation: no diastema (0); diastema between teeth (1); imbricated (2).
(64MG) p2 metaconid: absent (0); present (1).

In Cramauchenia normalis *the metaconid was scored as absent (0) following Soria (1981).*

(65MG) p3 labial cingulid: absent (0); present (1).
(66MG modified) p3 talonid: absent (0); reduced talonid (1); large talonid with crescentic lophid (2).

We modified the definition of character states 1 and 2 because we observed that the presence of talonid basin was not clear in several taxa.

(67MG) p3 trigonid basin: mesiodistally longer than talonid basin (0); same length as talonid basin (1).
(68MG) p3 hypoconid: absent (0); lingual of protoconid (1); directly distal of protoconid (2); labial of protoconid (3).
(69MG) p3 hypoconulid: absent (0); present (1).
(70MG modified) p3 metaconid: absent (0); present (1).

We modified the character definition to exclude the scoring of presence/absence of the paraconid, because it is often reduced (Jernvall 1995), and small cusps likely do not have a reliable phylogenetic signal (Jernvall 2000; Billet & Bardin 2019)

(71MG) p3 entoconid: absent or weak (0); well-developed (1).

We modified the character scoring of McGrath et al. *(2020b) for* Adiantoides leali *from "well-developed" to "absent or weak".*

(72MG) p4 entoconid: absent or weak (0); well-developed (1).
(20C) p4 talonid: small heel with cuspids indistinct (0); talonid fully developed with at least two cuspids (1); lophate (cuspids embedded in loph) (2).
(51C) p4 paraconid: present (0); reduced to absent (1).
(73MG) p4 labial cingulid: absent (0); present (1).
(74MG modified) p4 relative length of trigonid and talonid: trigonid mesiodistally longer than talonid (0); trigonid with same length as talonid (1).

We modified the character definition and character states because we observed that the presence of talonid basin was not clear in several taxa.

(75MG) p4 hypoconid: lingual of protoconid (0); directly distal of protoconid (1); labial of protoconid (2).

Upper molars

(43MG modified) M1-2 metaconule connections: joined to protocone (0); joined to hypocone (1); joined to crest uniting hypo- and protocone (2); joined to metacone (3); isolated (4); joined to hypoconoe on M1 and metaconule absent on M2 (5).†

We modified the character scoring of McGrath et al. *(2020b) for* Neobrachytherium morenoi *which has a metaconule joined to the hypocone (Soria 2001). We also modified the character definition to reflect the condition of* Lambdaconus suinus *where the metaconule is absent on the M2 (Soria 2001; Schmidt* et al. *2019a).*

(61MG) M3 metaconule: connected to protocone by crest (0); absent (1); not connected to protocone (2).
(53MG) M1 metaconule position: closer to hypocone (0); equidistant (1); closer to protocone (2).
(54MG) M2 metaconule position: closer to hypocone (0); equidistant (1); closer to protocone (2).

Appendix 2. — Continuation.

We modified the scoring of McGrath et al. *(2020b) for* Paranisolambda *from character state 1 to 0, after the observations of specimen DGM 1421M*

(14C modified) Upper molars parastyle: not forming distinct pillar (0); forming a distinct pillar (1).
(13C + 9M-C) Upper molar mesostyle: absent (0); present (1).
(59MG) M3 metastyle: absent (0); present (1).
(32C) Union of upper molar hypocone to protocone: distinct cusps (0); joined by a crest (1).
(40MG – Ordered) M1-2 paracone and metacone 'folds' (ridges between labial styles): absent (0); weak (1); strong (2).†
(41MG) M1-2 paracone and metacone concavities: both weak (0); paracone concavity well-developed (1); both well-developed (2).
(23C) Form of upper molar hypocone: cuspate (0); developed as a crescent (1).
(48C + 39MG) M1-2 hypocone: absent (0); present (1).

The character state for Lambdaconus lacerum *differs from McGrath* et al. *(2020b). The scoring was done following the specimens illustrated in Soria (2001: figs 3-9).*

(22C + 58MG) M3 hypocone: absent (0); present (1).
(55MG) M1 hypocone: directly distal of protocone (0); positioned more labially than protocone (1).
(56MG) M2 hypocone: directly distal of protocone (0); positioned more labially than protocone (1).
(22M-C + 50C) Cusp on precingulum anterior to paraconule: absent (0); present (1).

We modified the character states for Protolipterna, Miguelsoria *and* Ricardocifellia *after direct observations of the cast from Itaborai.*

(42C) Upper molar postcingulum: small (0); enlarged enclosing basin (1).
(48MG) M1-2 labial cingula: present (0); absent (1). †
(49MG) M3 labial cingulum: present (0); absent (1). †
(50MG modified) M1 mesiolingual cingulum: not connected to protocone and not forming basin (0); connected to protocone (1).
(51MG modified) M2 mesiolingual cingulum: not connected to protocone and not forming basin (0); connected to protocone (1).
(52MG modified) M3 mesiolingual cingulum: not connected to protocone and not forming basin (0); connected to protocone (1).

For characters 50MG, 51MG, and 52MG, we deleted the character state (2) "reaches lingual sulcus" as defined by McGrath et al. *(2020b) because it was only present in one taxon (*Diadiaphorus*). Therefore, we decided to exclude this character state and scored* Diadiaphorus *as (1) "connected to protocone".*

(49C modified) Molar size: M2 largest, M1 and M3 subequal (0); M3 largest or all molars subequal (1).

We modified the character definition to avoid the allometry (Billet & Bardin 2021).

(37MG) M1/P4 linguolabial width: subequal (ratio < or = 1.15) (0); M1 wider (> 1.15) (1).

Lower molars

(77MG modified) Position of paraconid on m1-2: directly lingual of protoconid (0); mesiolingual of protoconid (1); absent (2).

We modified the character state 1 of 77MG to "mesio-lingual of protoconid" instead of "mesial of protoconid" to better reflect the observed variation in the position of the protoconid.

(86MG) m3 paraconid: present (0); absent (1).
(78MG) Paralophid on m1-2: absent (0); terminates near midline (1); developed and reaching lingual edge of tooth (2).†
(90MG) m3 paralophid: absent (0); terminates near midline (1); reaches lingual edge of tooth (2).
(21C) Lower molar metaconid: is not developed as a distinct column (0); is developed as a distinct column (1).
(91MG) m3 metaconid: conical (0); mesiodistally extended (1).
(79MG) Entoconid on m1-2: as large as hypoconulid (0); larger than hypoconulid (1); smaller than hypoconulid (2); absent (3).†
(87MG modified) m3 entoconid: isolated (0); connected by crest to hypoconulid or to hypolophulid (1); absent (2).

We removed the character state 1 defined by McGrath et al. *(2020b) because it was not scored in any taxa of our sampling. We merged the character states 2 and 3 defined by McGrath* et al. *(2020b), as just one character state, because we did not observed enough variation to clearly scored them as different states in our taxonomic sample.*

(35C) Lower molar entoconid attachment to hypolophid: (0) posterior; (1) anterior.
(36C) Lower molar entoconid condition: (0) distinct cuspate; (1) developed as entolophid.
(88MG) m1-2 hypoconulid position: not on lingual border of tooth (0); on lingual border of tooth (1).
(89MG) m3 hypoconulid position: not on lingual border of tooth (0); on lingual border of tooth (1).
(17C modified) Lower molar cristid obliqua attachment to trigonid: median (0); lingual (at base of metaconid) (1).

We modified the wording of character state 1, to better describe the observed variation.

(37C) Lower molar talonid cusps: distinct (0); merged into crescent (1).
(81MG) m1-2 labial cingulids: absent (0); present (1).
(82MG) m3 labial cingulid: absent (0); present (1).
(83MG) m1-2 lingual cingulids: absent (0); present (1).
(84MG) m3 lingual cingulid: absent (0); present (1).
(85MG – Ordered) Hypsodonty index: HI < 0.85 (0); 0.85 < HI < 1.00 (1); HI > 1.00 (2).†

Note from McGrath et al. *(2020b): "Hypsodonty Index was measured only on m3s that were unworn enough so that the lophids were distinguishable from (i.e. thinner than) the cuspids".*

Digits

(1C) Digits in manus: five (0); reduced to three (1).
(2C) Digits in pes: five (0); reduced to three (1).
(38C) Lateral digits: subequal to or somewhat smaller than median digit (0); greatly reduced (1).
(92MG) Manus/pes: Functionally tridactyl (0); functionally or truly monodactyl, as shown by reduced second and/or fourth metapodials (1).

Astragalus

(3C) Astragalar body: low, without sharp crests (0); spool-like, with salient, subequal tibial and fibular crests (1).
(4C) Tibial trochlea of astragalus: restricted to dorsal surface (0); extending far posteroinferiorly (1).

Appendix 2. — Continuation.

(5C) Astragalar head: ovoid (0); semicylindrical, with major axis subparallel to that of tibial trochlea (1).
(6C) Navicular facet of astragalus: restricted to distoinferior part of head (0); well onto superior and inferior surfaces of head (1).
(7C) Cuboid facet on astragalus: present (0); lacking (1).
(8C) Medial collateral ligament facet on astragalus: present (0); lacking (1).
(9C) Astragalar ectal facet: shallow, facing inferiorly (0); deeply concave, facing outward (1).
(43C) Medial malleolar facet of astragalus: restricted to medial side of body (0); extending onto neck (1).
(46C) Medial side of astragalus: sublinear (0); with strong anterior flare (1).
(47C) Medial expansion of astragalar head: absent (0); present (1).

Calcaneus

(10C) Calcaneal neck: short, with cuboid facet subnormal to axis of element (0); long, with strongly oblique cuboid facet (1).
(11C) Sustentacular facet of calcaneus: subplanar, facing dorsodistally (0); anteroposteriorly concave, following same curvature as anterior part of ectal facet (1).
(44C) Dorsal beak on distal end of calcaneus: absent (0); present (1).
(45C) Peroneal tubercle of calcaneus: lateral (0); dorsal (1).

APPENDIX 3. — Character list reduced matrix.

To produce the reduced matrix, we merged characters from the extended matrix that coded independently adjacent teeth or cusps and showed redundant scoring. If a step matrix was used to constraint the character transitions in a character, this is indicated and the step matrices are described in the Appendix 4. In the character list below, the comments and justifications on modifications of the character definitions and character scorings with respect the extended matrix are in italics. If a character is treated as an ordered character in the analysis, this is indicated in parenthesis.

Note from Cifelli (1993): "Characters scored 0 indicate the presumed ancestral condition"

Note from McGrath *et al.* (2020b): "Characters involving cranial or mandibular dimensions were only recorded on adult specimens (i.e., M3/m3 fully erupted). Continuous characters rescaled to exhibit a range of 0-1 (see McGrath *et al.* 2020b, Table S2). All linear measurements taken to nearest 0.1 mm. *-continuous character. †-character adapted from Schmidt (2015)."

CONTINUOUS CHARACTERS

Skull

(3MG) Dorsoventral height of orbit/M1 mesiodistal length.*

(4MG) Width of palate between right and left M1/M1 mesiodistal length.*

Mandible

(5MG) Mandibular height (measured perpendicular to ventral edge of mandible) at posterior edge of m1/m1 length. *

(6MG) Mandibular height (measured perpendicular to ventral edge of mandible) at distal edge of m3/height at distal edge of p2.*

Upper incisors

(7MG) Length of upper incisor-P1 diastema/M1 mesiodistal length.*

DISCRETE CHARACTERS

Skull

(9MG) Orbit: open (0); closed (1).

(10MG modified – Ordered) Anterior edge of orbit directly over: P4 (0); M1 (1); M2 or M2-M3 (2).

(11MG) Posterior edge of infraorbital foramen directly dorsal of: P4 (0); P3 (1).

(12MG) Lateral edges of premaxillae: convergent (0); parallel (1).

Mandible

(23M-C) Mandibular symphysis: unfused (0); ankylosed (1).

(13MG – Ordered) Posterior most point of symphysis at level of: p3 (0); p2 (1); p1 (2).

Upper incisors

(14MG + 15MG modified) Number of upper incisors: three, small and incisiform (0); three, hypertrophied and tusk-like (1); one, small and incisiform (2); one, hypertrophied and tusk-like (3).

We merged characters 12 and 13 of the extended matrix (Appendix 2), as we noted they were extremely redundant and perfectly compatible. In this modified character definition, we assume that the number of incisors may be correlated with their shape in this taxonomic sample (i.e., if a taxon has three incisors, these are likely to be small and incisiform, whereas if a taxon has one incisor, it is likely to be hypertrophied and tusk-like). We used the step matrix A (Appendix 4).

Lower incisors

(16MG + 17MG modified) Number and relative size of lower incisors: three incisors, subequal (0); three incisors with the external being significantly larger than the internal (1); two incisors, subequal (2); two incisors with the external being significantly larger than the internal (3).

We used the step matrix A (Appendix 4).

Upper canines

(18MG + 19MG modified) Upper canine and diastema between P1 and next-most mesial tooth: canine present, diastema absent (0); canine absent, diastema present (1).

We merged characters 16 and 17 of the extended matrix (Appendix 2) because we assume that it is the absence of the canine that creates the diastema. Indeed, after the revision of Megadolodus *and* Villarroelia*, there were only two combinations (character states) represented in the datamatrix: canine present, diastema absent (character state 0), and canine absent, diastema present (character state 1).*

Lower canines

(20MG) Lower canine: incisiform (0); tusk-like (1).

(21MG) Diastema between c and p1: absent (0); present (1).

Upper premolars

(23MG) P2 protocone: absent (0); present (1).†

(3M-C) Postprotocrista of P3: P3 with an incipient or small protocone and a posterior edge not expanded posteriorly (0); small or medium-sized protocone present and postprotocrista expanded posteriorly (1).

(24MG + 31C+ 30MG modified) P3 mesostyle, paracone and metacone: mesostyle absent, paracone & metacone incipient on each other (or only paracone present) (0); mesostyle absent, paracone & metacone broadly spaced (1); mesostyle present, paracone & metacone broadly spaced (2).

We merge characters 22 and 23 of the extended matrix (Appendix 2). Based on the patterning cascade model of cusps (Jernvall 2000; Skinner & Gunz 2010), we hypothesize that the location and size of paracone and metacone is linked with the development of a mesostyle.

(26MG + 32 MG modified) P3-P4 hypocone: absent in P3-P4 (0); absent in P3 and present in P4 (1); present in P3-P4 (2).

We merged characters 24 and 25 of the extended matrix (Appendix 2). Taxa that were coded as "?" and "0" respectively in the extended matrix were scored here as "0" because none of the taxa showed a condition where the hypocone was absent in P4 and present in P3.

Appendix 3. — Continuation.

(25MG) P3 mesiolingual cingulum: not connected to protocone and not forming basin (0); connected to protocone forming basin (1); extends past protocone (2); absent (3).
(27MG) P3 paraconule: absent (0); present (1).
(28MG + 29C modified) P3-4 metaconule: absent in P3-4 (0); absent in P3 and present in P4 (1); present in P3-4 (2).

We merged characters 28 and 29 of the extended matrix (Appendix 2). Taxa that were coded as "?" and "0" respectively in the extended matrix were scored here as "0" because none of the taxa showed a condition where the metaconule was absent in P4 and present in P3.

(36MG modified) P4 metaconule connection: joined to protocone by crest (0); joined to hypocone by crest (1); isolated (2).
(29MG + 40C + 33MG modified) P3-4 parastyle: small (0); forming strong projection (1).

We merged characters 31 and 32 of the extended matrix (Appendix 2). None of the taxa showed a condition where the parastyle was small in P3 and forming a strong projection in P4, or viceversa. Therefore, for taxa in which the parastyle condition is known for only one of the teeth (P3 or P4), we assume that this condition is the same in the other tooth.

(15C) P4 metacone: (0) absent or closely appressed to paracone; (1) subequal to paracone and well separated from it.
(31MG) P4 mesiolingual cingulum: not connected to protocone and not forming basin (0); connected to protocone forming basin (1); extends past protocone (2); absent (3).
(16C + 34MG) P4 mesostyle: absent (0); present (1).
(35MG) P4 metastyle: absent (0); present (1).
(22MG) Cheek teeth: bunodont (0); bunoselenodont (1).

Lower premolars

(62MG – Ordered) Ratio of p2/p1 mesiodistal length: p2/p1 < or = 1.25 (0); 1.25 < p2/p1 < 1.45 (1); p2/p1 > or = 1.45 (2).
(63MG) p1-2 implantation: no diastema (0); diastema between teeth (1); imbricated (2).
(64MG) p2 metaconid: absent (0); present (1).
(65MG) p3 labial cingulid: absent (0); present (1).
(66MG modified) p3 talonid: absent (0); reduced talonid (1); large talonid with crescentic loph (2).
(67MG) p3 trigonid basin: mesiodistally longer than talonid basin (0); same length as talonid basin (1).
(68MG) p3 hypoconid: absent (0); lingual of protoconid (1); directly distal of protoconid (2); labial of protoconid (3).
(69MG) p3 hypoconulid: absent (0); present (1).
(70MG modified) p3 metaconid: absent (0); present (1).
(71MG + 72 MG modified) p3-4 entoconid: absent or weak in p3-p4 (0); absent or weak in p3 and well-developed in p4 (1); well-developed in p3-4 (2).

We merged characters 47 and 48 of the extended matrix (Appendix 2). Taxa that were coded as "?" and "0" respectively in the extended matrix were scored here as "0" because none of the taxa showed a condition where the entoconid was absent or weak in p4 and well-developed in p3.

(20C) p4 talonid: (0) small heel with cuspids indistinct; (1) talonid fully developed with at least two cuspids; (2) lophate.
(51C) p4 paraconid: (0) present; (1) reduced to absent.
(73MG) p4 labial cingulid: absent (0); present (1).
(74MG modified) p4 relative length of trigonid and talonid: trigonid mesiodistally longer than talonid (0); trigonid with same length as talonid (1).
(75MG) p4 hypoconid: lingual of protoconid (0); directly distal of protoconid (1); labial of protoconid (2).

Upper molars

(43MG modified) M1-2 metaconule connections: joined to protocone (0); joined to hypocone (1); joined to crest uniting hypo- and protocone (2); joined to metacone (3); isolated (4); joined to hypocone on M1 and metaconule absent on M2 (5).†
(61MG) M3 metaconule: connected to protocone by crest (0); absent (1); not connected to protocone (2).
(53MG + 54MG modified) M1-2 metaconule position: closer to hypocone on M1-2 (0); equidistant on M1-2 (1); closer to protocone on M1-2 (2); equidistant on M1, closer to protocone on M2 (3).

We used the step matrix B (Appendix 4).

(14C modified) Upper molar parastyle: not forming distinct pillar projecting labially (0); forming a distinct pillar projecting labially (1).
(13C + 9M-C) Upper molar mesostyle: absent (0); present (1).
(59MG) M3 metastyle: absent (0); present (1).
(32C) Union of upper molar hypocone to protocone: (0) distinct cusps; (1) joined by a crest.
(40MG + 41 MG modified) M1-2 paracone and metacone concavities and folds (ridges): no fold, well-developed concavities (0); weak fold, well-developed concavities (1); strong fold, weak concavities (2); strong fold, well-developed concavities (3).

In the model of character transitions, we allowed the direct transition from the state "no fold and well-developed concavities" to the state "strong fold, weak concavities" assuming a possible joint evolution of these structures. Anisolambda *was the only taxon scored as strong metacone and paracone folds and only the paracone concavity well-developed (character states 2 and 1 for characters 63 and 64 respectively in the extended matrix). We decided to score it as polymorphic (states 2 and 3 here), having strong folds, and both weak and well-developed concavities for the paracone and metacone. We used the step matrix B (Appendix 4).*

(23C) Form of upper molar hypocone: cuspate (0); developed as a crescent (1).
(48C + 39MG + 22C + 58MG modified) M1-3hypocone:absent in all molars (0); present on M1-2, absent on M3 (1); present in all molars (2).
(55MG + 56MG modified) M1-2 hypocone: directly distal of protocone in M1-2 (0); directly distal of protocone in M1 and positioned more labially than protocone in M2 (1); positioned more labially than protocone in M1-2 (2).

Prolicaphrium specillatum *was the only taxon scored as (0/1, 0) for characters 68 and 69 in the extended matrix (Appendix 2). We decided to score it here as having the hypocone directly distal of protocone in both, M1 and M2 (character state 0). Taxa scored as (?, 0) in the extended matrix were also scored here as character state 0.*

(22M-C + 50C) Cusp on precingulum anterior to paraconule: absent (0); present (1).
(42C) Upper molar postcingulum: small (0); enlarged enclosing basin (1).

Appendix 3. — Continuation.

(48MG + 49MG modified) M1-3 labial cingula: present in M1-3 (0); present in M1-2 and absent in M3 (1); absent in M1-3 (2).

We merged characters 72 and 73 of the extended matrix (Appendix 2). Taxa that were coded as "1" and "?" respectively in the extended matrix were scored here as "2" because none of the taxa showed a condition where the labial cingulum was present in M3 and absent in M1-2. We assume that if the labial cingulum is absent on M1-2 it is also absent on M3.

(50MG + 51 MG + 52MG modified) M1-3 mesiolingual cingulum: not connected to protocone and not forming a basin in M1-3 (0); not connected to protocone and not forming a basin in M1-2 and connected to protocone in M3 (1); not connected to protocone and not forming a basin in M1 and connected to protocone in M2-3 (2); connected to protocone in M1-3 (3).

Prolicaphrium specillatum *was the only taxon scored as (1, 0/1, 1) for characters 74, 75 and 76 in the extended matrix (Appendix 2). We decided to score it here as having mesiolingual cingulum connected to protocone in M1-3 (character state 3). Taxa scored in the extended matrix as (?, 0, 0) were scored here as having a mesiolingual cingulum not connected to protocone and not forming a basin in all the upper molars (character state 0). Taxa scored as (1, ?, ?) were scored as having a mesiolingual cingulum connected to protocone in all upper molars (character state 3). We used the step matrix C (Appendix 4).*

(49C modified) Molar size: M2 largest, M1 and M3 subequal (0); M3 largest or all molars subequal (1).

(37MG) M1/P4 linguolabial width: subequal (ratio < or = 1.15) (0); M1 wider (> 1.15) (1).

Lower molars

(77MG modified) Position of paraconid on m1-2: directly lingual of protoconid (0); mesiolingual of protoconid (1); absent (2).

(86MG) m3 paraconid: present (0); absent (1).

(78MG) Paralophid on m1-2: absent (0); terminates near midline (1); developed and reaching lingual edge of tooth (2).†

(90MG) m3 paralophid: absent (0); terminates near midline (1); reaches lingual edge of tooth (2).

(21C) Lower molar metaconid: (0) is not developed as a distinct column; (1) is developed as a distinct column.

(91MG) m3 metaconid: conical (0); mesiodistally extended (1).

(79MG) Entoconid on m1-2: as large as hypoconulid (0); larger than hypoconulid (1); smaller than hypoconulid (2); absent (3). †

(87MG modified) m3 entoconid: isolated (0); connected by crest to hypoconulid or to hypolophulid (1); absent (2).

(35C) Lower molar entoconid attachment to hypolophid: (0) posterior; (1) anterior.

(36C) Lower molar entoconid condition: (0) distinct cuspate; (1) developed as entolophid.

(88MG + 89MG modified) m1-3 hypoconulid position: not on lingual border of tooth in m1-3 (0); on lingual border of tooth in m1-2 and not on lingual border of tooth in m3 (1); on lingual border of tooth in m1-3 (2).

Brachytherium cuspidatum *was the only taxon scored as (0/1, 0) for characters 89 and 90 in the extended matrix (Appendix 2). We decided to score it here as having the hypoconulid on the lingual border of tooth in m1-3 (character state 2). Taxa scored as (0, ?) in the extended matrix were scored here as character state 0 because all the taxa on which the hypoconulid is not on the lingual border on m1-2, show the same condition on m3. Taxa scored as (?, 1) in the extended matrix were scored here as character state 2 because all the taxa on which the hypoconulid is on the lingual border on m3, show the same condition on m1-2.*

(17C modified) Lower molar cristid obliqua attachment to trigonid: median (0); lingual (at base of metaconid) (1).

(37C) Lower molar talonid cusps: distinct (0); merged into crescent (1).

(81MG + 82MG modified) m1-3 labial cingulids: absent in m1-3 (0); absent in m1-2 and present in m3 (1); present in m1-2 and absent in m3 (2); present in m1-3 (3).

(83MG + 84MG modified) m1-3 lingual cingulids: absent (0); present (1).

We merged characters 95 and 96 of the extended matrix (Appendix 2). Taxa that were coded as (0, ?) or (1, ?) in the extended matrix were scored here as "0" and "1" respectively because none of the taxa showed a condition where the lingual cingulid was absent in m1-2 and present in m3 or viceversa.

(85MG – Ordered) Hypsodonty index: HI < 0.85 (0); 0.85 < HI < 1.00 (1); HI > 1.00 (2).†

Digits

(1C) Digits in manus: five (0); reduced to three (1).

(2C) Digits in pes: five (0); reduced to three (1).

(38C) Lateral digits: subequal to or somewhat smaller than median digit (0); greatly reduced (1).

(92MG) Manus/pes: Functionally tridactyl (0); functionally or truly monodactyl, as shown by reduced second and/or fourth metapodials (1).

Astragalus

(3C) Astragalar body: low, without sharp crests (0); spool-like, with salient, subequal tibial and fibular crests (1).

(4C) Tibial trochlea of astragalus: restricted to dorsal surface (0); extending far posteroinferiorly (1).

(5C) Astragalar head: ovoid (0); semicylindrical, with major axis subparallel to that of tibial trochlea (1).

(6C) Navicular facet of astragalus: restricted to distoinferior part of head (0); well onto superior and inferior surfaces of head (1).

(7C) Cuboid facet on astragalus: present (0); lacking (1).

(8C) Medial collateral ligament facet on astragalus: present (0); lacking (1).

(9C) Astragalar ectal facet: shallow, facing inferiorly (0); deeply concave, facing outward (1).

(43C) Medial malleolar facet of astragalus: restricted to medial side of body (0); extending onto neck (1).

(46C) Medial side of astragalus: sublinear (0); with strong anterior flare (1).

(47C) Medial expansion of astragalar head: absent (0); present (1).

Appendix 3. — Continuation.

Calcaneus

(10C) Calcaneal neck: short, with cuboid facet subnormal to axis of element (0); long, with strongly oblique cuboid facet (1).

(11C) Sustentacular facet of calcaneus: subplanar, facing dorsodistally (0); anteroposteriorly concave, following same curvature as anterior part of ectal facet (1).

(44C) Dorsal beak on distal end of calcaneus: absent (0); present (1).

(45C) Peroneal tubercle of calcaneus: lateral (0); dorsal (1).

APPENDIX 4. — Step matrices used in the maximum parsimony analysis of the reduced matrix to set the costs and constrain the paths for transition among character states (see Appendix 3).

STEP MATRIX A

	0	1	2	3
0	0	1	1	1
1	1	0	2	1
2	1	2	0	1
3	1	1	1	0

STEP MATRIX B

	0	1	2	3
0	0	1	2	2
1	1	0	1	1
2	2	1	0	1
3	2	1	1	0

STEP MATRIX C

	0	1	2	3
0	0	1	2	1
1	1	0	1	2
2	2	1	0	1
3	1	2	1	0

APPENDIX 5. — Age ranges (in Ma) of the taxa included in the phylogenetic analyses. Abbreviation: **SALMA**, South American Land Mammal Age.

Taxon	Max Age	Min Age	Epoch/SALMAs	References
Simoclaenus sylvaticus Muizon & Cifelli, 2000	65.6	64	Tiupampan	(Muizon & Cifelli 2000; Woodburne *et al.* 2014)
Tiuclaenus Muizon & Marshall, 1987	65.6	64	Tiupampan	(Woodburne *et al.* 2014; Croft *et al.* 2020)
Miguelsoria parayirunhor (Paula Couto, 1952)	53	49.5	Itaboraian	(Cifelli 1983; Woodburne *et al.* 2014)
Protolipterna ellipsodontoides Cifelli, 1983	53	49.5	Itaboraian	(Woodburne *et al.* 2014; Zanesco *et al.* 2019)
Asmithwoodwardia scotti Paula Couto, 1952	53	49.5	Itaboraian	(Paula Couto 1952; Woodburne *et al.* 2014)
Paranisolambda prodromus (Paula Couto, 1952)	53	49.5	Itaboraian	(Cifelli 1983; Woodburne *et al.* 2014)
Ricardocifellia protocenica (Paula Couto, 1952)	53	49.5	Itaboraian	(Cifelli 1983; Woodburne *et al.* 2014)
Victorlemoinea prototypica Paula Couto, 1952	53	49.5	Itaboraian	(Paula Couto 1952; Woodburne *et al.* 2014)
Lamegoia conodonta Paula Couto, 1952	53	49.5	Itaboraian	(Paula Couto 1952; Woodburne *et al.* 2014)
Didolodus multicuspis Ameghino, 1897	46	39	Vacan-Barrancan	(Dunn *et al.* 2013; Woodburne *et al.* 2014; Croft *et al.* 2020)
Adiantoides leali Simpson & Minoprio, 1949	46	39	Vacan-Barrancan	(Cifelli & Soria 1983; Dunn *et al.* 2013; Woodburne *et al.* 2014; Croft *et al.* 2020)
Indalecia grandensis Bond & Vucetich, 1983	46	39	Vacan-Barrancan	(Cifelli & Soria 1983; Dunn *et al.* 2013; Woodburne *et al.* 2014; Croft *et al.* 2020)
Polymorphis Roth, 1899	38.2	38	Mustersan	(Dunn *et al.* 2013; Croft *et al.* 2020)
			Deseadan-Colhuehuapian	(Dozo & Vera 2010; Dunn *et al.* 2013)
Cramauchenia normalis Ameghino, 1902	29.4	20.1	Colhuehuapian-Laventan	(Cifelli & Guerrero 1997; Dunn *et al.* 2013; Croft *et al.* 2020)
Theosodon Ameghino, 1887	21	11.8		
Paramacrauchenia scamnata (Ameghino, 1902)	21	20.1	Colhuehuapian	(Soria 2001; Dunn *et al.* 2013)
Anisolambda Ameghino, 1901	53	38	Itaboraian-Mustersan	(Cifelli 1983; Dunn *et al.* 2013; Croft *et al.* 2020)
Megadolodus molariformis McKenna, 1956	13.5	11.8	Laventan	(Cifelli & Villarroel 1997)
Neodolodus colombianus Hoffstetter & Soria, 1986	13.5	11.8	Laventan	(Cifelli & Guerrero Díaz 1989)
Anisolophus australis (Burmeister, 1879)	18	15.6	Santacrucian	(Soria 2001; Cuitiño *et al.* 2016)
Anisolophus floweri (Ameghino, 1887)	18	15.6	Santacrucian	(Soria 2001; Cuitiño *et al.* 2016)
Brachytherium cuspidatum Ameghino, 1883	11.6	5.3	Late Miocene	(Schmidt 2015)
Diadiaphorus majusculus Ameghino, 1887	18	15.6	Santacrucian	(Soria 2001; Schmidt 2015; Cuitiño *et al.* 2016)
Diplasiotherium robustum Rovereto, 1914	4.7	3.7	Montehermosan	(Soria 2001; Prevosti *et al.* 2021)
Eoauchenia primitiva Ameghino, 1887	4.7	3.7	Montehermosan	(Soria 2001; Prevosti *et al.* 2021)
Epitherium laternarium Ameghino, 1888	4.7	3.7	Montehermosan	(Soria 2001; Prevosti *et al.* 2021)
Lambdaconus lacerum (Ameghino, 1902)	21	17.5	Colhuehuapian-Pinturan	(Soria 2001; Dunn *et al.* 2013)
Lambdaconus suinus Ameghino, 1897	29.4	24.2	Deseadan	(Soria 2001; Dunn *et al.* 2013)
Neobrachytherium intermedium (Moreno & Mercerat, 1891)	8.5	3.7	Huayquerian-Montehermosan	(McGrath *et al.* 2020a, 2020b; Prevosti *et al.* 2021)
Neobrachytherium morenoi (Rovereto, 1914)	8.5	3.7	Huayquerian-Montehermosan	(McGrath *et al.* 2020a, 2020b; Prevosti *et al.* 2021)
Neolicaphrium recens Frenguelli, 1921	2	0.78	Ensenadan	(Cione & Tonni 1995; Bond *et al.* 2001)
Picturotherium migueli Kramarz & Bond, 2005	19.04	17.5	Pinturan	(Kramarz & Bond 2005; Dunn *et al.* 2013)
Proectocion Ameghino, 1904	41.7	39	Barrancan	(Dunn *et al.* 2013; Croft *et al.* 2020)
Mesolicaphrium sanalfonense (Cifelli & Guerrero, 1997)	13.5	11.8	Laventan	(Cifelli & Guerrero 1997)
Prolicaphrium specillatum Ameghino, 1902	21	20.1	Colhuehapian	(Soria 2001; Dunn *et al.* 2013)
Proterotherium cervioides Ameghino, 1883	11.6	5.3	Late Miocene	(Schmidt 2015)
Protheosodon coniferus Ameghino, 1897	29.4	24.2	Deseadan	(Dunn *et al.* 2013; Croft *et al.* 2020)
Tetramerorhinus cingulatum (Ameghino, 1891)	18	15.6	Santacrucian	(Soria 2001; Cuitiño *et al.* 2016)
Tetramerorhinus lucarius Ameghino, 1894	18	15.6	Santacrucian	(Soria 2001; Cuitiño *et al.* 2016)
Tetramerorhinus mixtum (Ameghino, 1894)	18	15.6	Santacrucian	(Soria 2001; Cuitiño *et al.* 2016)
Thoatheriopsis mendocensis Soria, 2001	15.9	11.6	Middle Miocene	(Villafañe *et al.* 2012)
Thoatherium minusculum Ameghino, 1887	18	15.6	Santacrucian	(Soria 2001; Cuitiño *et al.* 2016)
Uruguayodon alius Corona, Perea & Ubilla, 2019	0.78	0.12	Middle Pleistocene	(Corona *et al.* 2019)
Villarroelia totoyoi Cifelli & Guerrero, 1997	13.5	11.8	Laventan	(Cifelli & Guerrero 1997)